EG&G-EAST-8608
August 1989

Received by OSTI

MAY 21 1990

INFORMAL REPORT

A COMPARISON OF RELAP5 AND TRAC LOCA CALCULATIONS FOR THE K-14.1 CHARGE AT SRS

C. B. Davis

DO NOT MICROFILM
COVER

Idaho National Engineering Laboratory

Managed by the U.S. Department of Energy

EG&G Idaho

Work performed under DOE Contract No. DE-AC07-76ID01570

DISTRIBUTION OF THIS DOCUMENT IS UNLIMITED

DISCLAIMER

This report was prepared as an account of work sponsored by an agency of the United States Government. Neither the United States Government nor any agency thereof, nor any of their employees, makes any warranty, express or implied, or assumes any legal liability or responsibility for the accuracy, completeness, or usefulness of any information, apparatus, product, or process disclosed, or represents that its use would not infringe privately owned rights. Reference herein to any specific commercial product, process, or service by trade name, trademark, manufacturer, or otherwise does not necessarily constitute or imply its endorsement, recommendation, or favoring by the United States Government or any agency thereof. The views and opinions of authors expressed herein do not necessarily state or reflect those of the United States Government or any agency thereof.

DISCLAIMER

Portions of this document may be illegible in electronic image products. Images are produced from the best available original document.

EGG-EAST--8608

DE90 010923

A COMPARISON OF RELAP5 AND TRAC LOCA CALCULATIONS FOR THE K-14.1 CHARGE AT SRS

C. B. Davis

Published August 1989

EG&G Idaho Inc.
Idaho Falls, Idaho 83415

Prepared for the U. S. Department of Energy
Idaho Operations Office
Under DOE Contract No. DE-AC07-76ID01570

MASTER

DISTRIBUTION OF THIS DOCUMENT IS UNLIMITED

ABSTRACT

Calculations of a loss-of-coolant accident (LOCA) in K-Reactor at the Savannah River Site (SRS) were performed using the RELAP5 computer code. The results of the RELAP5 calculation were then compared with a TRAC calculation previously performed by Savannah River Laboratory. The calculations represented the early (flow instability) portion of a LOCA initiated by a double-ended guillotine break in the plenum inlet piping in K-Reactor.

A RELAP5 model of K-Reactor was developed to perform the calculations. The model represented all six external loops and represented the the reactor vessel in a three-dimensional manner.

The RELAP5 and TRAC results were compared to illustrate and understand differences and similarities between calculations performed with independent computer codes and input models. The variation between the independent calculations provided an indication of the uncertainty in the calculated results with both codes. Results of the comparison were generally favorable as differences between the calculated results for the water plenum and tank bottom pressures were generally less than the values currently assumed in Savannah River's FLOWTRAN uncertainty studies.

DISCLAIMER

This report was prepared as an account of work sponsored by an agency of the United States Government. Neither the United States Government nor any agency thereof, nor any of their employees, makes any warranty, express or implied, or assumes any legal liability or responsibility for the accuracy, completeness, or usefulness of any information, apparatus, product, or process disclosed, or represents that its use would not infringe privately owned rights. Reference herein to any specific commercial product, process, or service by trade name, trademark, manufacturer, or otherwise does not necessarily constitute or imply its endorsement, recommendation, or favoring by the United States Government or any agency thereof. The views and opinions of authors expressed herein do not necessarily state or reflect those of the United States Government or any agency thereof.

SUMMARY

A calculation of a loss-of-coolant accident (LOCA) in K-Reactor at the Savannah River Site (SRS) was performed using the RELAP5 computer code. The results of the RELAP5 calculation were then compared with a TRAC calculation previously performed by Savannah River Laboratory. Both calculations represented the flow instability portion of a LOCA initiated by a double-ended guillotine break in the the inlet piping in K-Reactor. The RELAP5 and TRAC results were compared to illustrate and understand differences and similarities between calculations performed with independent computer codes and input models. The variation between the RELAP5 and TRAC calculations provided an indication of the uncertainty in the calculated results with both codes.

A RELAP5 model of K-Reactor was developed to perform the LOCA calculations described in this report. The model was based on a six-loop, three-dimensional RELAP5 model of the L-Reactor although modifications were made to represent K-Reactor. Specifically, the modifications included changing the model of the core to represent the Mark 22 assemblies present in the K-14.1 charge and representing the K-Reactor top shield.

The RELAP5 and TRAC LOCA calculations were in remarkably good agreement. The overall hydraulic response of the process system was similar with both codes. The flow out both sides of the double-ended break generally agreed to within 2%. The total flow through the core generally agreed to within 1.3%.

The RELAP5 and TRAC calculations of the boundary conditions needed for detailed calculations of assembly response were also in good agreement. Specifically, the calculated water plenum pressures in the sector attached to the broken loop were generally within 1 psi. The deviations between the RELAP5 and TRAC results were slightly larger in the sectors attached to unbroken loops, but were generally within 2 psi. The deviations between the differential pressures across the assemblies were also generally less than 1.1 psi in the broken sector and 2.0 psi in the unbroken sectors.

Deviations between calculated gas plenum and tank bottom pressures were generally less than 0.7 and 0.5 psi, respectively. Thus, the deviations between the RELAP5 and TRAC results were generally less than the uncertainty values currently used by Savannah River in determining flow instability power limits.

The analysis of the results indicated that the blanket gas system significantly affects the response of the gas plenum pressure during the flow instability portion of a LOCA. The gas plenum pressure directly affects tank bottom pressure. Consequently, RELAP5 calculations were performed to investigate the sensitivity of the results to the modeling of the blanket gas system. Specifically, sensitivity calculations were used to determine the effects of blanket gas system nodalization and the composition of the blanket gas.

In both the RELAP5 and TRAC models, the blanket gas system was modeled as a simple pipe of the appropriate volume that was connected to the gas plenum. Sensitivity calculations with one, five, and ten control volumes in the pipe showed that converged results were obtained with five control volumes. However, the RELAP5 and TRAC models of the blanket gas system are relatively simple representations of the actual system. The simple models may not adequately represent the hydraulic response of the blanket gas system during the first few seconds of the LOCA because of their simple representation of the hydraulic resistance and because the actual flow circuit, with contains active components such as gas blowers, is not simulated. The uncertainty in the RELAP5 and TRAC results caused by the use of simple models of the blanket gas system was not evaluated in this study.

A sensitivity calculation was also performed to determine the effect of the blanket gas composition. The blanket gas was assumed to be air in the RELAP5 and TRAC calculations described previously although helium is actually used in the plant. RELAP5 calculated gas plenum and tank bottom pressures that were as much as 1.0 psi higher with helium than with air because helium's lower density resulted in more volumetric flow from the blanket gas system into the gas plenum.

A review of the RELAP5 and TRAC results indicated that both codes calculated nearly isothermal expansions of the blanket gas. Although the actual expansion characteristics of the blanket gas during a LOCA are not known, the assumption that the gas expands isentropically will yield a lower pressure than assuming an isothermal expansion. Bounding hand calculations indicated that the maximum difference between an isentropic expansion and the expansion calculated by RELAP5 was about 1.4 psi for air and 2.4 psi for helium. The bounding hand calculations also indicated that the net effect of assuming an isentropic expansion of helium versus the RELAP5 calculation of a nearly isothermal expansion of air was to lower the gas plenum pressure by 1.4 psi.

In summary, the RELAP5 and TRAC LOCA calculations were generally in excellent agreement, providing improved confidence in the results obtained with both codes. The analysis of the results indicates some uncertainty due to the expansion characteristics of the blanket gas. Accounting for the uncertainty in the expansion characteristics and the differences between air and helium, the maximum bias in the TRAC calculation of gas plenum pressure was estimated to be 1.4 psi. However, this estimate does not include any contribution to uncertainty resulting from the simple model of the blanket gas system.

ACKNOWLEDGMENTS

The author thanks R. Shaw, J. Cozzuol, and S. Rodriguez for their support in the development of the RELAP5 model used in this analysis; C. McKenzie, E. Jenkins, and N. Larson for their support in preparing the report graphics; and R. Hanson and P. Wheatley for their review and assistance. E. Schaub of Savannah River Laboratory performed the TRAC calculations described in this report and contributed significantly in the analysis of the results.

CONTENTS

ABSTRACT ii

SUMMARY iii

ACKNOWLEDGMENTS vi

1. INTRODUCTION 1

2. CODE AND MODEL DESCRIPTION 3

   2.1 Code Description 3
   2.2 Model Description 4

3. RESULTS 11

   3.1 Steady-State Results 11
   3.2 LOCA Results 13
   3.3 Sensitivity Calculations 17

4. CONCLUSIONS 22

5. REFERENCES 24

APPENDIX A--DETAILED COMPARISON OF THE RELAP5 AND TRAC RESULTS 52

APPENDIX B--GAS EXPANSION HAND CALCULATIONS 72

FIGURES

1. Nodalization of the six-loop model of K-Reactor 26

2. Nodalization of loop 1 27

3. Schematic of the three-dimensional vessel model and fuel ..... assemblies 28

4. Nodalization of the two-dimensional plenum model 29

5. Nodalization of the three-dimensional tank model 30

6. Cutaway view of the vessel model 31

7. Nodalization of a typical lumped assembly and the hot assembly 32

8. Nodalization of the gas plenum, top shield, reactor vent paths, ... and blanket gas system 33

9. Nodalization of the septifoil system 34

10. Nodalization of the ECS 35

11. A comparison of calculated flows out the heat exchanger side ..... of the break 36

12. A comparison of calculated flows out the plenum side ..... of the break 37

13. A comparison of total calculated flow through the assemblies 38

14. A comparison of calculated pressures in the gas plenum 39

15. A comparison of calculated pressures in ring 2 sector 5 ..... of the water plenum 40

16. A comparison of calculated pressures in ring 2 sector 5 ..... at the tank bottom 41

17. A comparison of calculated differential pressures across ..... the assemblies in ring 2 sector 5 42

18. A comparison of calculated pressures in ring 2 sector 2 ..... of the water plenum 43

19. A comparison of calculated pressures in ring 2 sector 2 ..... at the tank bottom 44

20. A comparison of calculated differential pressures across ..... the assemblies in ring 2 sector 2 45

21. The effect of blanket gas nodalization on gas plenum pressure 46

22. The effect of blanket gas nodalization on blanket gas flow 47

23. The effect of blanket gas composition on gas plenum pressure 48

24. The effect of blanket gas composition on blanket gas flow 49

A-1. A comparison of calculated pressures in ring 1 sector 1 ..... of the water plenum 54

A-2. A comparison of calculated pressures in ring 1 sector 1 ..... at the tank bottom 54

A-3. A comparison of calculated differential pressures across ..... the assemblies in ring 1 sector 1 54

A-4. A comparison of calculated pressures in ring 1 sector 2 ..... of the water plenum 55

A-5. A comparison of calculated pressures in ring 1 sector 2 ..... at the tank bottom 55

A-6. A comparison of calculated differential pressures across ..... the assemblies in ring 1 sector 2 55

A-7. A comparison of calculated pressures in ring 1 sector 3 ..... of the water plenum 56

A-8. A comparison of calculated pressures in ring 1 sector 3 ..... at the tank bottom 56

A-9. A comparison of calculated differential pressures across ..... the assemblies in ring 1 sector 3 56

A-10. A comparison of calculated pressures in ring 1 sector 4 ..... of the water plenum 57

A-11. A comparison of calculated pressures in ring 1 sector 4 ..... at the tank bottom 57

A-12. A comparison of calculated differential pressures across ..... the assemblies in ring 1 sector 4 57

A-13. A comparison of calculated pressures in ring 1 sector 5 ..... of the water plenum 58

A-14. A comparison of calculated pressures in ring 1 sector 5 ..... at the tank bottom 58

A-15. A comparison of calculated differential pressures across ..... the assemblies in ring 1 sector 5 58

A-16. A comparison of calculated pressures in ring 1 sector 6 ..... of the water plenum 59

A-17. A comparison of calculated pressures in ring 1 sector 6 ..... at the tank bottom 59

A-18. A comparison of calculated differential pressures across ..... the assemblies in ring 1 sector 6 59

A-19. A comparison of calculated pressures in ring 2 sector 1 ..... of the water plenum 60

A-20. A comparison of calculated pressures in ring 2 sector 1 ..... at the tank bottom 60

A-21. A comparison of calculated differential pressures across ..... the assemblies in ring 2 sector 1 60

A-22. A comparison of calculated pressures in ring 2 sector 2 ..... of the water plenum 61

A-23. A comparison of calculated pressures in ring 2 sector 2 ..... at the tank bottom 61

A-24. A comparison of calculated differential pressures across ..... the assemblies in ring 2 sector 2 61

A-25. A comparison of calculated pressures in ring 2 sector 3 ..... of the water plenum 62

A-26. A comparison of calculated pressures in ring 2 sector 3 ..... at the tank bottom 62

A-27. A comparison of calculated differential pressures across ..... the assemblies in ring 2 sector 3 62

A-28. A comparison of calculated pressures in ring 2 sector 4 ..... of the water plenum 63

A-29. A comparison of calculated pressures in ring 2 sector 4 ..... at the tank bottom 63

A-30. A comparison of calculated differential pressures across ..... the assemblies in ring 2 sector 4 63

A-31. A comparison of calculated pressures in ring 2 sector 5 ..... of the water plenum 64

A-32. A comparison of calculated pressures in ring 2 sector 5 ..... at the tank bottom 64

A-33. A comparison of calculated differential pressures across ..... the assemblies in ring 2 sector 5 64

A-34. A comparison of calculated pressures in ring 2 sector 6 ..... of the water plenum 65

A-35. A comparison of calculated pressures in ring 2 sector 6 ..... at the tank bottom 65

A-36. A comparison of calculated differential pressures across ..... the assemblies in ring 2 sector 6 65

A-37. A comparison of calculated pressures in ring 3 sector 1 ..... of the water plenum 66

A-38. A comparison of calculated pressures in ring 3 sector 1 ..... at the tank bottom 66

A-39. A comparison of calculated differential pressures across ..... the assemblies in ring 3 sector 1 66

A-40. A comparison of calculated pressures in ring 3 sector 2 ..... of the water plenum 67

A-41. A comparison of calculated pressures in ring 3 sector 2 ..... at the tank bottom 67

A-42. A comparison of calculated differential pressures across ..... the assemblies in ring 3 sector 2 67

A-43. A comparison of calculated pressures in ring 3 sector 3 of the water plenum 68

A-44. A comparison of calculated pressures in ring 3 sector 3 at the tank bottom 68

A-45. A comparison of calculated differential pressures across the assemblies in ring 3 sector 3 68

A-46. A comparison of calculated pressures in ring 3 sector 4 of the water plenum 69

A-47. A comparison of calculated pressures in ring 3 sector 4 at the tank bottom 69

A-48. A comparison of calculated differential pressures across the assemblies in ring 3 sector 4 69

A-49. A comparison of calculated pressures in ring 3 sector 5 of the water plenum 70

A-50. A comparison of calculated pressures in ring 3 sector 5 at the tank bottom 70

A-51. A comparison of calculated differential pressures across the assemblies in ring 3 sector 5 70

A-52. A comparison of calculated pressures in ring 3 sector 6 of the water plenum 71

A-53. A comparison of calculated pressures in ring 3 sector 6 at the tank bottom 71

A-54. A comparison of calculated differential pressures across the assemblies in ring 3 sector 6 71

B-1. Illustration of the gas expansion process 76

TABLES

1. Calculated and measured process initial conditions 50

2. Calculated and measured initial conditions for the secondary side of the heat exchangers 51

A COMPARISON OF RELAP5 AND TRAC LOCA CALCULATIONS FOR THE K-14.1 CHARGE AT SRS

1. INTRODUCTION

The possibility of the occurrence of a flow instability during a loss-of-coolant accident (LOCA) at the reactors at the Savannah River Site (SRS) is currently the subject of many analyses. Savannah River Laboratory (SRL) currently sets assembly power and effluent temperature limits[1] to prevent any assembly from experiencing flow instability during a LOCA. SRL uses a suite of computer codes to calculate reactor response during a LOCA. TRAC-PF1/MOD1[2] and FLOWTRAN[3] are the primary computer codes used to calculate the thermal-hydraulic response of the reactors. TRAC is used to calculate system thermal-hydraulic response and to provide assembly boundary conditions. In particular, TRAC provides water plenum and tank bottom pressures. Assembly response is then calculated with FLOWTRAN. The uncertainty in the boundary conditions supplied by TRAC has been estimated and the uncertainty propagated through the FLOWTRAN calculations to obtain a conservative power limit.

The TRAC computer code was developed to calculate LOCAs in commercial pressurized water reactors (PWRs). The code has undergone extensive assessment[4] with both separate-effects and integral data to demonstrate its applicability for representing LOCAs in PWRs. The uncertainty in the code for calculating a LOCA initiated by a large cold leg break in a PWR has also been estimated through the Code Scaling and Uncertainty (CSAU) method.[5]

TRAC's applicability for representing a LOCA in the reactors at the SRS has not been demonstrated as conclusively as for PWRs, partly because applicable, integral LOCA experiments have not been performed. Furthermore, the lack of integral experimental LOCA data makes the determination of uncertainty in the TRAC results difficult. The uncertainty in the TRAC system calculations will ultimately be addressed through the CSAU method.[6]

A quicker method of checking the estimated uncertainty in the TRAC calculations is to compare TRAC results with those from an independent computer code. SRL requested that the Idaho National Engineering Laboratory (INEL) perform independent system thermal-hydraulic calculations using the RELAP5[7] computer code. Specifically, SRL requested that INEL perform a calculation of the flow instability portion of a LOCA that was initiated by a double-ended guillotine break in an inlet line to the water plenum. A corresponding TRAC calculation was performed by Schaub[8] for the K-14.1 charge in K-Reactor.

To satisfy SRL's request, a new RELAP5 model of K-Reactor was developed. INEL previously developed[9] a one-dimensional, two-loop model of the L-Reactor at SRS. However, the one-dimensional model did not provide sufficient detail within the water plenum to independently check the pressure gradients as calculated by TRAC. Consequently, the INEL developed a six-loop, three-dimensional RELAP5 model of the L-Reactor.[10] Minor modifications to the three-dimensional L-Reactor model allowed it to represent K-Reactor. The three-dimensional RELAP5 model of K-Reactor allowed reasonable comparisons to be made with the results of SRL's TRAC model.

The three-dimensional RELAP5 model of K-Reactor was then used to perform a LOCA calculation. The remainder of this report describes the RELAP5 code and the three-dimensional model of K-Reactor (Section 2), and the comparison between the TRAC and RELAP5 calculations (Section 3). Conclusions and references are presented in Sections 4 and 5, respectively.

2. CODE AND MODEL DESCRIPTION

A brief description of the RELAP5 code and the three-dimensional thermal-hydraulic input model of K-Reactor are provided in Sections 2.1 and 2.2, respectively.

2.1 Code Description

The RELAP5/MOD3 computer code (see Reference 7) is being developed at the INEL with the support of the United States Nuclear Regulatory Commission. The code provides advanced, thermal-hydraulic, system analysis capability. RELAP5/MOD3 is based on the RELAP5/MOD2[11] code, which has been used extensively around the world. The code version used in this analysis was RELAP5/MOD2.5 version 392, a preliminary version of RELAP5/MOD3.

RELAP5 is an advanced, one-dimensional, fast-running, user-convenient systems analysis computer code. The code is based on a nonhomogeneous, nonequilibrium two-phase fluid model that utilizes a six-equation formulation for the conservation of mass, energy, and momentum. In addition to the basic hydrodynamic model, the code has special process models to represent phenomena associated with abrupt flow area changes, choked flow, horizontally and vertically stratified flow, boron tracking, noncondensible gas (up to five can be specified), and crossflow (flow perpendicular to the main flow path). The development of the crossflow model allows a multidimensional flow analysis capability in regions where multidimensional fluid momentum is not significant. RELAP5 can also represent core neutronics and plant control systems.

RELAP5/MOD3 and its predecessor RELAP5/MOD2 have been used for many different applications. These applications include thermal-hydraulic analysis of commercial light water reactors, including pressurized and boiling water reactors, advanced light water reactor concepts, production reactors, and various experimental facilities. The code has also been used to model Department of Energy reactors in addition to those at Savannah

River, including N-Reactor[12] and the Advanced Test Reactor.[13] The code has benefited from extensive application and comparison with experimental data by many different organizations throughout the world. Recent assessments of RELAP5/MOD2, which are generally applicable to RELAP5/MOD2.5, are described in References 14 and 15.

2.2 Model Description

A six-loop, three-dimensional RELAP5 model was developed at the INEL to represent the SRS L-Reactor as described in Reference 10. However, because the external loops in L-Reactor and K-Reactor are nearly identical, K-reactor was simulated with only minor modifications. The three-dimensional RELAP5 model is illustrated in Figure 1 and explicitly represents the six loops present in the plant. The nodalization of the model was generally based on the nodalization of the one-dimensional, two-loop model described in Reference 9.

Figure 2 documents in detail the nodalization used in loop 1. The nodalization was identical in the other five loops except for component numbers, which can be obtained by adding a multiple of 50 to the values shown in Figure 2. Component numbers thus range from 100 to 147 for loop 1, 150 to 197 for loop 2, 200 to 247 for loop 3, etc. The loop nodalization in the three-dimensional model was identical to that used in the two-loop model except that the plenum inlet nozzle (component 147) was explicitly represented.

The variations between individual loops were explicitly represented in the three-dimensional model. (In contrast, the loops were "averaged" in the two-loop model.) Identical loss coefficients were used in all six loops except for variations caused by bends that were not present in all loops. Each modeled loop represented the Bingham pump, heat exchangers, isolation valve, rotovalves, and connecting piping. Each loop in the plant contains two parallel heat exchangers, rotovalves, and connecting piping. The two parallel flow paths were lumped together into a single flow path in the model.

The reactor tank was modeled in a three-dimensional manner with the crossflow model, which allows a limited multidimensional flow analysis capability. The crossflow model uses a simplified momentum equation to represent flow perpendicular to the main flow path. The crossflow model neglects the momentum flux or spacial acceleration terms but accounts for temporal acceleration and friction terms.

A three-dimensional noding scheme was employed using the crossflow model as shown schematically in Figure 3. The moderator tank and water plenum were modeled with six azimuthal sectors and three radial rings. The primary flow direction was oriented vertically. The crossflow model was used at the radial and azimuthal junctions. Each crossflow junction was connected to the midplane of the adjacent volumes. Thirteen fuel assemblies (12 lumped and one hot) connected the plenum and the bottom of the moderator tank. The fuel assemblies were modeled as one-dimensional components. Crossflow junctions were used to connect the top of the fuel assemblies with the midplane of the water plenum volumes.

The nodalization of the water plenum and the moderator tank are illustrated in Figures 4 and 5. The six azimuthal sectors correspond to the six external loops. Sector 1, which contains plenum components 811, 821, and 831, is connected to loop 1 while sector 2, which contains components 812, 822, and 832, is connected to loop 2. The other loops and sectors are connected similarly. The inner, middle, and outer radial rings are referred to as rings 1, 2, and 3, respectively. The three rings were based on SRL's five-ring TRAC model.[16] Ring 1 in the RELAP5 model represents the inner two rings in the TRAC model. Similarly, ring 2 in the RELAP5 model represents rings 3 and 4 in the TRAC model. Ring 3 in the RELAP5 model corresponds to ring 5 in the TRAC model. A simplified radial nodalization was originally used because of computer memory limitations in RELAP5/MOD2 and the INEL Cyber 176. Significantly more computer memory is available with RELAP5/MOD2.5 and the Cray X-MP/24, and a five ring model could be supported if desired. The comparisons between RELAP5 and TRAC results presented later indicate that the three ring model appears to give adequate results.

The axial divisions in the vessel, illustrated in Figure 6, were based on the two-loop model. Specifically, the water plenum was modeled with a single level. The moderator tank below the top shield was represented with three levels. The height (65 in.) of the lowest level in the moderator tank was set to obtain AC pump aspiration at the correct moderator level based on the two-loop benchmark comparisons.[17]

The radial and azimuthal form loss coefficients in the water plenum and moderator tank were originally calculated from Idel'chik[18] based on flow across a tube bundle. The loss coefficients in the plenum were then adjusted to match data from the 1985 AC Process Flow Tests (see Reference 16). Specifically, the radial loss coefficients were adjusted to match data from Test I while the azimuthal loss coefficients were adjusted to match Test D. The azimuthal loss coefficients were adjusted by multiplying by a constant, while different multipliers were used to adjust the radial loss coefficients at the outer radii of rings 1 and 2. The magnitudes of the adjustments were relatively small, less than a factor of two.

A lumped, average fuel assembly model was attached to each cell in the inner two rings in both the water plenum and the tank bottom. No fuel assemblies were attached to the outer ring in the model because the region contained no active fuel assemblies in the reactor. Each lumped fuel assembly model represented an average Mark 22 assembly and accounted for the effects of different flow zones. The lumping process of the fuel assemblies was accomplished in four steps. First, a separate-effects RELAP5 model of an individual assembly from each of the five flow zones present in the K-14.1 charge (see Reference 8) was developed. The five individual assemblies were then driven with nominal tank bottom pressures and flow rates. Second, loss coefficients and/or surface roughness were adjusted until the total assembly pressure drop and the distribution of pressure drop within the assembly was consistent with the correlations presented by Koffman[19] for each flow zone. Note that only loss coefficients were adjusted in the unheated regions of the assembly and that only surface roughness was adjusted in the heated region. The adjusted loss coefficients and the surface roughness were generally close to the expected values. Third, the number, flow zone, and power of the Mark 22 assemblies contained

in each control volume in the vessel were then obtained using data from References 8 and 16. Finally, the individual assembly models were then lumped into an average assembly in such a manner as to preserve the flow versus pressure response.

In addition to the average assembly, a single "hot" channel was attached to sector 5 of ring 1, in anticipation of a LOCA initiated by a break in loop 5. The hot channel represented the 4-in. position at on-line computer (OLC) number 344, which contained a Mark 22 assembly belonging to flow zone 3. OLC position 344 was selected because it was the highest-powered assembly residing in sector 5 in the data presented in Reference 8.

Lumped fuel assembly component numbers were based on the component numbers of the control volumes in the water plenum and moderator tank to which they were connected. For example, assembly component 11 connected water plenum component 811 and moderator tank component 711. Figure 7 shows the nodalization used to represent a typical lumped assembly (component 15) and the hot assembly (component 17). The lumped and hot assemblies were all modeled axially with seven control volumes: five representing the heated length and one representing the inlet and endfitting regions. The primary, annular flow paths within the heated length were modeled with a single, lumped flow path. The minor flow paths through the purge channels were neglected. In the lumped assembly models, the fuel and target annuli were lumped into an equivalent, double-sided heat structure for heat transfer purposes. In the hot assembly, each fuel and target annulus was modeled with a separate heat structure. The universal sleeve housing was also modeled with a separate heat structure that thermally connected the assembly and the moderator tank.

The gas plenum was modeled in a one-dimensional manner, with three vertically oriented control volumes, because significant pressure variations were not expected there. Thus, the model of this region (see Figure 8) was identical to that used previously with the two-loop model. Flow paths through the top shield were generally based on King's[20] description of the region. The 1/4-in. annular gap between the top shield and the reactor tank top shell and the annular gaps between the 1 in. permanent sleeves and the

housings inside the permanent sleeves were combined into a single flow path (component 797). This flow path connected the bottom of the gas plenum and the top of the moderator space.

The model of the top shield flow path through the 4-in. positions was modified to represent K-Reactor geometry as described in Reference 8. The bearing and nonbearing 4-in. tubes were modeled separately to account for the 1-in. diameter hole located in the bearing tubes near the bottom of the gas plenum. The 594 nonbearing tubes, including 519 annuli and 75 vacant tubes, were combined into a single flow path (component 799) that connected the center of the gas plenum with the top of the moderator space. The 73 bearing tubes, including 61 annuli and 12 vacant tubes, were combined into a single flow path (components 801 and 802) that also connected the center of the gas plenum with the top of the moderator space. The connections between the one-dimensional gas plenum and the three-dimensional moderator tank were selected somewhat arbitrarily. Components 799 and 801, the 4-in. flow paths, were connected to the moderator tank at ring 1 sector 5 and ring 2 sector 2, respectively. Component 797, the flow path through the 1/4-in. annular gap was connected to the moderator tank at ring 3 sector 1. The connection of the one-dimensional gas plenum to the three-dimensional moderator tank can cause some artificial asymmetry in the flow to the moderator tank. To date, this artificial asymmetry has not caused any significant problems.

The model also contained a detailed description of the reactor vent paths as shown in Figure 8. These vent paths include the gas ports, vacuum breakers, and U-tube (also called the supplementary pressure relief system or downcomer). Three gas ports were lumped into one flow path in the model. Similarly, the two vacuum breakers were lumped into one flow path. The blanket gas system, which controls gas plenum pressure during normal operation, was also modeled.

The models of the reactor vent paths and blanket gas system were generally identical to the corresponding models in the two-loop model as described in Reference 9. However, some improvements were made in the representation of the vacuum breaker and the blanket gas system as a result of preliminary comparisons between RELAP5 and TRAC LOCA calculations that

were performed as part of this study. Specifically, two changes were made to the model of the blanket gas system. First, the blanket gas system was modeled with five volumes rather than one because sensitivity calculations indicated that the calculated results were not adequately converged when the region was modeled with a single volume. Second, the connection between the blanket gas system and the gas plenum was changed from component 800 to component 810. The change in the junction connection resulted in a more realistic acceleration of the flow from the blanket gas system to the gas plenum during the first few seconds of a LOCA because component 800 contained liquid at the start of the transient which resulted in a larger "average" density at the junction and thus a slower acceleration of the fluid.

Improvements to the RELAP5 model of the vacuum breaker were also made as a result of the comparisons with TRAC. As described in Reference 9, the area at the exit of the vacuum breaker standpipes in the RELAP5 model was adjusted to match the hydraulic resistance reported in the SARIS manual.[21] The net result of this adjustment was that the majority of the hydraulic resistance was placed at the exit (top) of the vacuum breakers in the RELAP5 model. In contrast, most of the resistance was placed at the inlet to the vacuum breaker in the TRAC model.[22] A review of the vacuum breaker geometry indicated that there are substantial losses near the inlet of the vacuum breaker caused by the lifting lug hood and the bends in the flow path near the vacuum breaker pot. As a result, more mechanistic loss coefficients were calculated throughout the vacuum breakers. The total resistance in the RELAP5 model was then adjusted to match the experimentally derived value described in Reference 22, with the total resistance divided nearly equally between the inlet and outlet junctions of the vacuum breaker. The improvements to the models of the vacuum breakers and the blanket gas system described above should be incorporated into all RELAP5 models of SRS reactors, including the two-loop model.

The piping connecting the outlet of the heat exchangers with the septifoils in the moderator tank was modeled as illustrated in Figure 9. The ring header was divided into two control volumes, with two corresponding, distinct septifoils extending up into the moderator tank. Each of the two septifoils in the model was connected to three sectors in

the inner ring to provide uniform azimuthal cooling. The radial distribution of the septifoils that occurs in the plant was neglected in the model for simplicity. Loss coefficients in the model were adjusted to yield about 6200 gpm total septifoil flow at nominal operating conditions with a Mark 16B-31A charge.

Although not utilized in the K-14.1 LOCA calculations, a detailed model of the ECS was illustrated as shown in Figure 10. Details of this model are presented in Reference 9.

The model was generally based on a mechanistic, "first-principle" representation of the actual geometry. Form loss coefficients were also based on "first-principle" estimates that included the effects of area changes, bends, etc. However, because of complicated geometries, some loss coefficients could not be readily estimated and were adjusted based on comparisons with data. These complicated geometries included the muffs at the outlet of the reactor tank, water plenum inlet nozzles, fuel assemblies, vacuum breakers, and septifoil system.

The RELAP5 control system was used to model the macroscopic effects of elbow and pump cavitation in each of the six external loops. Details of the cavitation models are presented in Reference 23.

Components not discussed in detail above were generally modeled the same as with the two-loop model described in Reference 9.

The three-dimensional model is currently undergoing a quality assurance review. As a consequence, the model used in the LOCA calculations described in Section 3 was not formally quality assured. Based on the quality assurance completed to date, the results obtained with a quality-assured version of the model are not likely to vary materially from the results shown in Section 3.

3.0 RESULTS

The RELAP5 model described in Section 2.2 was used to analyze a LOCA for the K-14.1 charge. This section documents the results of the analysis. Section 3.1 provides a comparison of the steady-state results as calculated by RELAP5 with the corresponding TRAC results described in Reference 8. Section 3.2 compares results of the two calculations during the LOCA. Results of sensitivity calculations performed with the RELAP5 model are described in Section 3.3.

3.1 Steady-State Results

Plant parameters were measured in K-Reactor during the K-13.2 charge as described in Reference 8. Since the K-13.2 and K-14.1 charges are hydraulically equivalent, the K-14.1 steady state was based on the measured K-13.2 conditions. Tables 1 and 2 show the K-14.1 steady state as calculated by RELAP5 and TRAC as well as the available measured values from the K-13.2 charge. The calculated results from both codes were generally in excellent agreement with each other and the data. As shown in Table 1, the core power was 1326 MW in both calculations and 1326.5 MW in the data. Since the purpose of the task was to compare the results of the RELAP5 and TRAC LOCA calculations, the RELAP5 core power was adjusted to make the RELAP5 results consistent with the TRAC results rather than an exact match with the data. Similarly, the heat exchanger cooling water temperature (see Table 2) was adjusted in RELAP5 so that the average process temperature was about the same with both codes. As a result of the slight adjustment in cooling water temperatures, the average pump suction and plenum inlet temperatures were in excellent agreement in the two calculations. The differences in calculated temperatures were generally less than $1^{o}C$ and within the expected uncertainty in the data. The calculated process temperatures were about $3^{o}C$ higher than the measured values, partly because the input cooling water temperature was higher (originally due to a minor error in the TRAC calculation) and partly because the modeled heat exchangers were apparently not quite as efficient as the actual components.

Calculated pump flows were also in good agreement between the two codes as illustrated in Table 1. (Note that the corresponding measured values were not available for comparison.) The total flow through the pumps was about 1.3% higher in the RELAP5 calculation. This small difference between total loop flows can be traced to the benchmark comparisons with 1985 AC Process Flow Test I (see References 10 and 16) where RELAP5 and the data were about 1.6% higher than the TRAC calculated flow. The comparison between calculated and measured average loop temperature rise also indicates that the TRAC calculated flow might be slightly lower than the actual flow. Even though the total RELAP5 calculated loop flow appears to agree slightly better with the data than TRAC, the difference is probably insignificant considering the uncertainty in the data.

The calculated septifoil flow was about 10% higher in the TRAC calculation than in the RELAP5 calculation. The different septifoil flow can also be attributed to the benchmarking with both models. The RELAP5 and TRAC septifoil models were adjusted to provide 6200 and 6800 gpm, respectively, for AC Test I. The measured septifoil flow for Test I was not reported but both calculated flows are within the range of generally quoted septifoil flows. The 10% difference in septifoil flows should not significantly affect system response during a LOCA.

Calculated and measured water plenum pressures are also shown in Table 1. Note that the measured and calculated pressures correspond to different plenum radii; the measurement represents the pressure at a radius of zero while the calculated values represent cell-centered pressures in ring 1. The calculated cell-centered pressures are reasonably comparable to the measured centerline pressure because test data (see Reference 16) show that the plenum pressure profile is relatively flat near the center of the plenum. The measured plenum centerline pressure was between the calculated values and within 2 psi of both. The maximum deviation between calculated plenum pressures was about 5 psi at steady state. The differences between the measured plenum centerline pressure and the two calculated values could be caused by minor differences in loop flow. For example, a 1.2% reduction in total core flow, which is consistent with the reduction that would occur if the sparjets were modeled explicitly, would bring the RELAP5 calculated centerline pressure into agreement with the measured value. Thus, the

differences between calculated and measured plenum pressures do not appear significant considering the uncertainty in the loop flows.

Table 2 compares calculated and measured heat exchanger initial conditions. The deviation between measured inlet temperature and the input temperature in the calculation was discussed previously. The inlet flow rates in the calculations were about 10% lower than the measured value to account for the density difference between light water, used as the secondary fluid in the plant, and heavy water, used in the calculations. Reducing the flow rate in the calculations to account for fluid property differences between light and heavy water results in an accurate calculation of temperature rise across the heat exchangers with both codes. However, fluid property differences result in about a 9% reduction in secondary-side heat transfer coefficient when light water is replaced with heavy water. The reduction in heat transfer coefficient associated with using heavy water was partially responsible for the less than actual efficiency of the model heat exchangers mentioned previously. RELAP5 has the capability to simultaneously use light water and heavy water on the secondary and process sides of the heat exchanger, but this feature was not utilized in the K-14.1 calculation to be consistent with TRAC.

3.2 LOCA Results

The analyzed LOCA was initiated by a double-ended guillotine break in the plenum inlet piping. The break was assumed to occur at the flange between the piping and the plenum inlet nozzle in loop 5. The LOCA was assumed to occur at 0 s. The RELAP5 calculation was run beyond the potential period of flow instability and was terminated at 5 s.

The break flows calculated with RELAP5 were in excellent agreement with the results calculated by TRAC. The flows through the heat exchanger side of the break are shown in Figure 11. The difference in calculated flows during the transient was generally less than 2% of the total, and in fact, was less than the difference at steady state. The agreement in the minor flow oscillations caused by pressure waves between 0.0 and 0.5 s was considered quite remarkable. One slight difference between calculations was that elbow cavitation (see Reference 23) was obtained in the broken loop

between 1.5 and 2.5 s with the RELAP5 model, resulting in a slight decrease in flow. The TRAC model did not represent cavitation. However, the similarity of the RELAP5 and TRAC results indicates that cavitation did not significantly affect the hydraulic response of the broken loop.

Figure 12 compares flows through the plenum side of the break. After 0.5 s, the difference in calculated flows was generally less than 2% of the total. Note that the apparent large difference between the calculated results at 0.0 s is an artifact of the post-processing of the TRAC results and does not reflect an actual difference between calculations. The RELAP5 volumetric flow was obtained by summing the phasic volumetric flows. The gas volumetric flow was calculated as junction gas velocity times junction void fraction times junction area; the liquid flow was calculated similarly. The TRAC volumetric flow was obtained by dividing the break mass flow rate by the density in the nozzle cell adjacent to the break. In both calculations, air was initially flowing into the plenum nozzle at a rate in excess of 24,000 gpm. However, because the fluid in the first nozzle cell was initially liquid in the TRAC calculation, the volumetric flow appeared zero at the start of the LOCA but, in fact, was not.

The total flow into the assemblies was also in excellent agreement as illustrated in Figure 13. The calculated flow rates displayed nearly identical trends. The total assembly flow decreased sharply in response to the break, reached a minimum value between 0.2 and 0.4 s, and then recovered slightly. The maximum difference between the two calculations was less than 5% of the total flow. During the time period when the limits would be set, between 1 and 2 s, the difference between calculations was less than 1.3%. The good agreement between the two flow rates indicates that cavitation, which was represented in a best-estimate fashion in the RELAP5 model but not in the TRAC model, was insignificant for this transient. A review of the RELAP5 results indicated that cavitation was not predicted to occur in any of the intact loops.

The gas plenum pressures from the RELAP5 and TRAC calculations are compared in Figure 14. The gas plenum was represented in a one-dimensional manner in the RELAP5 model and in a three-dimensional manner in the TRAC model. However, the variation between cells in the TRAC model was not

significant, and Figure 14 presents typical results (from cell 1). The qualitative trends of the two calculations were similar. In both calculations, the pressure decreased as the blanket gas expanded in response to the break. The gas ports cleared at about 1 s in both calculations but the flow of air was insufficient to make up for the break flow, and the pressure continued to decrease until the vacuum breakers cleared at about 2 s. The vacuum breakers allowed enough air into the gas plenum to make up for the flow out the break and to relieve the vacuum than had been drawn in the gas plenum. Gas plenum pressure recovered nearly to atmospheric pressure by 3 s in both calculations. The calculated gas plenum pressures were also in good quantitative agreement. The calculated pressures were within 0.7 psi during the time period when limits would be set (between 1 and 2 s). The maximum difference between calculations was 1.5 psi, occurred after the vacuum breakers cleared, and thus should not affect limits.

One of the primary reasons for comparing the RELAP5 and TRAC calculations was to determine similarities and differences in the key boundary conditions required by FLOWTRAN: water plenum and tank bottom pressures. Figures 15 and 16 compare calculated water plenum and tank bottom pressures in the break sector, where the most restrictive power limit is normally obtained. The RELAP5 results shown in the figures were taken from ring 2 while the TRAC results presented were obtained by averaging the ring 3 and 4 values. (Recall that ring 2 of the RELAP5 model corresponded exactly to rings 3 and 4 of the TRAC model.)

The calculated water plenum pressures (Figure 15) were generally in excellent agreement. Deviations between the two calculations were less than 1.0 psi during the time period when limits would be set. The pressure oscillations calculated by both codes before 0.5 s caused generally larger deviations than were observed after 0.5 s. However, the deviations before 0.5 s are not significant because the oscillations are generally smoothed prior to input into FLOWTRAN. The calculated tank bottom pressures (Figure 16) were also in excellent agreement. Deviations between the two calculations were less than 0.5 psi between 1 and 2 s. Once again, larger deviations were obtained before 0.5 s during the period of pressure oscillations.

Assembly differential pressures are compared in Figure 17. The assembly differential pressures were obtained by subtracting the tank bottom pressures shown in Figure 16 from the water plenum pressures shown in Figure 15 and adding 9.6 psi to account for the gravitational head. The resulting quantity represents the differential pressure that drives flow through the assembly. As expected based on the previous comparisons, the assembly differential pressures were also in excellent agreement. Deviations between the two calculations were less than 1.1 psi during the time period when limits would be set.

The comparisons of the multidimensional variation in vessel pressures are further illustrated in Figures 18 through 20 which show plenum pressure, tank bottom pressure, and assembly differential pressures for ring 2 sector 2 of the RELAP5 model. Since sector 2 is located opposite of the break sector, the results presented in Figures 15 through 20 bound the calculated pressure comparisons for the other sectors. The difference in calculated plenum pressures was generally within 2 psi. However, the actual difference in calculated plenum pressures would be larger except for the compensating effects caused by the RELAP5 steady-state pressure exceeding the TRAC pressure. Preliminary comparisons between RELAP5 and TRAC for a Mark 16B-31A charge (L-1.1) in which both codes had the same initial plenum pressures showed a 5 psi difference in sector 2 and a 1 psi difference in sector 5.

The comparison between calculated tank bottom pressures in sector 2 (Figure 19) is similar to that discussed previously for sector 5 (Figure 16) because the gradient in calculated tank bottom pressures was relatively small. Relatively good agreement was also obtained in the calculation of assembly differential pressures as shown in Figure 20. The deviation between the RELAP5 and TRAC calculations was generally less than 2 psi.

The results presented for sectors 2 and 5 generally bound the results for the other sectors. For completeness, Appendix A contains comparisons between RELAP5 and TRAC calculations of water plenum pressure, tank bottom pressure, and assembly differential pressure for each ring and sector in the RELAP5 model. The results are generally similar to those discussed previously. However, the difference between the calculated results for the

outer ring is larger than discussed previously (almost 10 psi). The difference between results can be traced to the benchmark comparisons discussed in References 15 and 16 in which the RELAP5 results were in better agreement with the data. However, the calculated difference in pressure in the outermost ring is of little practical significance since no Mark 22 assemblies are connected to this ring.

3.3 Sensitivity Calculations

The response of the gas plenum pressure was studied thoroughly during this analysis. Preliminary comparisons between the RELAP5 and TRAC calculations revealed more substantial differences in the gas plenum pressure than in other parameters. Calculations were performed to investigate the sensitivity of the gas pressure to the models of the blanket gas system and the vacuum breakers and the composition of the blanket gas. This section describes the results of these sensitivity calculations.

The gas plenum pressure was found to be sensitive to the nodalization of the blanket gas system. Figure 21 shows the calculated gas plenum pressure for cases with the blanket gas system modeled with one, five, and ten control volumes. In each case, the total volume of the blanket gas system was based on the volume of the 6-in. gas line and the drain and overflow tanks described in the SARIS manual (see Reference 21). The total volume of the blanket gas system was represented with a single control volume in previous RELAP5 models (References 10 and 23). With the five- and ten-node models, the drain and overflow tanks were represented with a single control volume and the 6-in. pipe was divided evenly into the remaining volumes.

Figure 21 shows that the calculated results were not converged when the blanket gas system was modeled with one control volume but were converged when five or more control volumes were used. The blanket gas nodalization affected gas plenum pressure by as much as 0.8 psi. The finer nodalization affected the clearing of the vacuum breakers and hence the time at which the minimum pressure occurred but did not affect the value of the minimum pressure. The effect of nodalization on gas plenum pressure was caused by the effect of the spacial pressure gradient on the temporal acceleration of

the blanket gas into the plenum as shown in Figure 22. Note that the RELAP5 and TRAC results presented in Section 3.2 were obtained with five-node and ten-node representations of the blanket gas system, respectively.

The gas plenum pressure was also found to be sensitive to the manner in which the blanket gas system was connected to the gas plenum. In previous RELAP5 models, the blanket gas was connected to the middle control volume in the gas plenum, which contained the liquid interface at steady state. In the RELAP5 model described in Section 2.2, the blanket gas was connected to the upper volume in the gas plenum. With the "old" connection, the acceleration of blanket gas into the gas plenum during the LOCA was slowed by the presence of liquid in the downstream volume which resulted in a larger average density at the junction. The "new" connection resulted in a more realistic acceleration of the gas flow into the gas plenum during the first few seconds of the LOCA. The change in junction connections resulted in an increase of about 1 psi in the minimum gas plenum pressure during the LOCA.

The sensitivity calculations described above show that the results were sensitive to the modeling of the blanket gas system. This system, which was modeled similarly with both RELAP5 and TRAC, was represented as a passive pipe, with one end connected to the gas plenum. The volume of the pipe was based on the values presented in the SARIS manual. In contrast with the simple model used with the codes, the blanket gas system in the plant is a relatively complicated, active system. During normal operation, about 100 standard cubic feet per minute of helium flows through the blanket gas system. Gas blowers draw helium from the gas plenum and force it through separators, catalytic recombiners, valves, preheaters and coolers that have been retired in place, and back to the gas plenum. The uncertainty in the RELAP5 and TRAC results caused by the use of simple models to represent the blanket gas system was not evaluated in this study.

The calculated gas plenum pressure was also sensitive to the modeling of the vacuum breakers. In previous RELAP5 models, the majority of the resistance was placed at the outlet of the vacuum breakers. When the resistance was more mechanistically distributed as described in Section 2.2, the timing of the clearing of the vacuum breakers was affected. As shown in

Figure 14, the vacuum breakers cleared at 2 s when the resistance was distributed mechanistically. In previous calculations, see Reference 23 for an example, the vacuum breakers cleared at about 1 s. The delayed clearing of the vacuum breakers resulted in lower minimum gas plenum pressures. Uncertainty in the magnitude and distribution of the vacuum breaker resistance has the potential to affect the overall uncertainty in the calculated results.

A calculation was also performed to investigate the sensitivity of the results to blanket gas composition. In the TRAC calculation and all the RELAP5 calculations described previously, the blanket gas was modeled as air. In the reactor, however, the blanket gas is helium. During a LOCA, air will flow into the process system after the gas ports and the vacuum breakers clear. TRAC currently cannot represent helium, and neither code can currently represent the mixing of helium and air. (The capability is expected shortly with RELAP5.) A RELAP5 calculation was performed using helium as the blanket gas and as the supply gas for the vacuum breakers and gas ports to determine the sensitivity of the results.

The effect of blanket gas composition on gas plenum pressure, as calculated by RELAP5, is shown in Figure 23. Calculated gas plenum pressures with helium were higher by as much as 1.0 psi than with air. The lower density of helium caused a more rapid acceleration of gas into the gas plenum (see Figure 24), resulting in more volumetric flow into the gas plenum. The additional volumetric flow into the gas plenum caused higher gas plenum pressures and consequently, higher tank bottom and water plenum pressures during the first 2 s of the LOCA.

Based on the results shown in Figure 24, it would appear that calculations performed with air should be conservative because air results in lower gas plenum and tank bottom pressures and thus a lower margin to onset of nucleate boiling, flow instability, and cavitation. However, the magnitude of the calculated difference between air and helium may not be correct because of a limitation in RELAP5. The effect of the different noncondensibles on gas plenum pressure should be manifested in two ways. First, there is the effect of noncondensible density on the acceleration of flow from the blanket gas system to the gas plenum. This effect can be

adequately simulated by the code. Second, the pressure of a noncondensible gas during expansion can depend of the ratio of specific heats (hereafter referred to as the isentropic coefficient). The isentropic coefficient for helium, about 1.66, exceeds that for air, about 1.40. Thus, for the same break flow and no inflow from the blanket gas system, an isentropic expansion of helium would result in a lower pressure than air. The effect of the different isentropic coefficients may not be adequately simulated because the code calculates a near isothermal expansion. (The code closely couples liquid and gas temperatures in control volumes containing significant amounts of liquid.) As described in Appendix B, a review of the calculated results with RELAP5 showed that the effective expansion coefficient of the gas in the gas plenum was about 1.1 with both air and helium.

Although the actual effective gas expansion coefficient during a LOCA is not known, it clearly should be between isothermal and isentropic. Based on the rapid nature of the gas expansion during a double-ended guillotine break, an isentropic expansion would normally be expected. However, the potential mixing of the gas with the liquid in the top shield and moderator tank regions during a LOCA would act to make the expansion more isothermal. Intuitively, it appears that the effective expansion coefficient of the gas should be closer to isentropic than isothermal. Certainly, an isentropic expansion results in lower pressures and thus less margin to the onset of nucleate boiling and cavitation. Since RELAP5 predicts a nearly isothermal expansion, the calculated gas plenum pressure, and thus tank bottom pressure, may be too large. TRAC also may calculate gas plenum and tank bottom pressures that are too large since it appears to calculate a nearly isothermal expansion.

As described in Appendix B, hand calculations were performed to estimate the maximum bias in the RELAP5 calculated results. The hand calculations assumed an isentropic gas expansion between 0.0 and 1.5 s. The time of 1.5 s was selected as the approximate time at which the flow instability limits would be set. According to the hand calculations, isentropic expansions resulted in gas plenum pressures at 1.5 s that were 1.4 and 2.4 psi lower than calculated with RELAP5 for air and helium, respectively. The hand calculations also showed that an isentropic

expansion to 1.5 s would cause the gas plenum pressure to be about the same with either helium or air. The hand calculations thus indicated that the effect on pressure of helium's larger isentropic coefficient could effectively negate the increase in pressure caused by its smaller density. Thus, RELAP5 may have overstated the increase in pressure (up to 1.0 psi) caused by the use of helium versus air. However, even in the bounding case of an isentropic expansion, similar gas plenum pressures would be obtained with helium and air.

4.0 CONCLUSIONS

The RELAP5 and TRAC calculations of a LOCA initiated by a double-ended guillotine break in a plenum inlet line for the K-14.1 charge were in remarkably good agreement with each other.

The overall hydraulic response of the process system was similar with both codes. As described in Section 3.2, the break flow generally agreed within 2%. The total flow through the core generally agreed within 1.3%.

The RELAP5 and TRAC calculations of the boundary conditions needed for detailed assembly calculations with FLOWTRAN were also in good agreement. The deviations between the RELAP5 and TRAC results for water plenum and tank bottom pressures at the limiting location and limiting time were less than 1.0 and 0.5 psi, respectively. These deviations are well within the uncertainty values currently used by Savannah River Laboratory in determining flow instability power limits.

The blanket gas system significantly affects gas plenum pressure, and hence tank bottom pressure, during the flow instability portion of a LOCA. Five or more control volumes are adequate to provide converged results with the current, simple models of the blanket gas system. However, the simple models may not adequately represent the hydraulic response of the blanket gas system during the first few seconds of the LOCA because of their simple representation of the hydraulic resistance and because the actual flow circuit, with contains active components such as gas blowers, is not simulated. The uncertainty in the RELAP5 and TRAC results associated with using such simple models of the blanket gas system has not been evaluated.

The effect of modeling the blanket gas as air rather than helium was examined but not conclusively determined during this analysis. RELAP5 calculated gas plenum and tank bottom pressures that were as much as 1.0 psi higher with helium than with air because helium's lower density resulted in more volumetric flow from the blanket gas system into the gas plenum.

However, this result may not be correct because RELAP5 (and TRAC) may not accurately calculate the expansion of the blanket gas during the first few seconds of the LOCA. The expansion calculated by RELAP5 was nearly isothermal, with an effective expansion coefficient of about 1.1. Since the actual gas expansion could be near isentropic, RELAP5 may be calculating gas plenum and tank bottom pressures that are as much as 1.4 to 2.4 psi too high for air and helium, respectively. Bounding hand calculations indicated that the effect of helium's larger isentropic coefficient on pressure could effectively negate the increase in pressure caused by its smaller density. Thus, RELAP5 may have overstated the increase in pressure caused by the use of helium versus air.

5. REFERENCES

1. Limits Methodology for a Large Break LOCA in an SRP Reactor, DPSTM-110-LOCA, Draft B, to be published.

2. Safety Code Development Group, TRAC-PF1/MOD1: An Advanced Best-Estimate Computer Program for Pressurized Water Reactor Thermal-Hydraulic Analysis, NUREG/CR-3858 LA-10157-MS, July 1986.

3. FLOWTRAN: An Algorithm for Describing the Thermal-Hydraulic Behavior of SRP Assemblies, DPSTM-140, Volume 3.

4. M. S. Sahota and F. L. Addessio, TRAC-PF1/MOD1 Developmental Assessment, NUREG/CR-4278, LA-10445-MS, August 1985.

5. K. R. Katsma et al, Quantifying Reactor Safety Margins: Application of Code Scaling, Applicability, and Uncertainty Methodology to a Large Break Loss of Coolant Accident, NUREG/CR-5249 (Draft), November 1988.

6. M. A. Bolander et al, Development of a Phenomena Identification and Ranking Table for Thermal-Hydraulic Phenomena during a Double Ended Guillotine Break LOCA in a SRS Production Reactor, EGG-EAST-8618, August 1989.

7. V. H. Ransom et al, SCDAP/RELAP5/MOD1 Code Manual, Volumes 1 and 2, EG&G Idaho Inc., February 1988 (Draft).

8. E. G. Schaub, TRAC Calculations of the Initial Flow Decay in K-14.1, DPST-89-326, to be published.

9. J. M. Cozzuol and C. B. Davis, Description of the Two-Loop RELAP5 Model of the L-Reactor at the Savannah River Site, EGG-EAST-8449, to be published.

10. M. A. Bolander and C. B. Davis, Benchmarking the Six-Loop, Three-Dimensional RELAP5 L-Reactor Model with Savannah River Reactor Test Data, EGG-EAST-8556, June 1989 (Draft).

11. V. H. Ransom et al, RELAP5/MOD2 Code Manual, Volumes 1 and 2, EG&G Idaho Inc., NUREG/CR-4312, EGG-2396, August 1985.

12. M. A. Bolander and C. D. Fletcher, Simulation of Cold Leg Manifold Break and Station Blackout Sequences in the N-Reactor, EGG-TFM-7891, February 1988.

13. J. D. Burtt et al, Advanced Test Reactor Large Break Loss-of-Coolant Accident Break Spectrum Study, EGG-TFM-8082, April 1988.

14. P. D. Wheatley et al, RELAP5/MOD2 Code Assessment at the Idaho National Engineering Laboratory, NUREG/CR-4454, EGG-2428, March 1986.

15. R. W. Shumway et al, Applicability of RELAP5/MOD2 to N-Reactor Safety Analysis Part-1 "Quick-Look Evaluation", EGG-TFM-8026, February 1988.

16. L. D. Koffman et al, TRAC Calculations of the Initial Flow Decay in L-1.1, DPST-87-737, December 18, 1987.

17. C. B. Davis et al, Benchmarking the RELAP5 L-Reactor Model with Savannah River Reactor Test Data, EGG-EAST-8336, April 1989.

18. I. E. Idel'chik, Handbook of Hydraulic Resistance, Coefficients of Local Resistance and of Friction, AEC-TR-6630, 1966.

19. L. D. Koffman, Analysis of CMX Hydraulic Data for the Mark 22, DPST-88-795, December 16, 1988.

20. J. F. King, Flow Paths Through the Reactor Top Shield, DPST-87-680, December 1987.

21. J. P. Morin, Process Water System Hydraulic and Heat Transfer Data Base for Savannah River Simulator, DPST-83-282-TL, January 1982.

22. R. E. Pevey and J. W. Reece, TRAC Model of Reactor Vent Paths, DPST-87-738, December 18, 1987.

23. C. B. Davis, Pump Cavitation in L-Reactor During a LOCA Initiated by a Large Break in a Plenum Inlet Line, EGG-EAST-8148, June 1988.

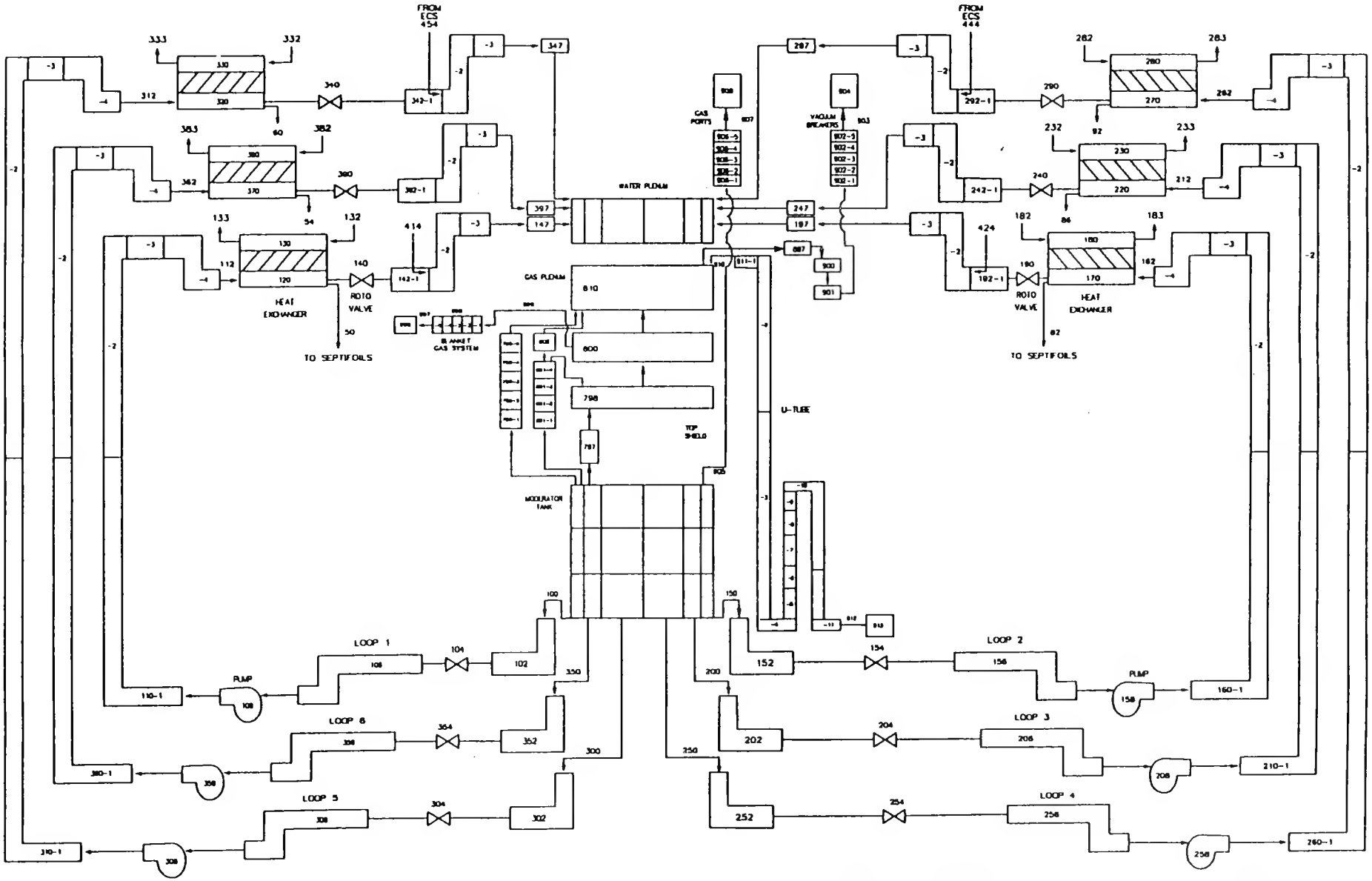

Figure 1. Nodalization of the six-loop model of K-Reactor.

CCK01190

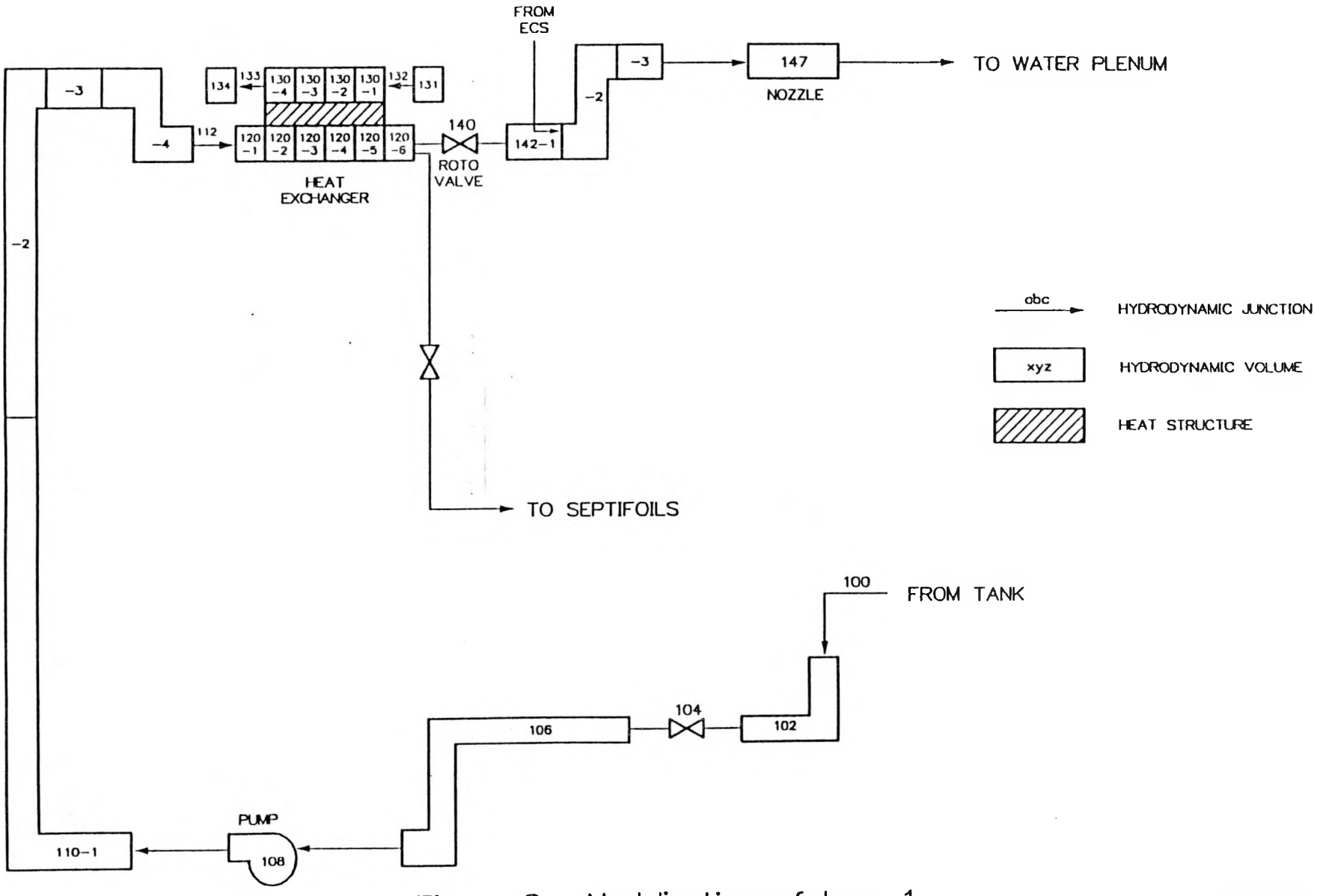

Figure 2. Nodalization of loop 1.

CCK01163

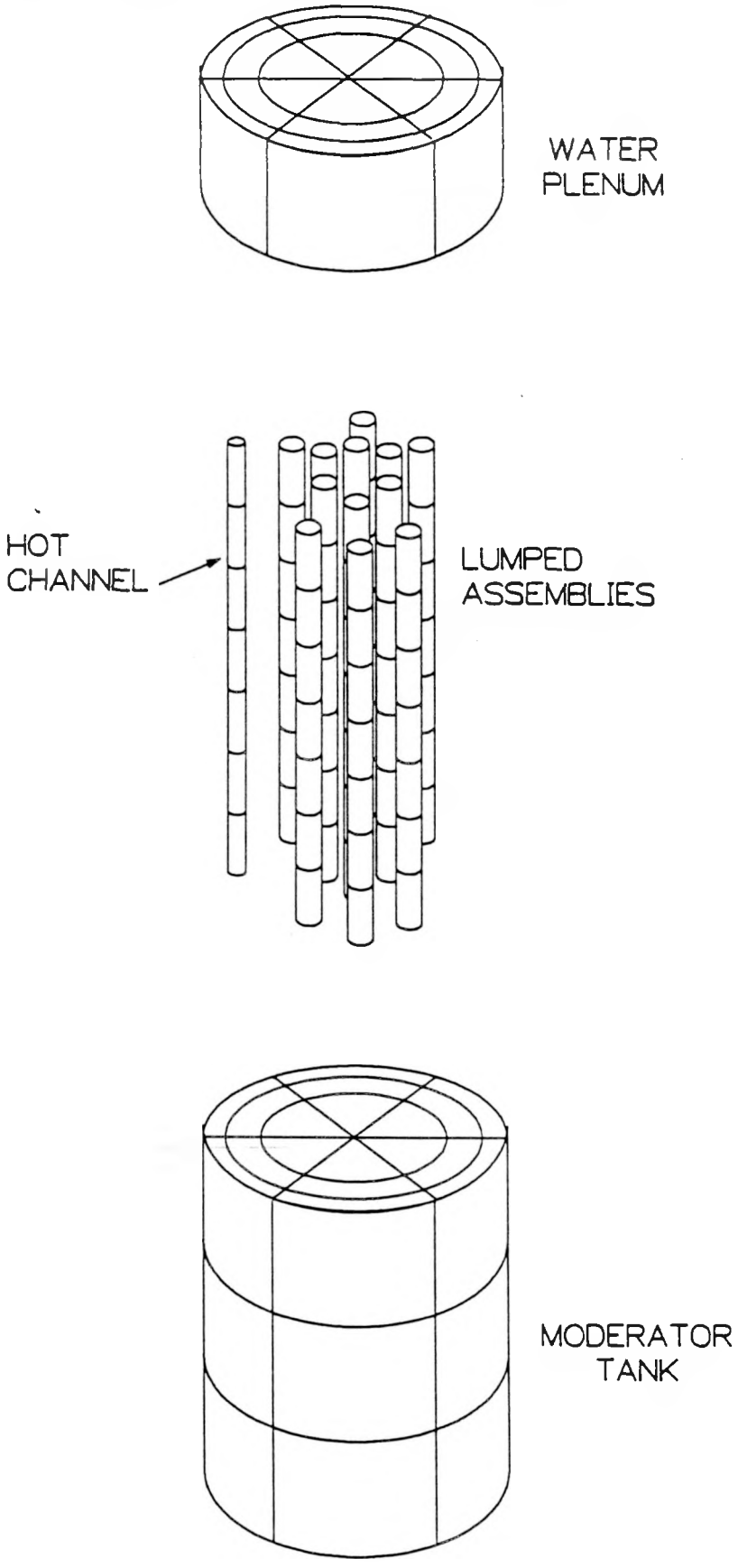

Figure 3. Schematic of the three-dimensional vessel model and fuel assemblies.

CCK01138

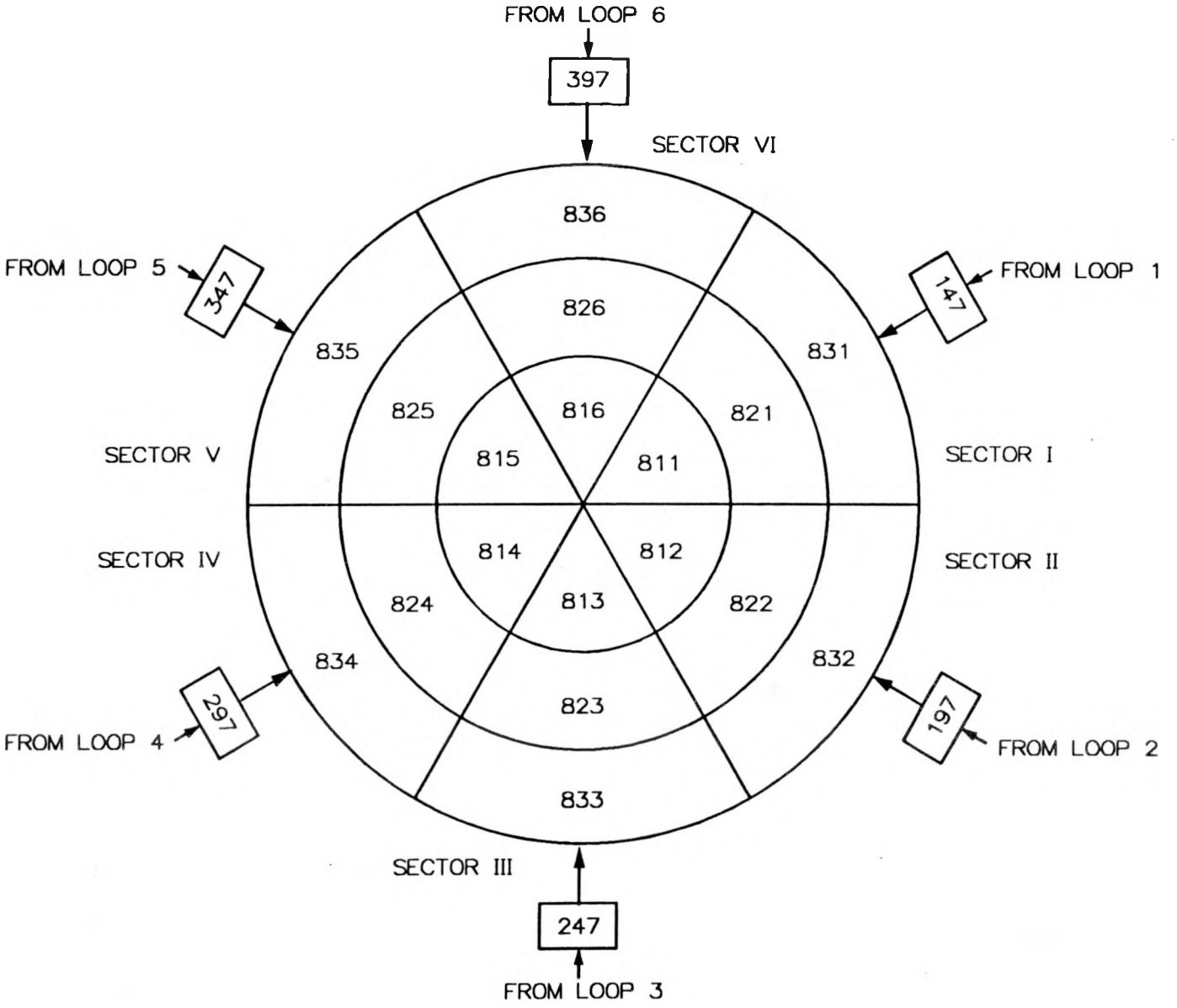

Figure 4. Nodalization of the two-dimensional plenum model.

CCK01131

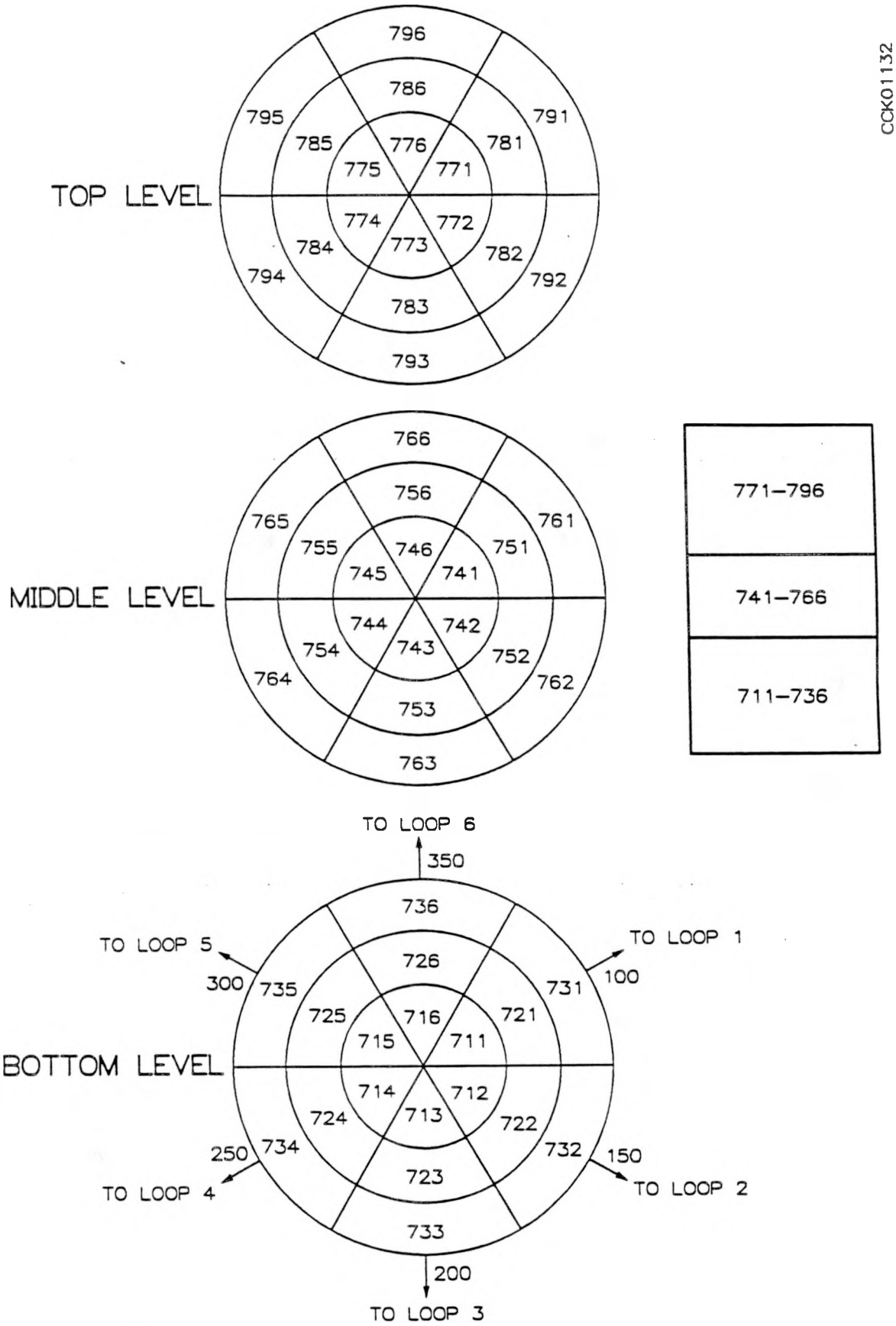

Figure 5. Nodalization of the three–dimensional tank model.

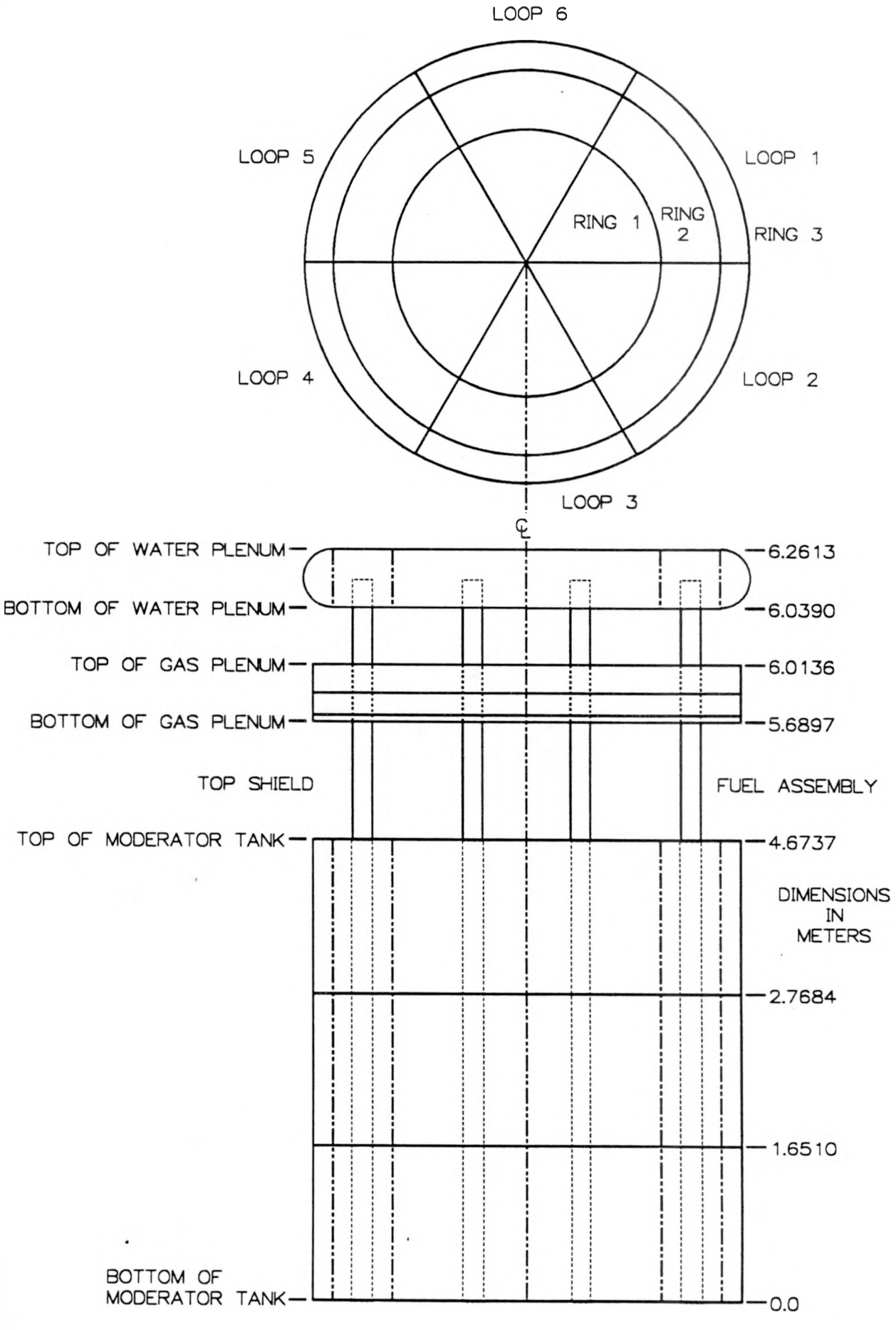

Figure 6. Cutaway view of the vessel model.

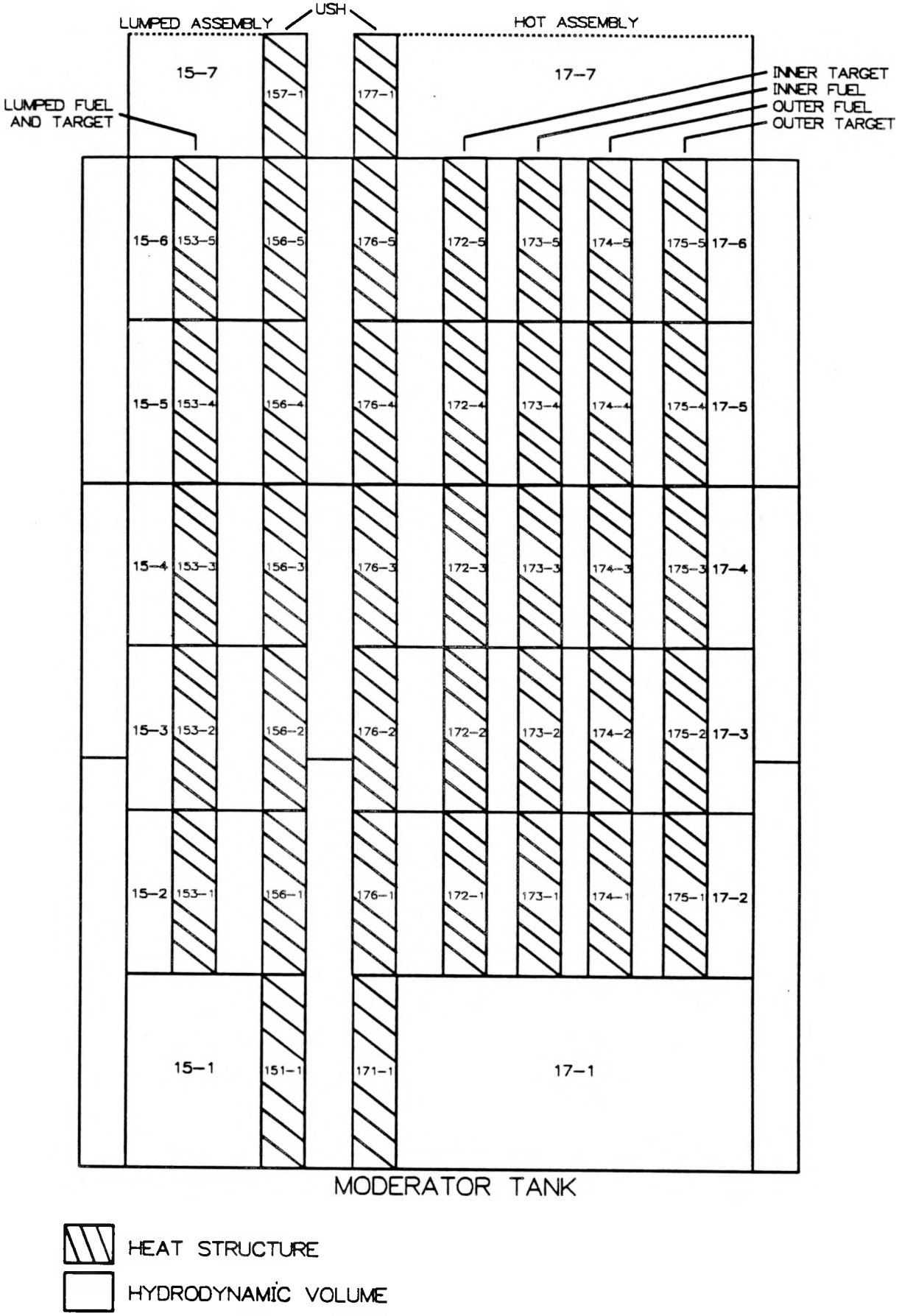

CCK01136

Figure 7. Nodalization of a typical lumped assembly and the hot assembly.

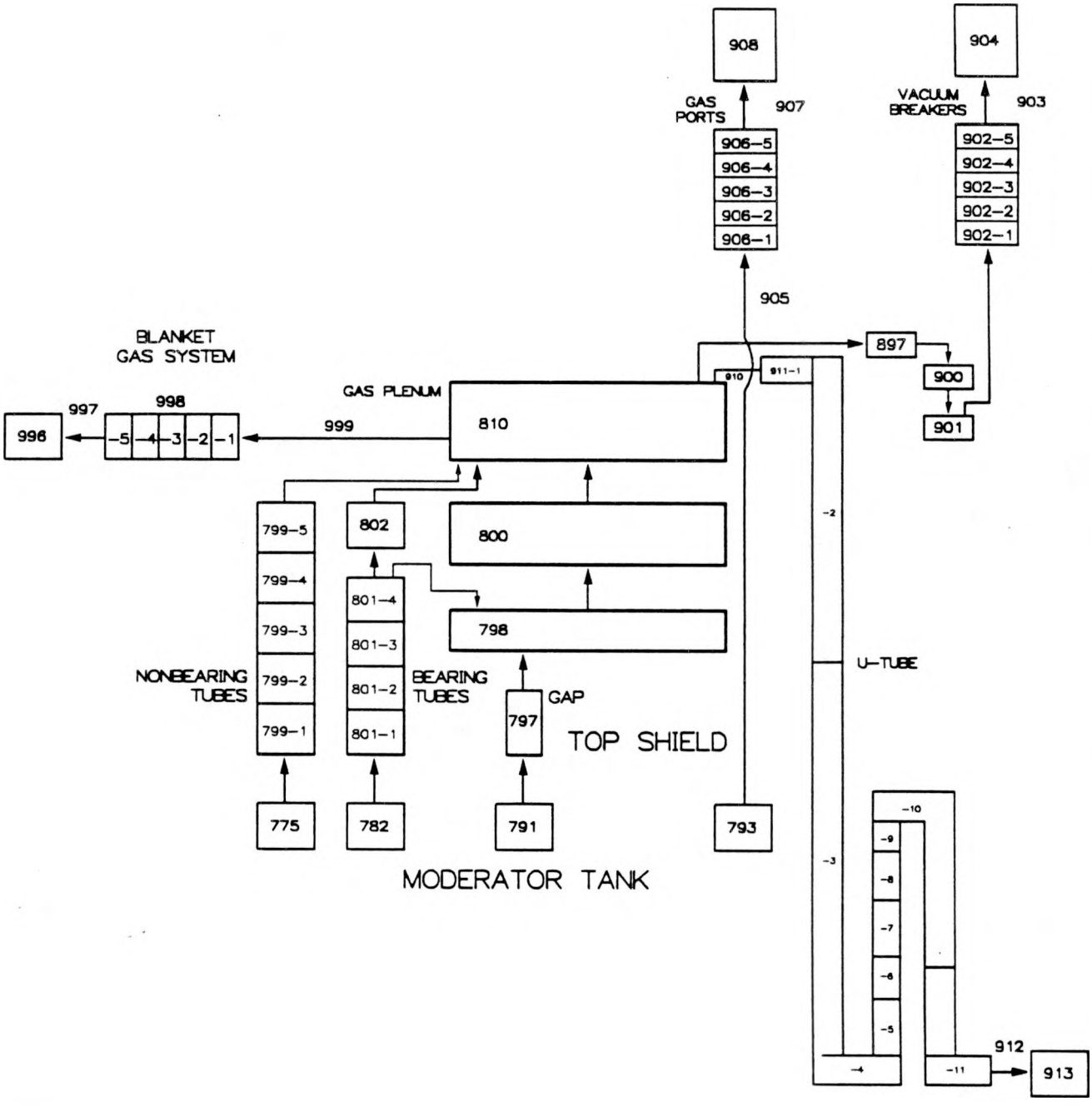

Figure 8. Nodalization of the gas plenum, top shield, reactor vent paths, and blanket gas system.

CCK01188

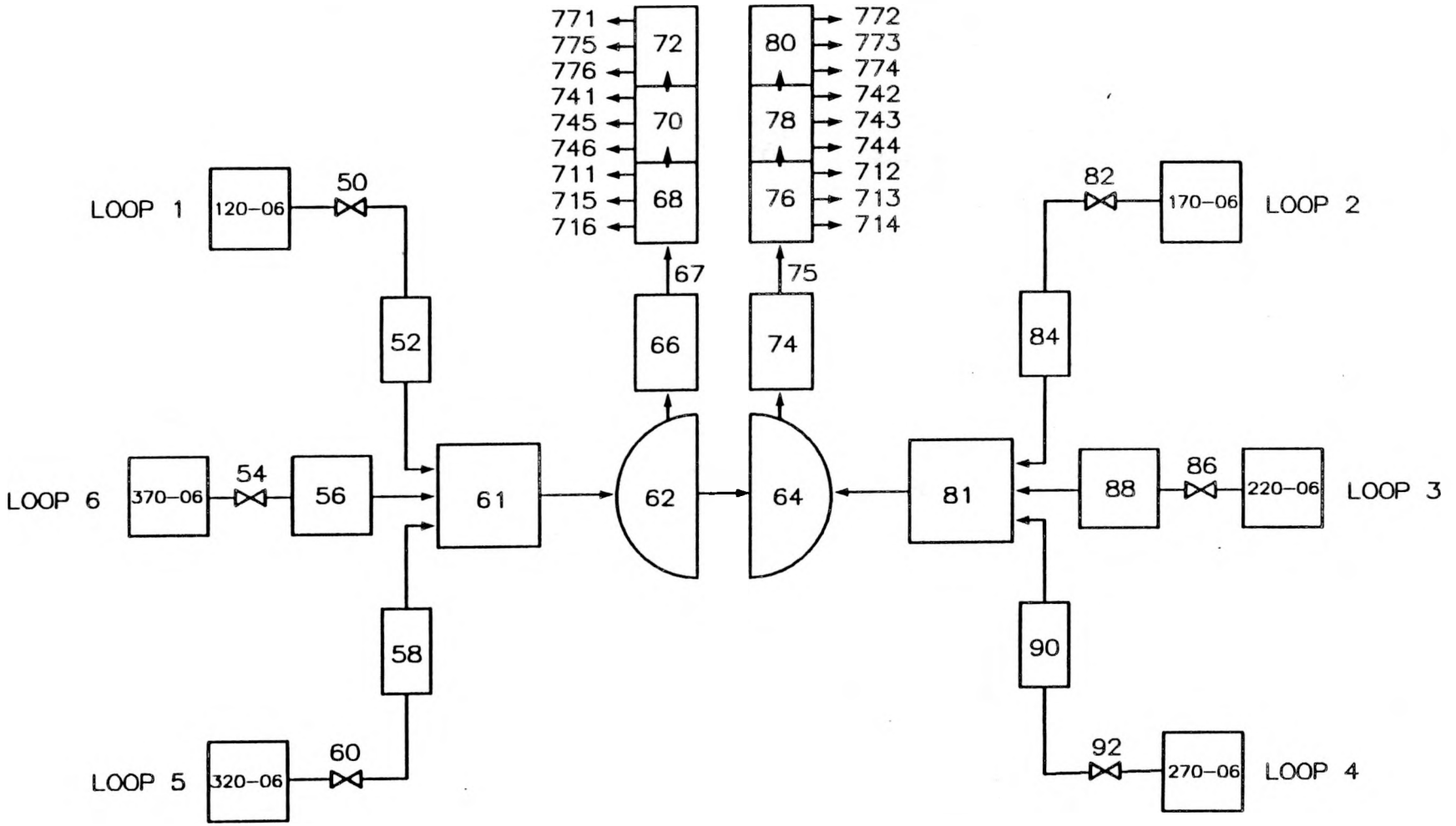

Figure 9. Nodalization of the septifoil system.

CCK01130

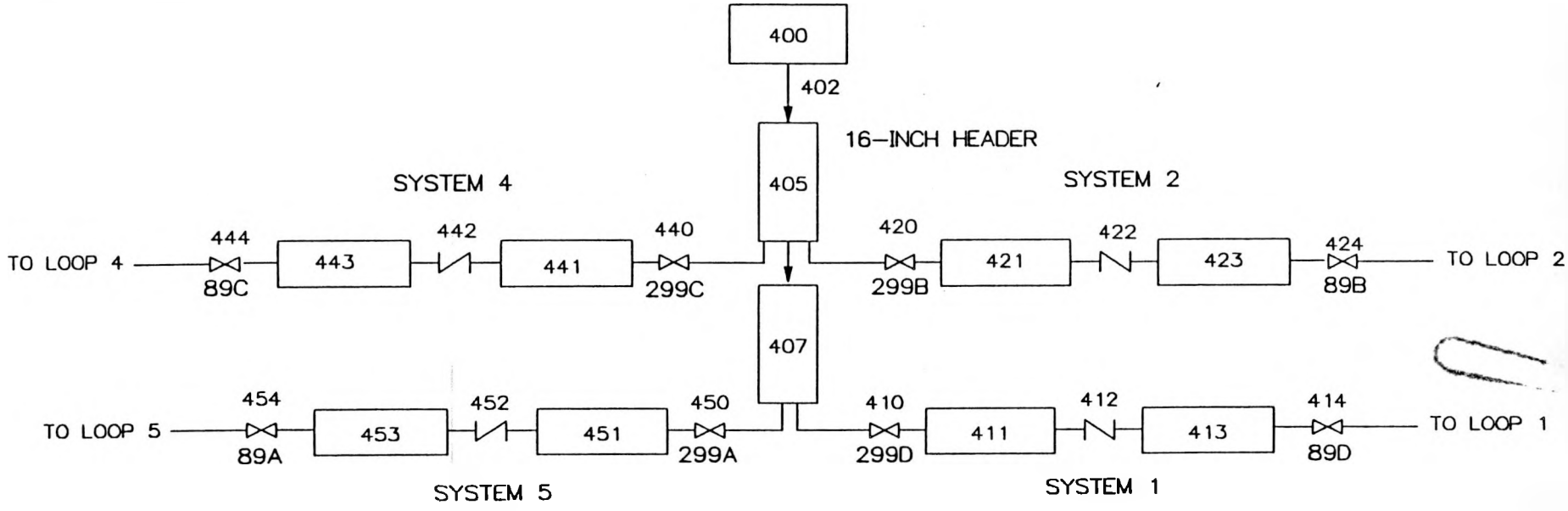

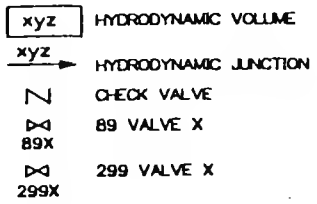

Figure 10. Nodalization of the ECS.

CCK01134

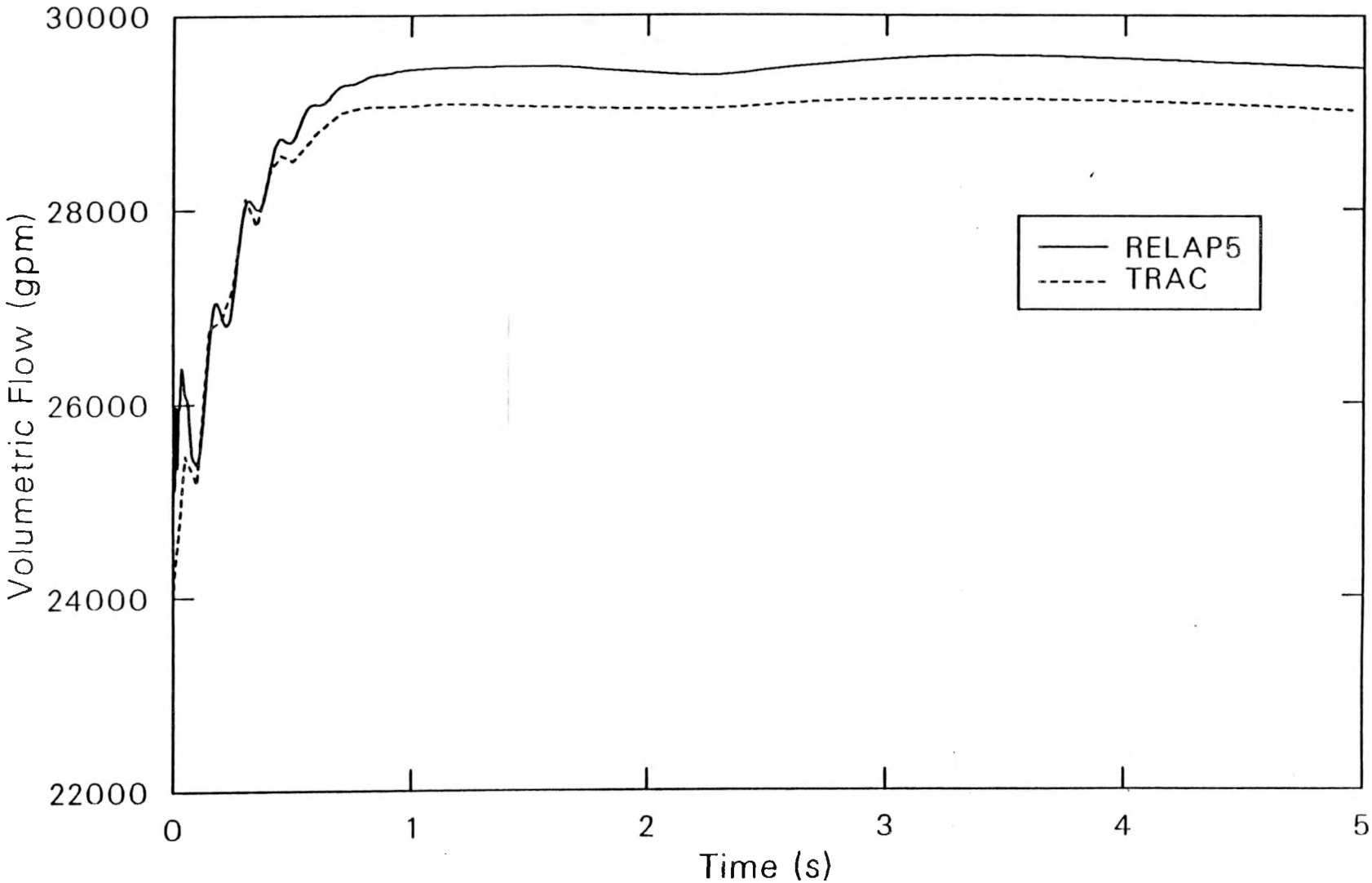

Figure 11. A comparison of calculated flows out the heat exchanger side of the break.

CBD0689-11

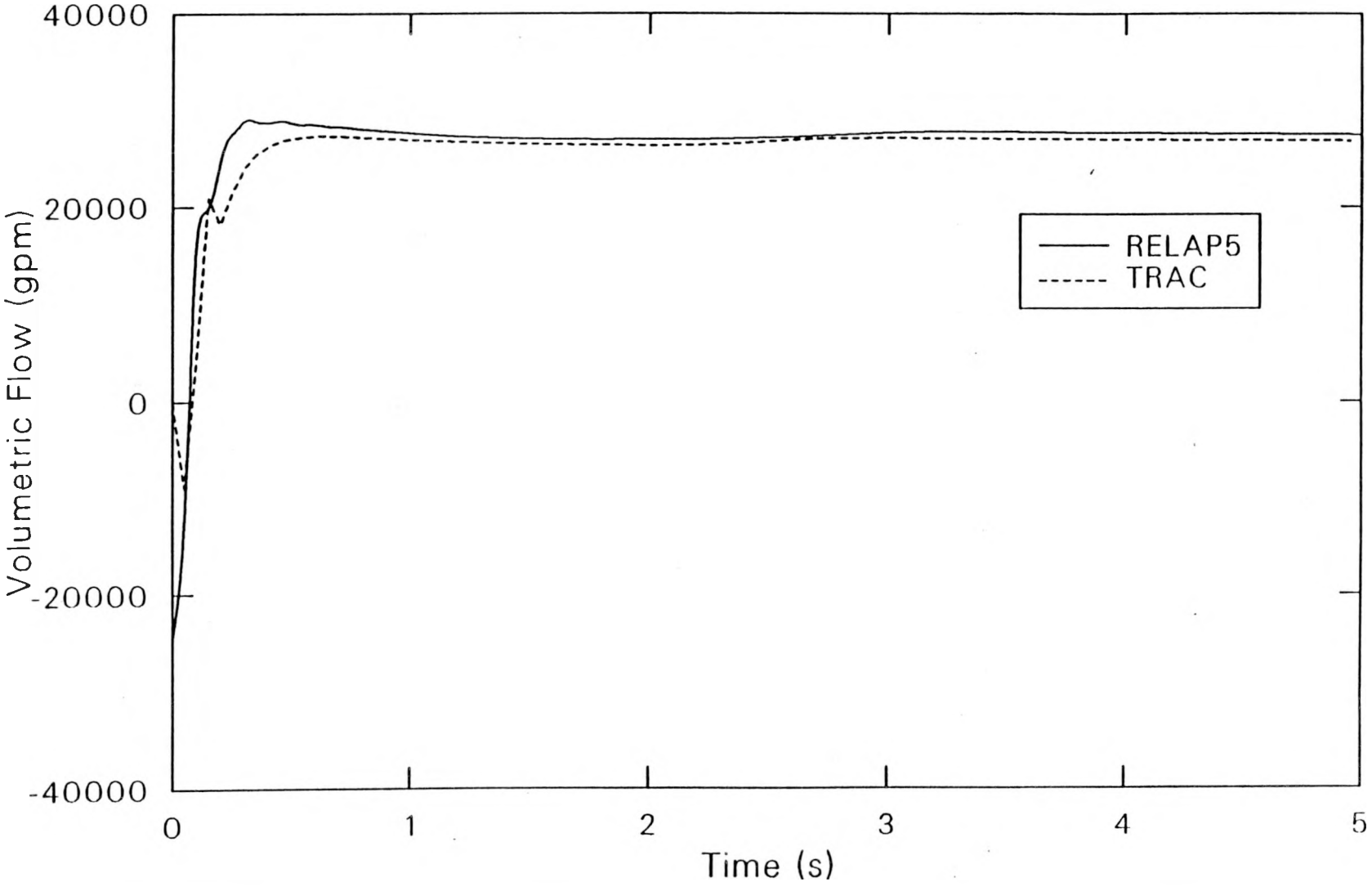

Figure 12. A comparison of calculated flows out the plenum side of the break.

CBD0689-12

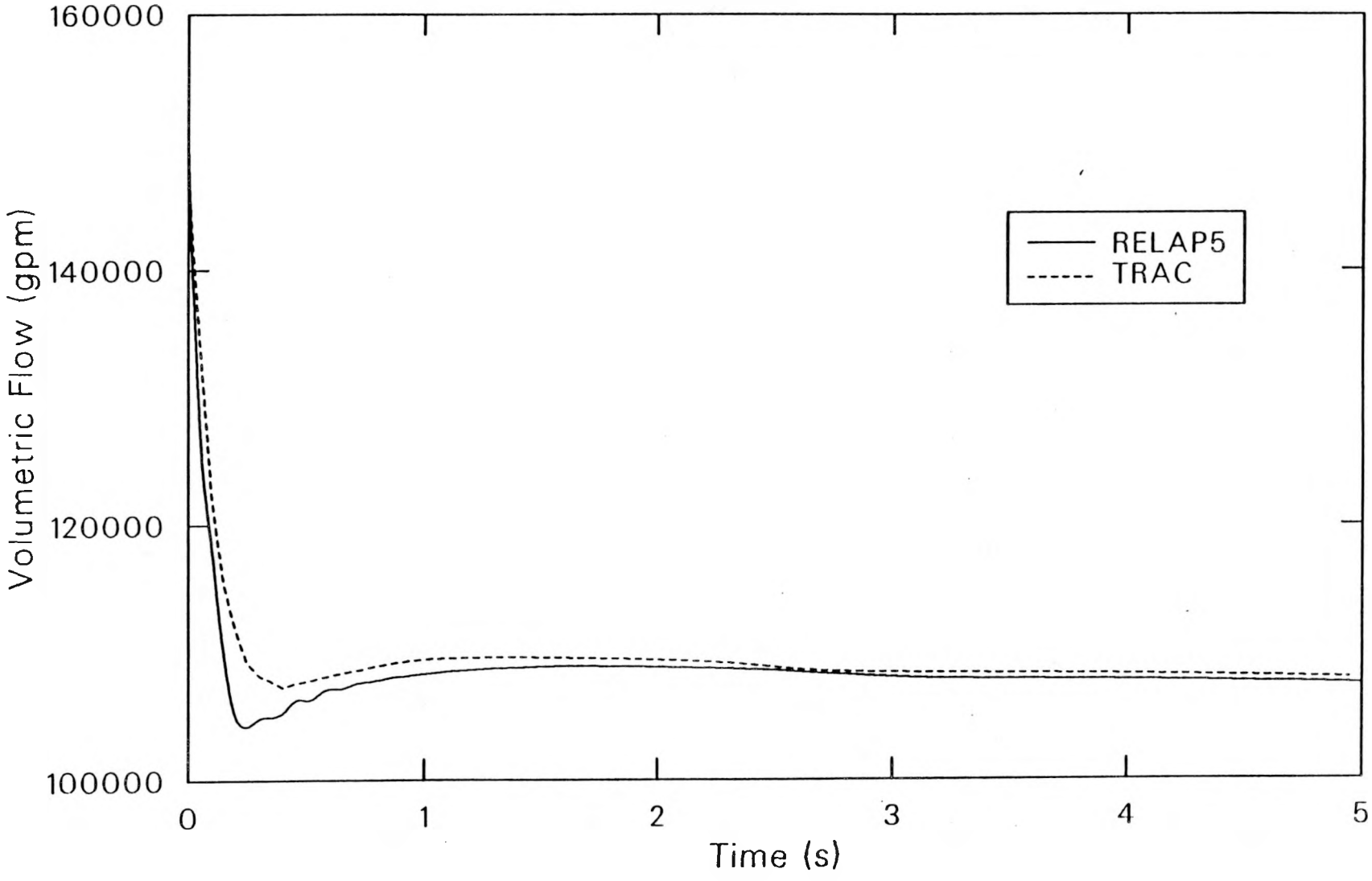

Figure 13. A comparison of total calculated flow through the assemblies.

CBD0689-13

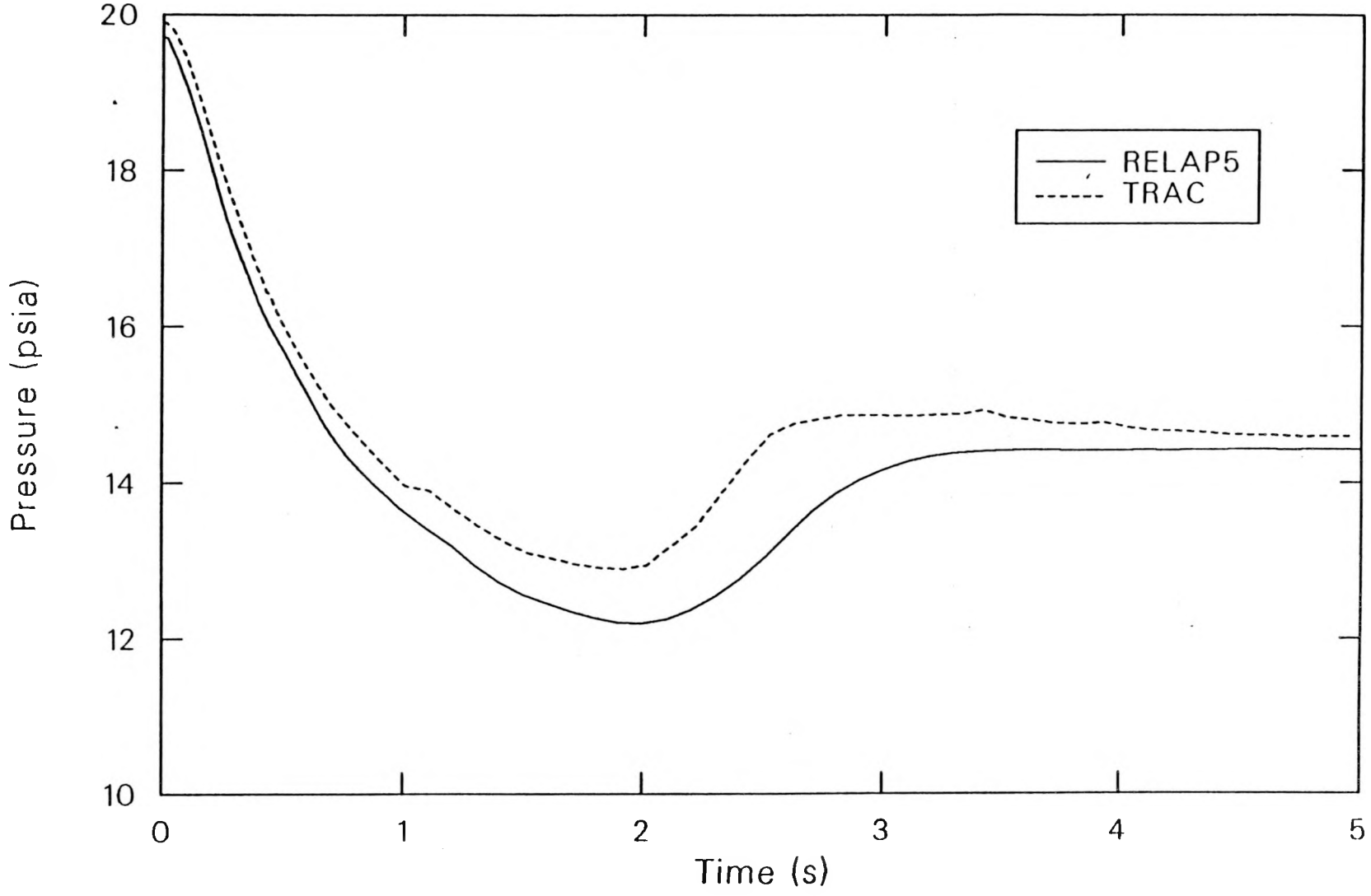

Figure 14. A comparison of calculated pressures in the gas plenum.

CBD0689-14

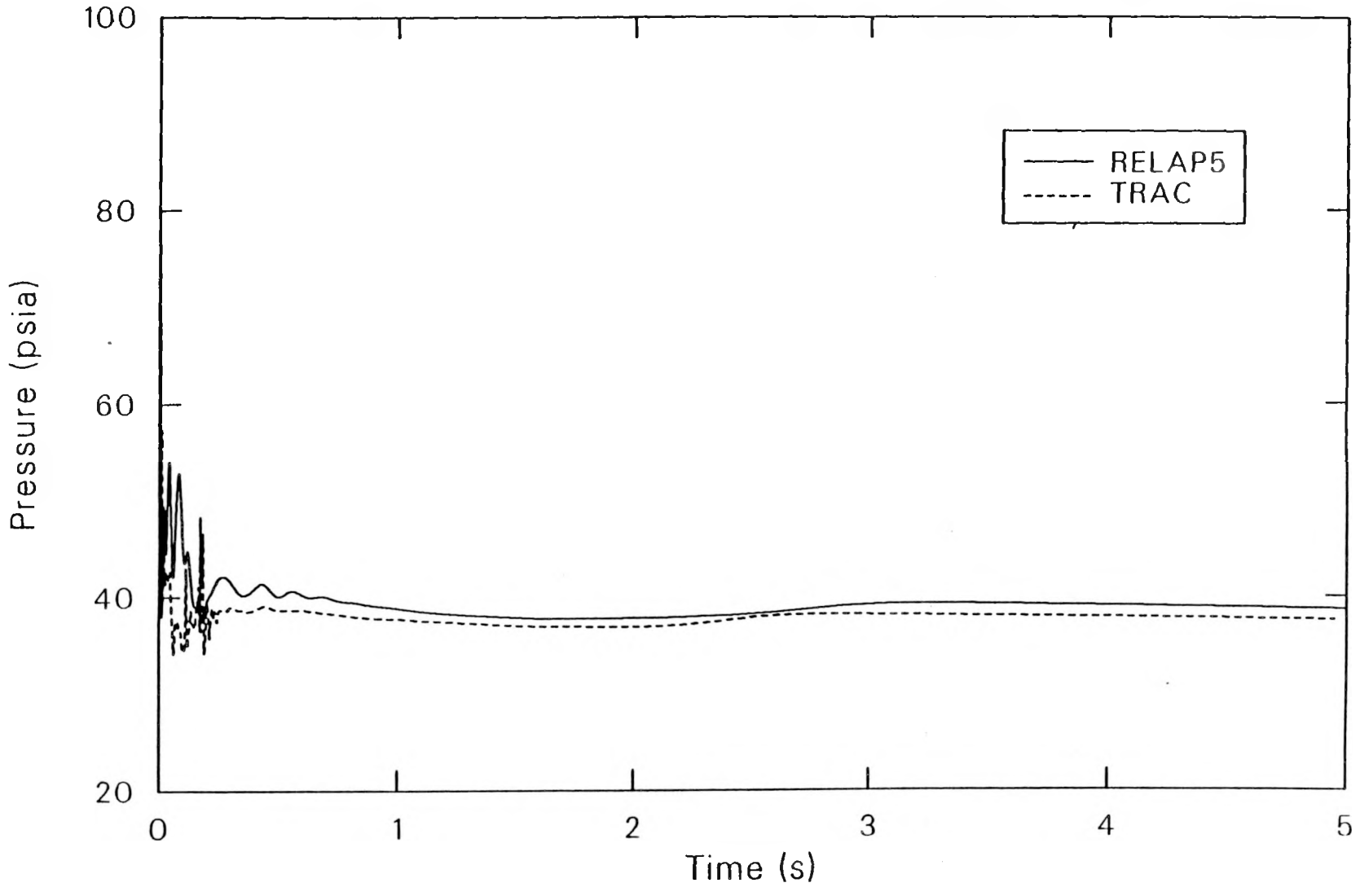

Figure 15. A comparison of calculated pressures in ring 2 sector 5 of the water plenum.

CBD0689-15

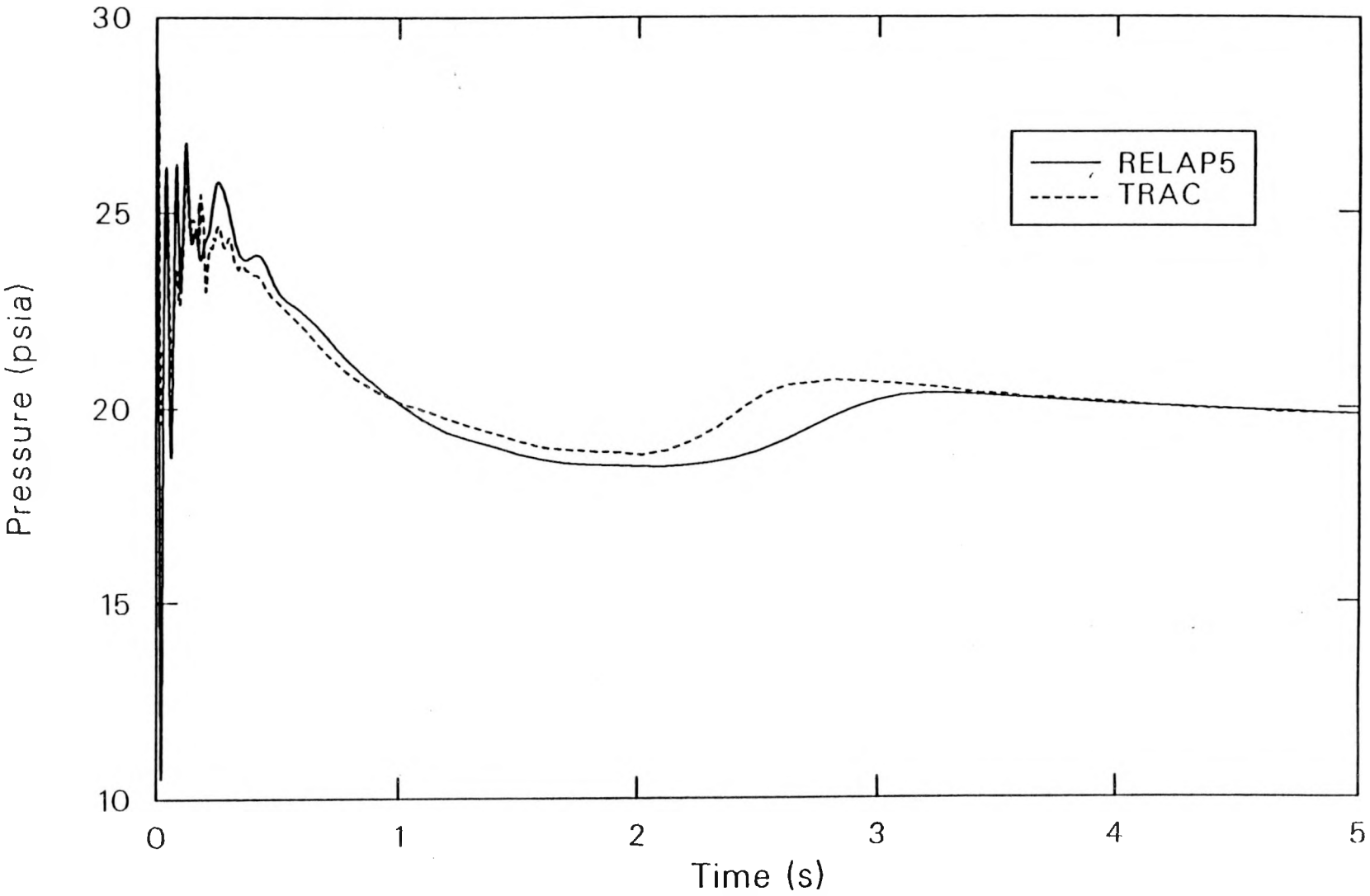

Figure 16. A comparison of calculated pressures in ring 2 sector 5 at the tank bottom.

CBD0689-16

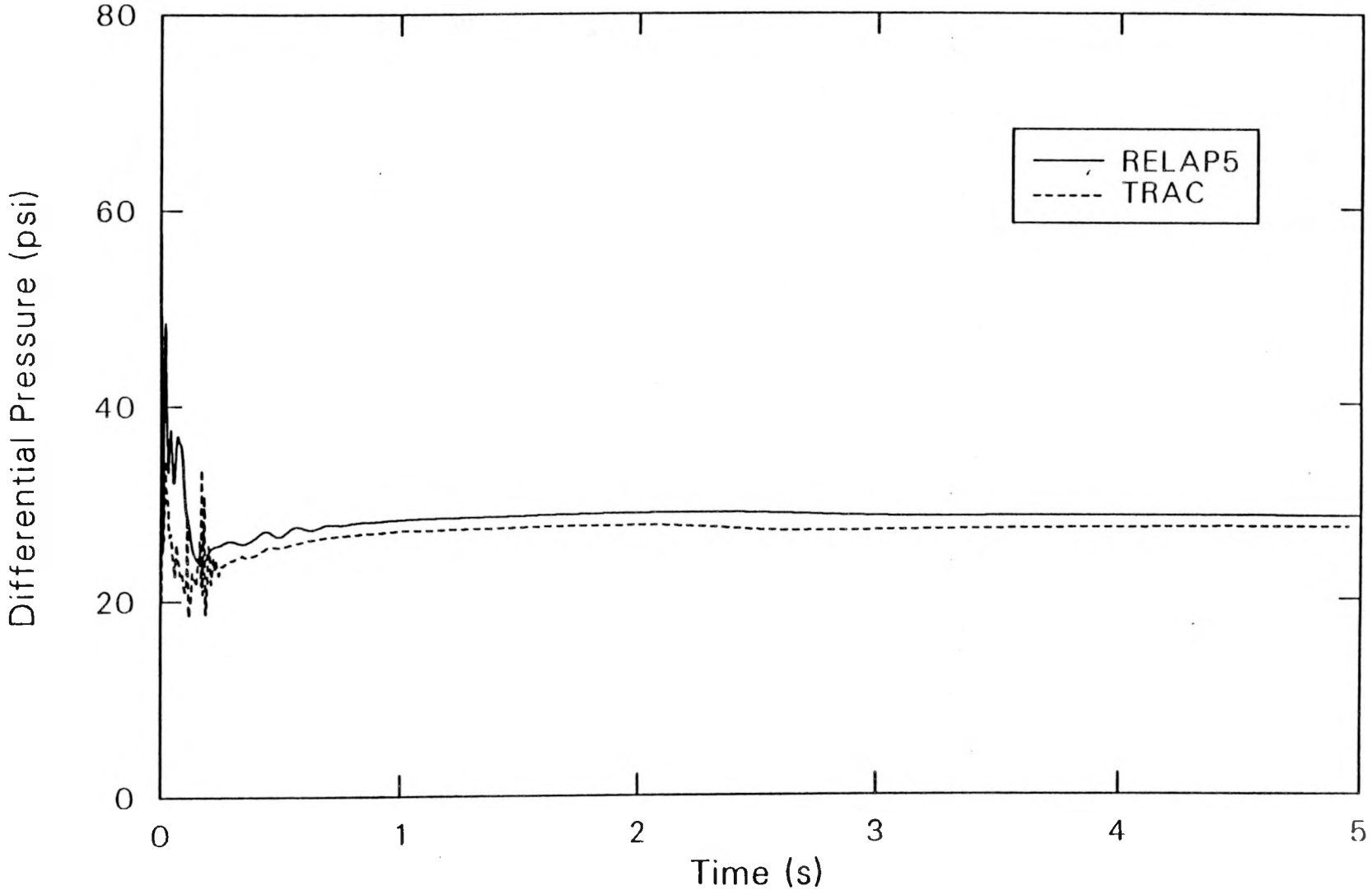

Figure 17. A comparison of calculated differential pressures across the assemblies in ring 2 sector 5.

CBD0689-17

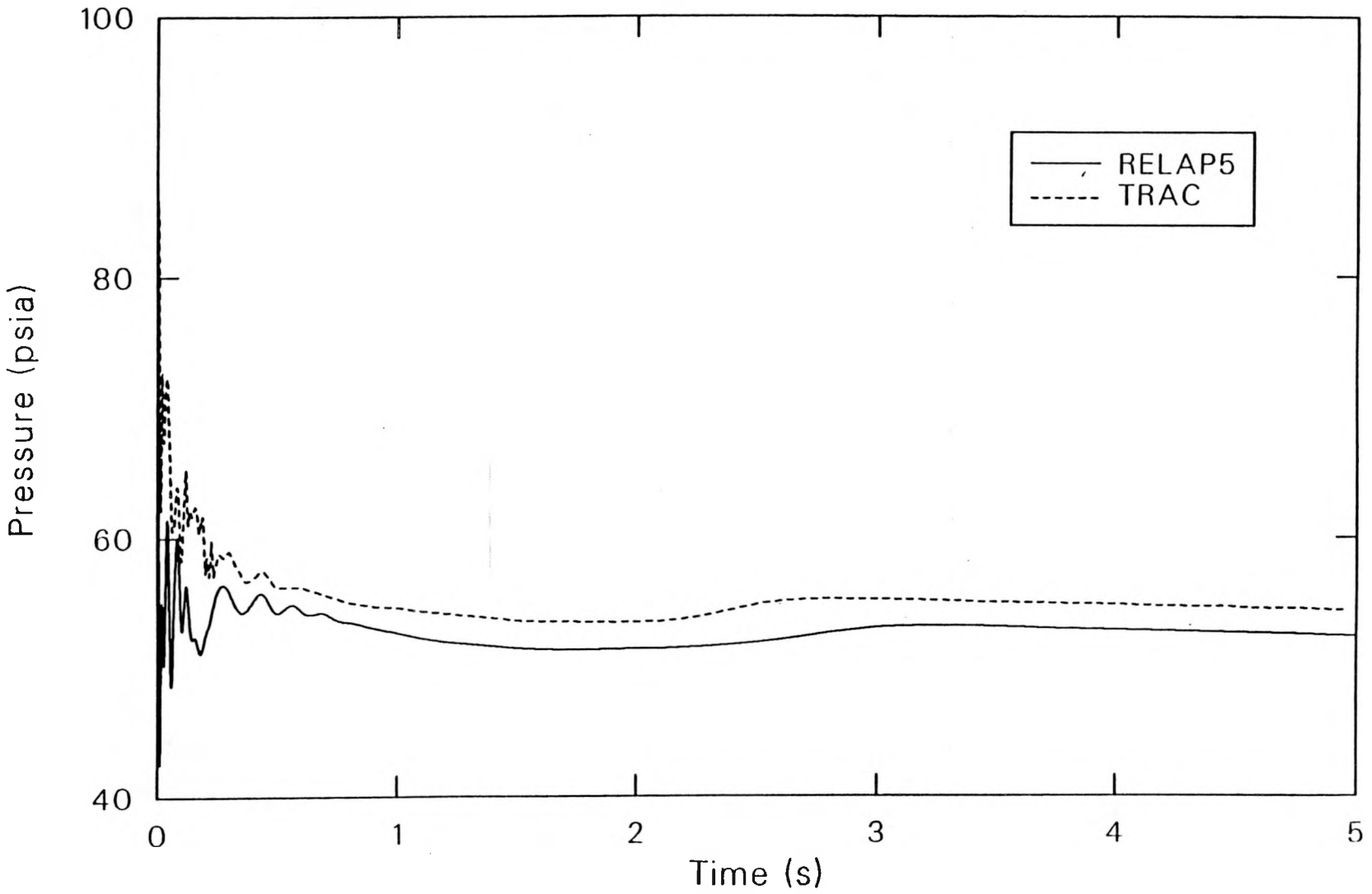

Figure 18. A comparison of calculated pressures in ring 2 sector 2 of the water plenum.

CBD0689-18

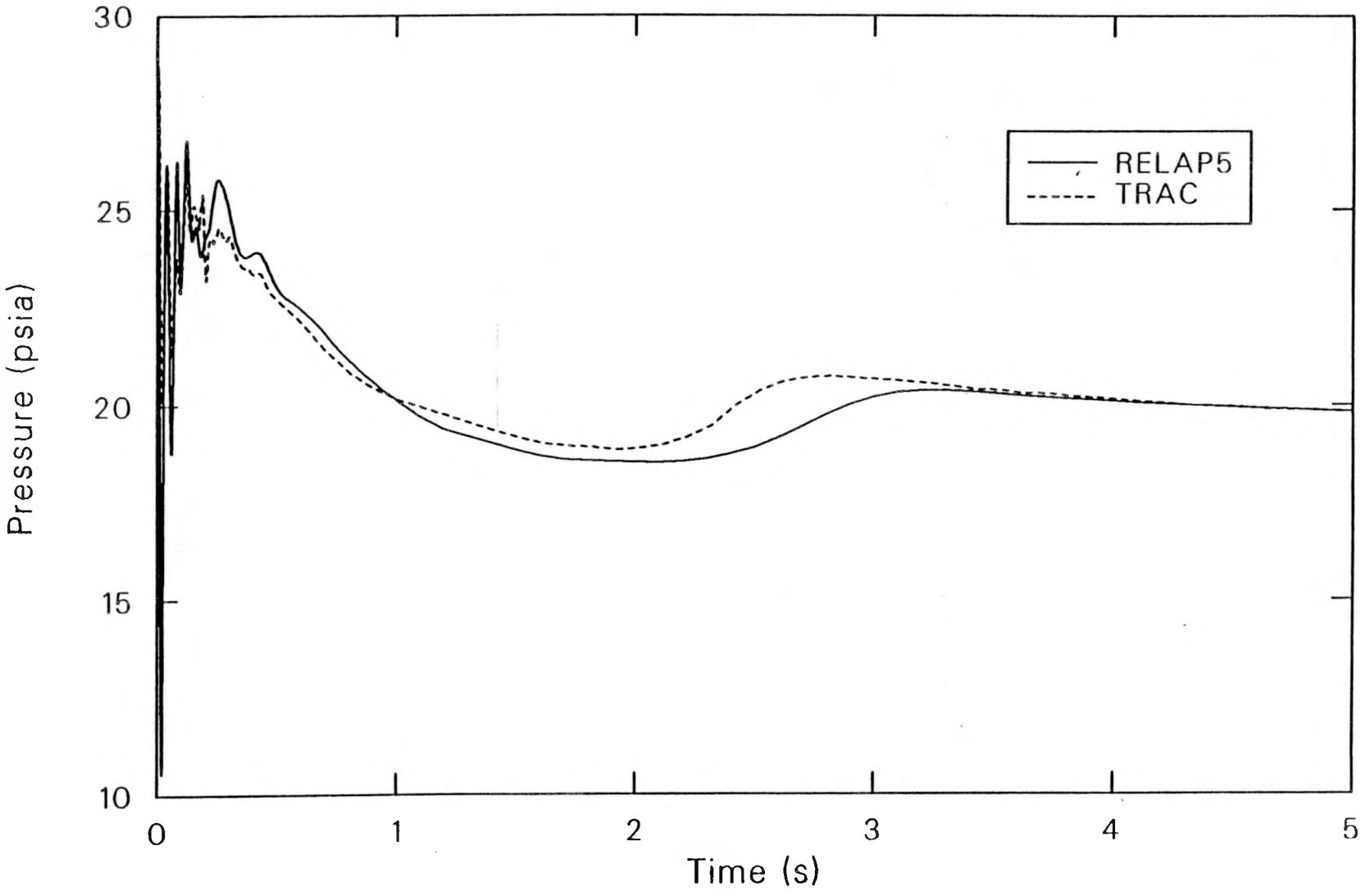

Figure 19. A comparison of calculated pressures in ring 2 sector 2 at the tank bottom.

CBD0689-19

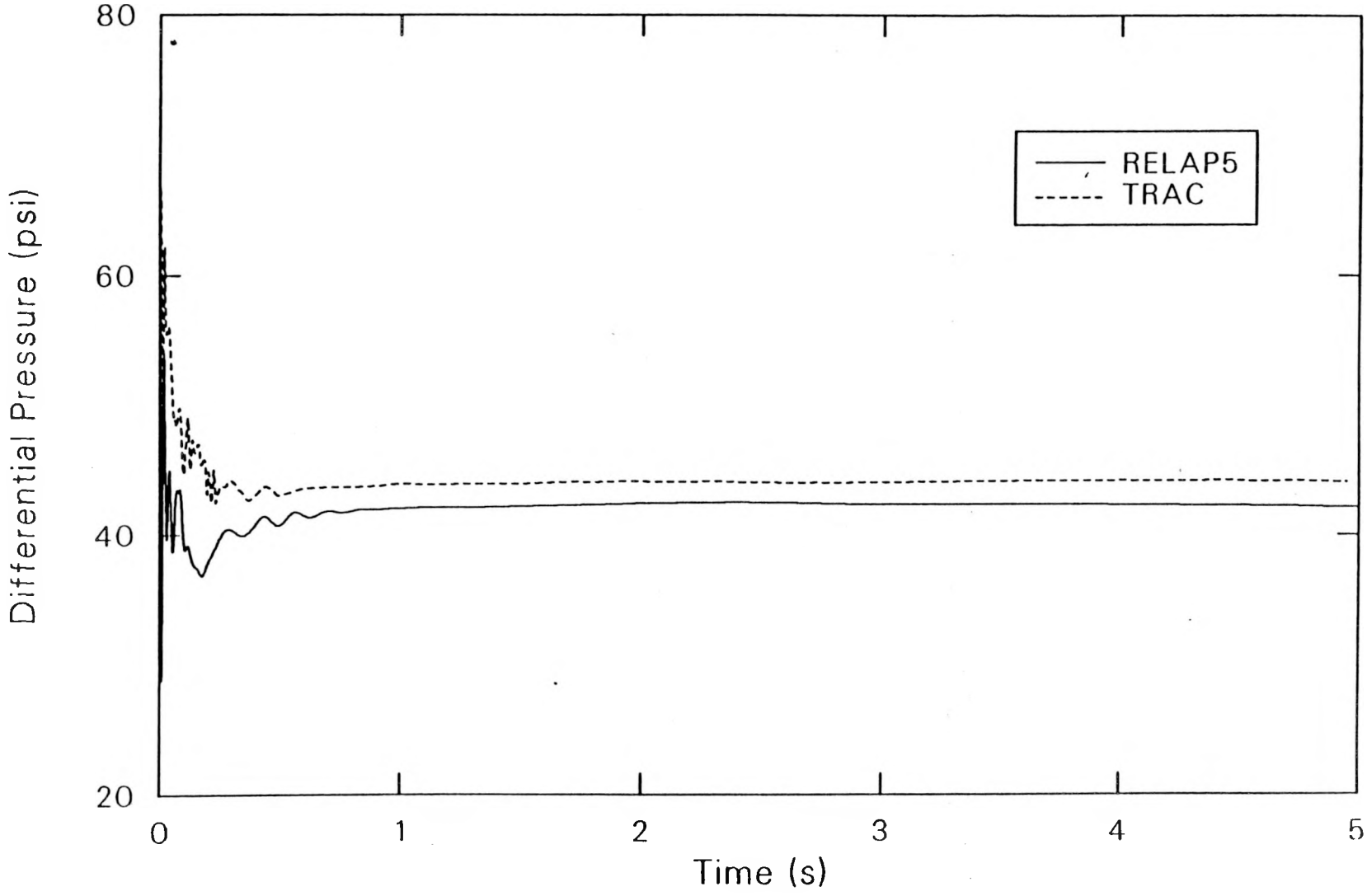

Figure 20. A comparison of calculated differential pressures across the assemblies in ring 2 sector 2.

CBD0689-20

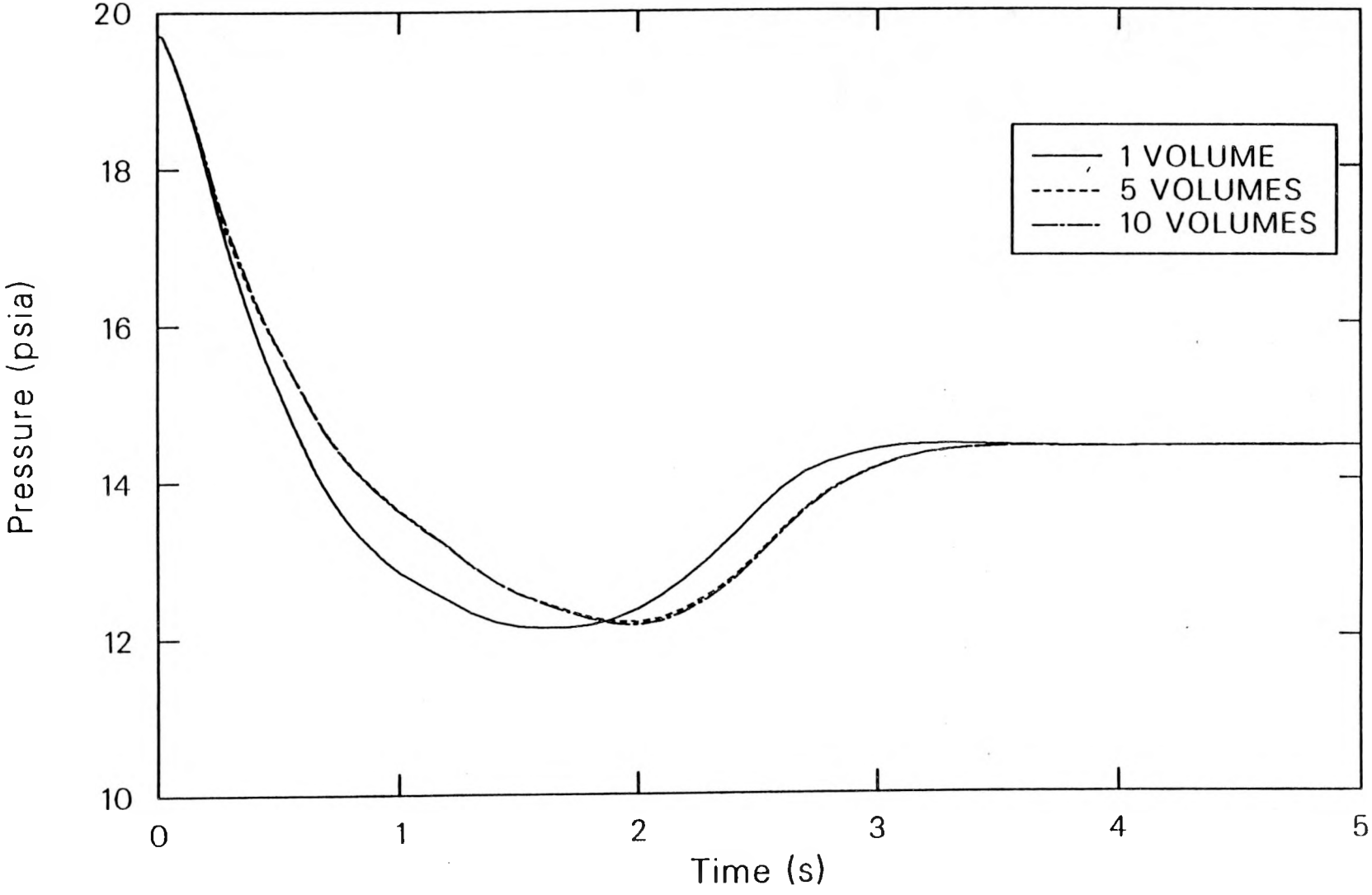

Figure 21. The effect of blanket gas nodalization on gas plenum pressure.

CBD0689-21

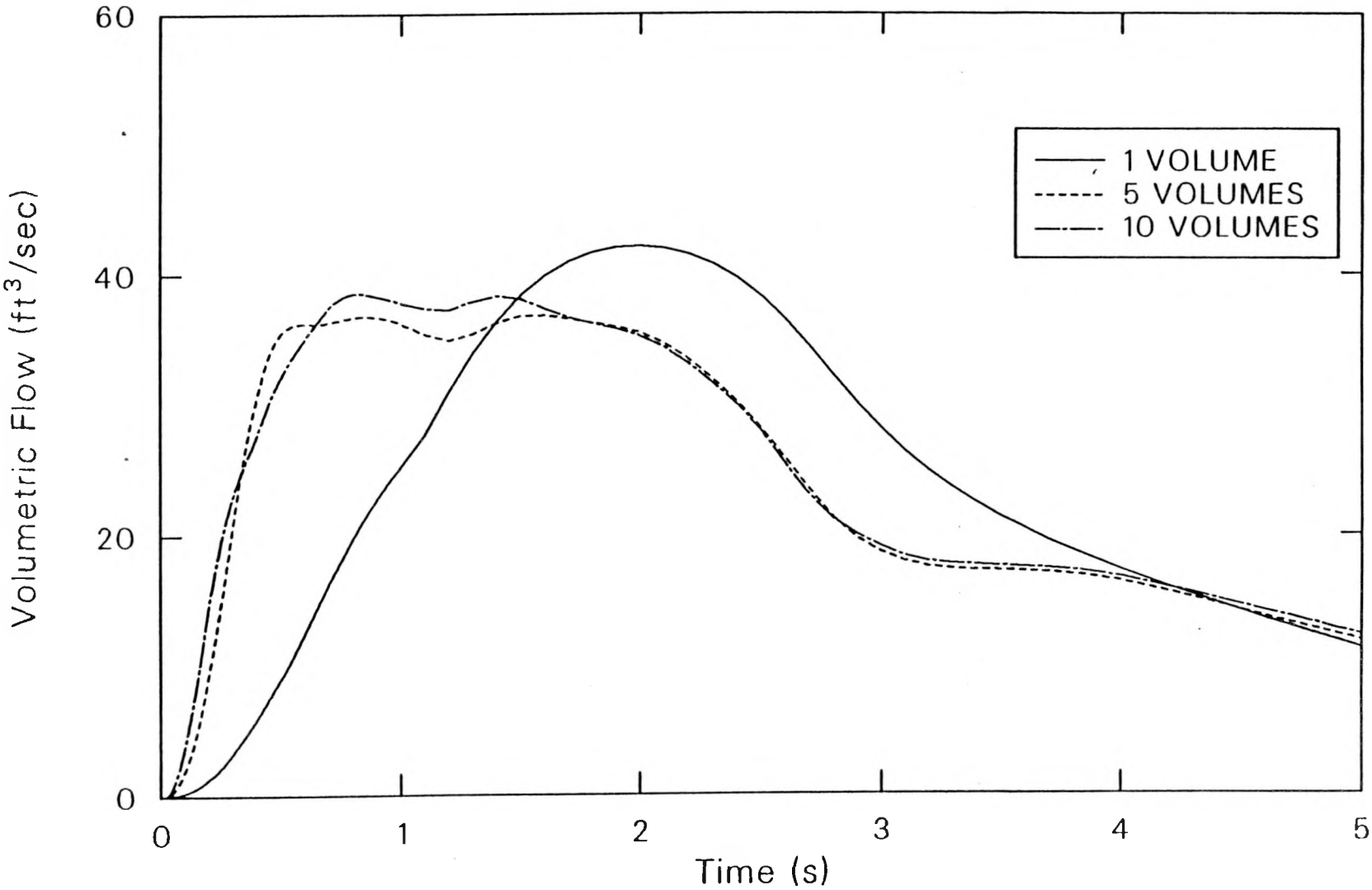

Figure 22. The effect of blanket gas nodalization on blanket gas flow.

CBD0689-22

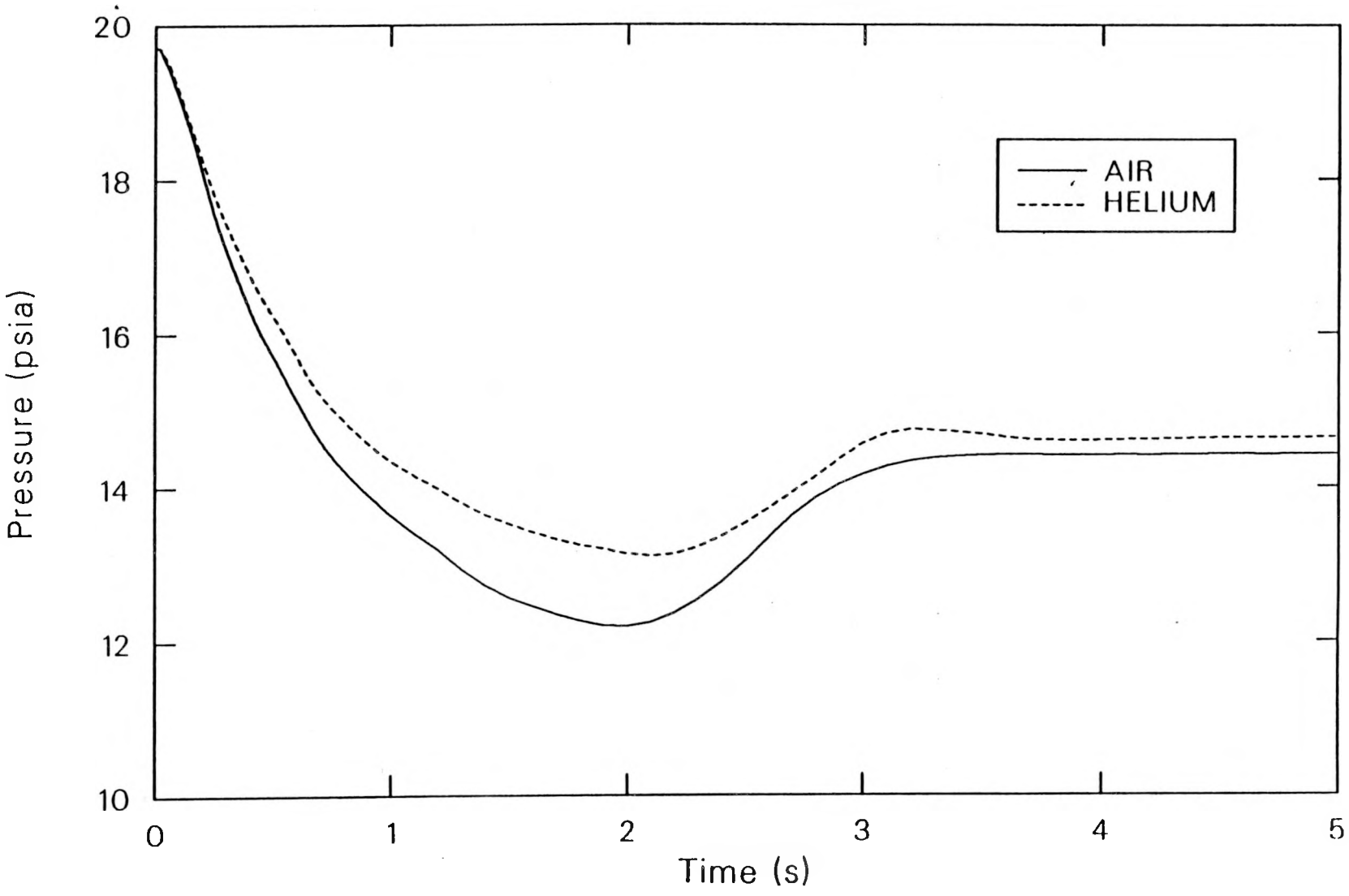

Figure 23. The effect of blanket gas composition on gas plenum pressure.

CBD0689-23

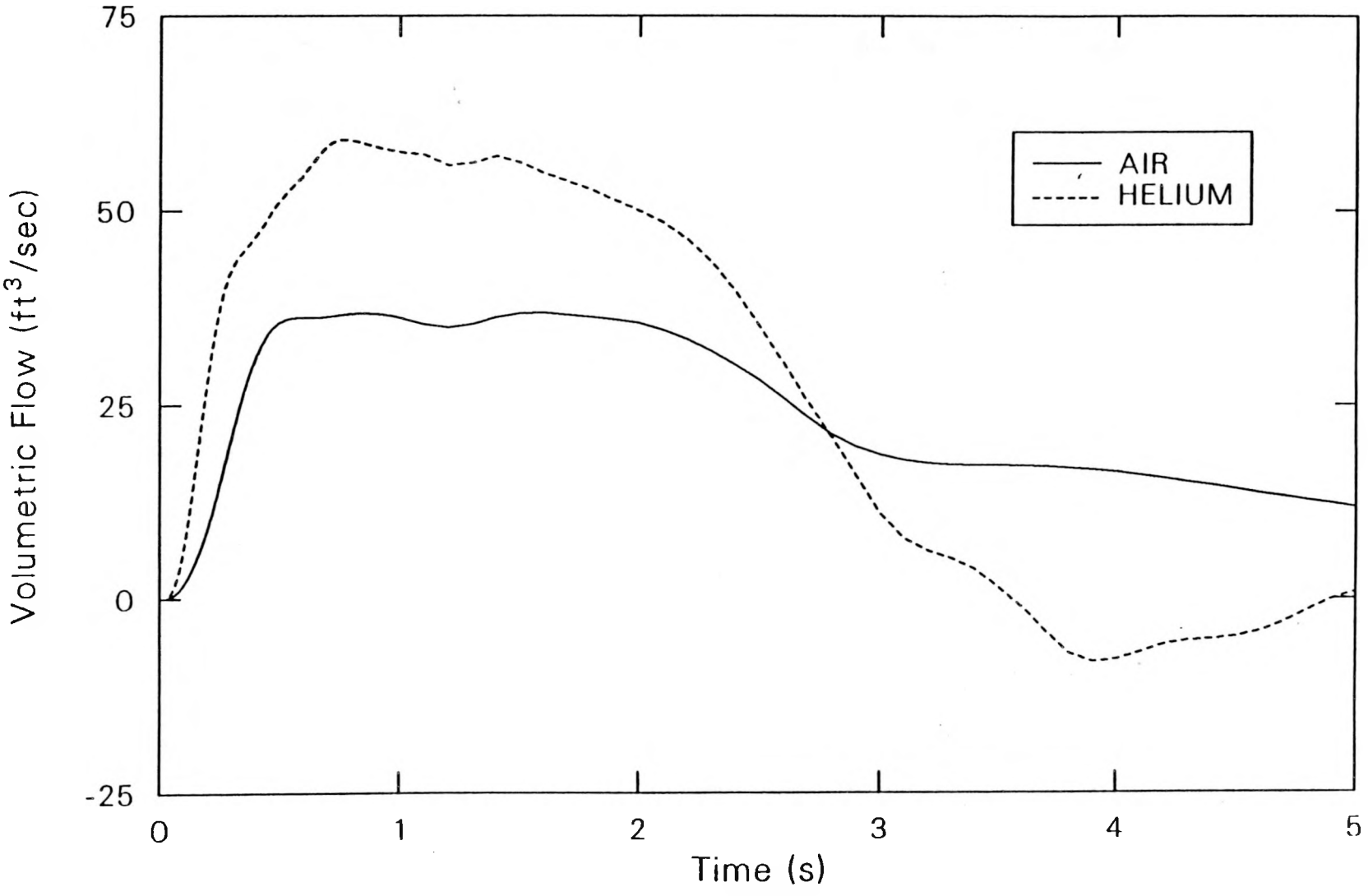

Figure 24. The effect of blanket gas composition on blanket gas flow.

CBD0689-24

TABLE 1. CALCULATED AND MEASURED PROCESS INITIAL CONDITIONS.

Parameter	RELAP5 (K-14.1)	TRAC (K-14.1)	MEASURED (K-13.2)
Core power, MW	1326.0	1326.0	1326.5
Temperature, ^{o}C			
Pump suction loop 1	58.3	58.8	55.1
Pump suction loop 2	57.3	58.3	55.7
Pump suction loop 3	58.9	59.9	56.1
Pump suction loop 4	58.4	58.4	52.8
Pump suction loop 5	58.7	58.1	55.2
Pump suction loop 6	59.0	57.3	55.5
Pump suction average	58.4	58.5	55.1
Plenum inlet loop 1	29.3	29.3	26.4
Plenum inlet loop 2	28.9	29.2	25.3
Plenum inlet loop 3	29.8	29.9	26.7
Plenum inlet loop 4	29.4	28.6	26.0
Plenum inlet loop 5	29.4	28.6	26.4
Plenum inlet loop 6	29.8	29.1	25.9
Plenum inlet average	29.4	29.1	26.3
Average loop temperature rise	29.0	29.4	28.8
Flow, gpm			
Pump 1	26228	26041	NA[1]
Pump 2	26105	26158	NA
Pump 3	26654	26667	NA
Pump 4	26230	25261	NA
Pump 5	26115	25334	NA
Pump 6	26657	26476	NA
Total pump	157989	155937	NA
Septifoil	5931	6591	NA
Plenum pressure, psia			
Ring 1	80.9	77.3[2]	79.4[3]
Ring 2	89.3	85.4	NA
Ring 3	100.5	105.9	NA

1. Not available.

2. Pressure in rings 1, 2, and 3 correspond to the average of TRAC rings 1 and 2, the average of rings 3 and 4, and ring 5, respectively.

3. Measured centerline pressure.

TABLE 2. CALCULATED AND MEASURED INITIAL CONDITIONS FOR THE SECONDARY SIDE OF THE HEAT EXCHANGERS.

Parameter	RELAP5 (K-14.1)	TRAC (K-14.1)	MEASURED (K-13.2)
Temperature, ^{o}C			
Inlet	14.0	15.7	13.2
Outlet	43.6	44.8	43.2
Average temperature rise	29.6	29.1	30.0
Total flow, gpm	155909	155909	170480

APPENDIX A
DETAILED COMPARISON OF THE RELAP5 AND TRAC RESULTS

APPENDIX A
DETAILED COMPARISON OF THE RELAP5 AND TRAC RESULTS

This appendix thoroughly documents the comparisons between the RELAP5 and TRAC calculations described in Section 3.2 of the main body of this report. Figures A-1 through A-54 present comparisons of water plenum pressure, tank bottom pressure, and assembly differential pressure for each ring and sector in the RELAP5 model. The reader is referred to the main body for a discussion of the results.

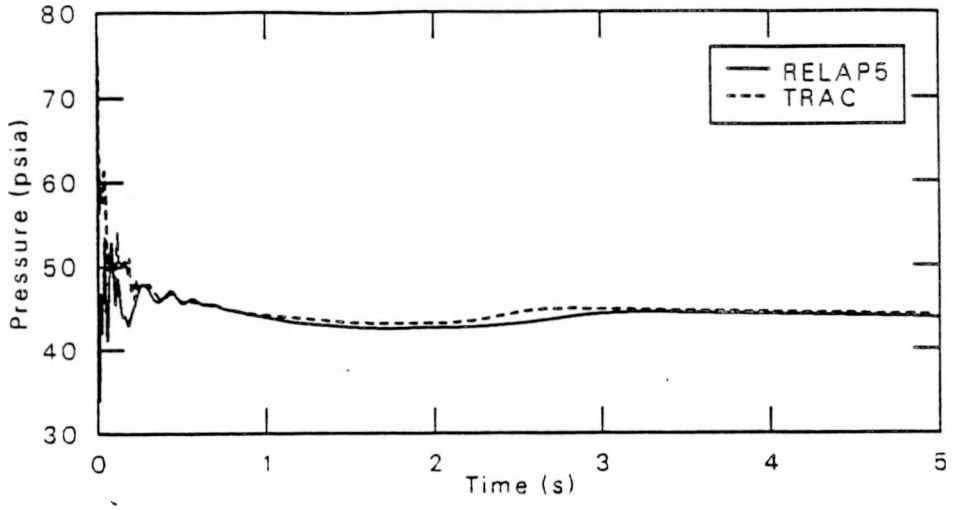

Figure A-1. A comparison of calculated pressures in ring 1 sector 1 of the water plenum.

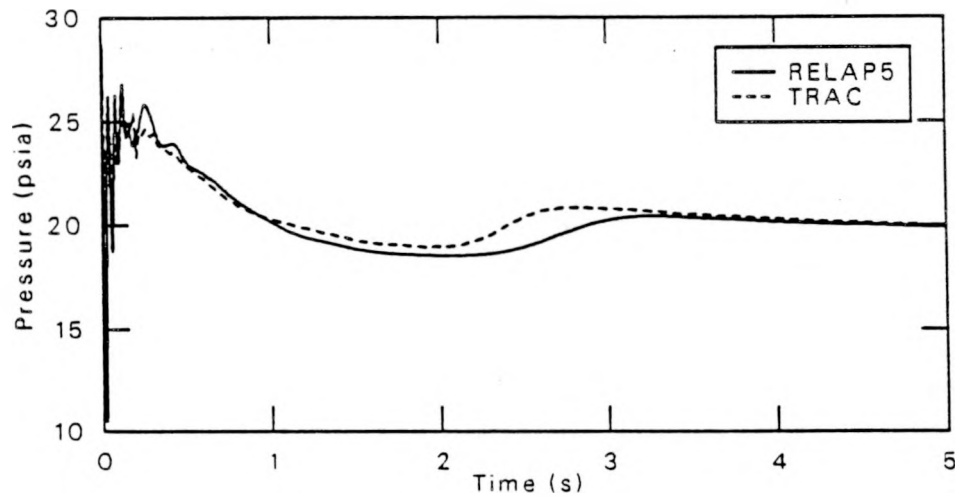

Figure A-2. A comparison of calculated pressures in ring 1 sector 1 at the tank bottom.

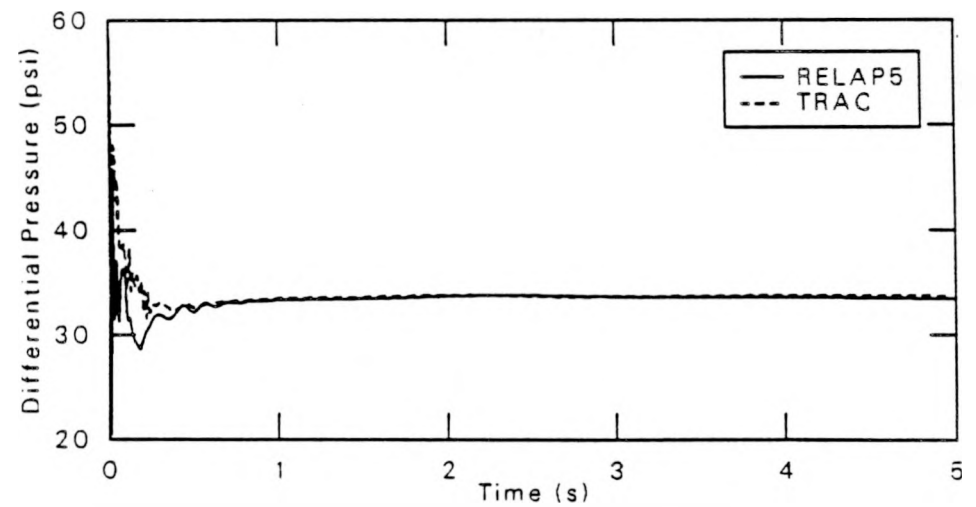

Figure A-3. A comparison of calculated differential pressures across the assemblies in ring 1 sector 1.

CBD0689 A1-3

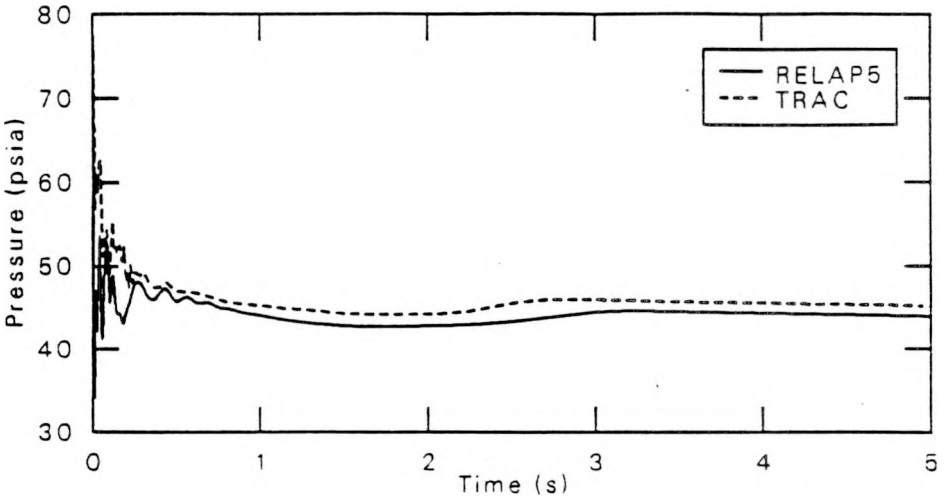

Figure A-4. A comparison of calculated pressures in ring 1 sector 2 of the water plenum.

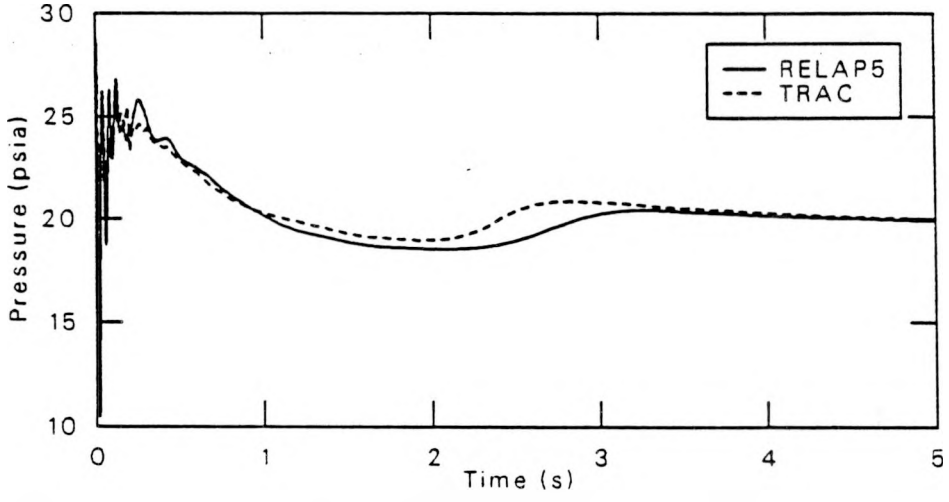

Figure A-5. A comparison of calculated pressures in ring 1 sector 2 at the tank bottom.

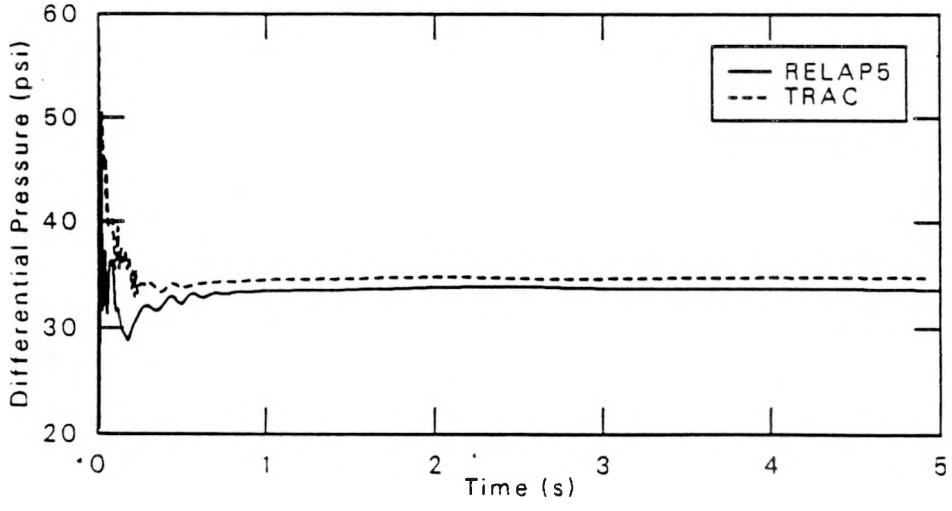

Figure A-6. A comparison of calculated differential pressures across the assemblies in ring 1 sector 2.

CBD0689 A4-6

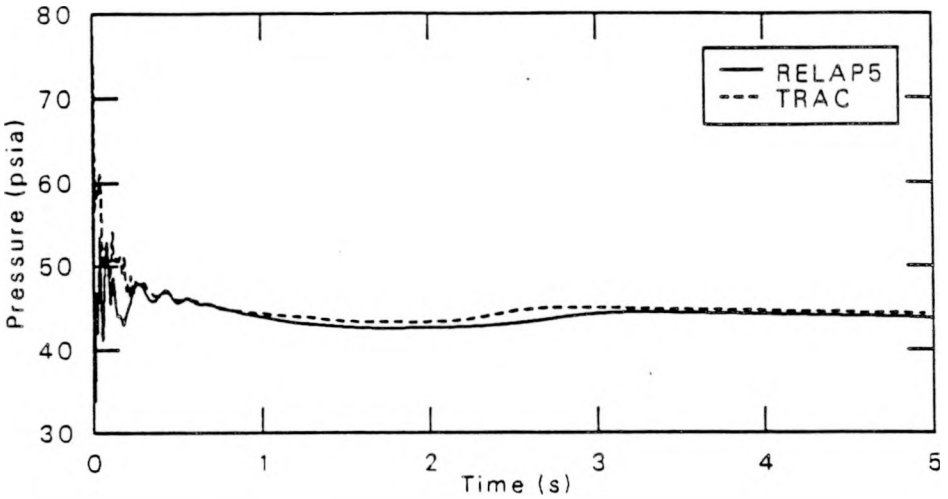

Figure A-7. A comparison of calculated pressures in ring 1 sector 3 of the water plenum.

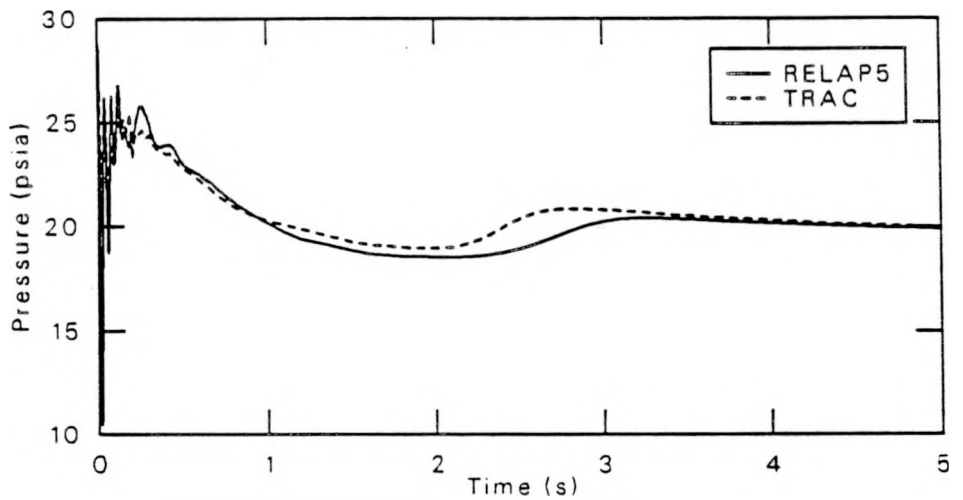

Figure A-8. A comparison of calculated pressures in ring 1 sector 3 at the tank bottom.

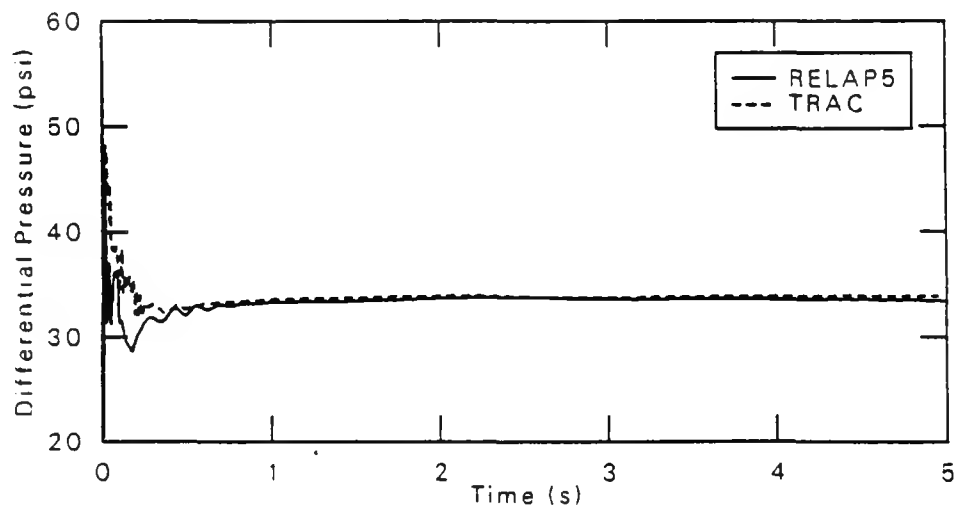

Figure A-9. A comparison of calculated differential pressures across the assemblies in ring 1 sector 3.

CBD0689 A7-9

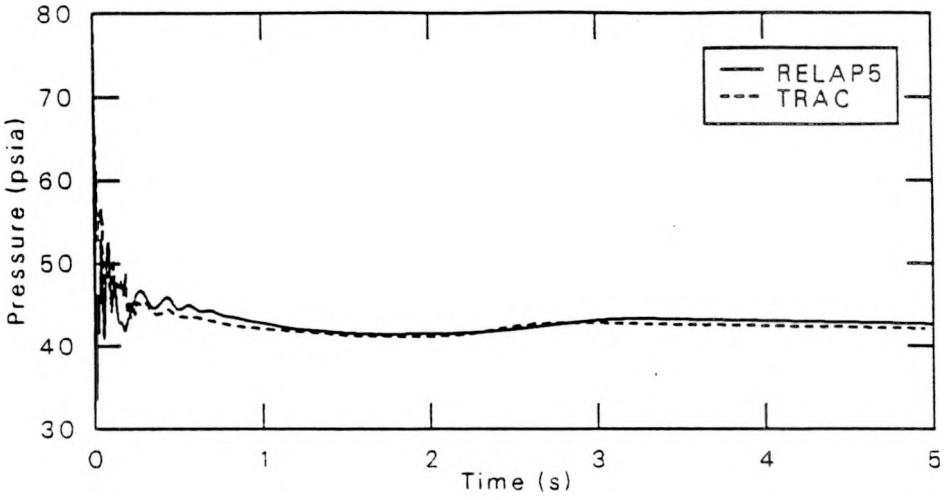

Figure A-10. A comparison of calculated pressures in ring 1 sector 4 of the water plenum.

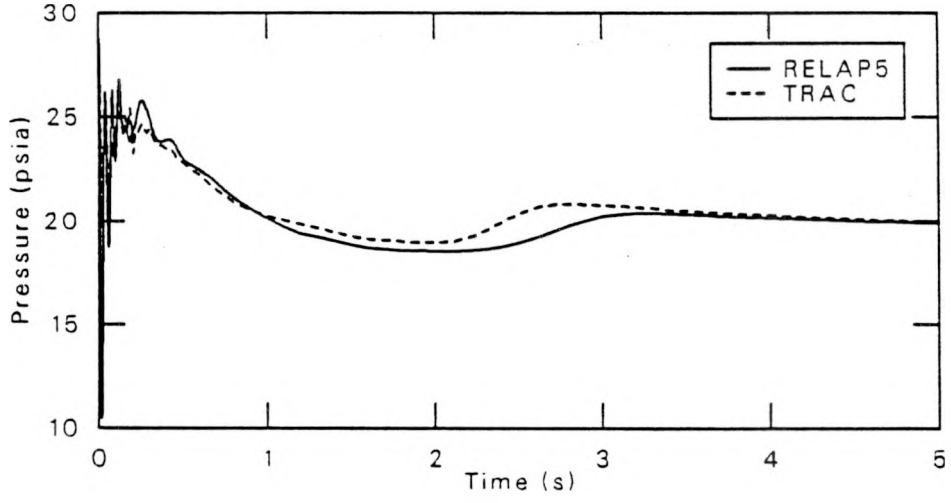

Figure A-11. A comparison of calculated pressures in ring 1 sector 4 at the tank bottom.

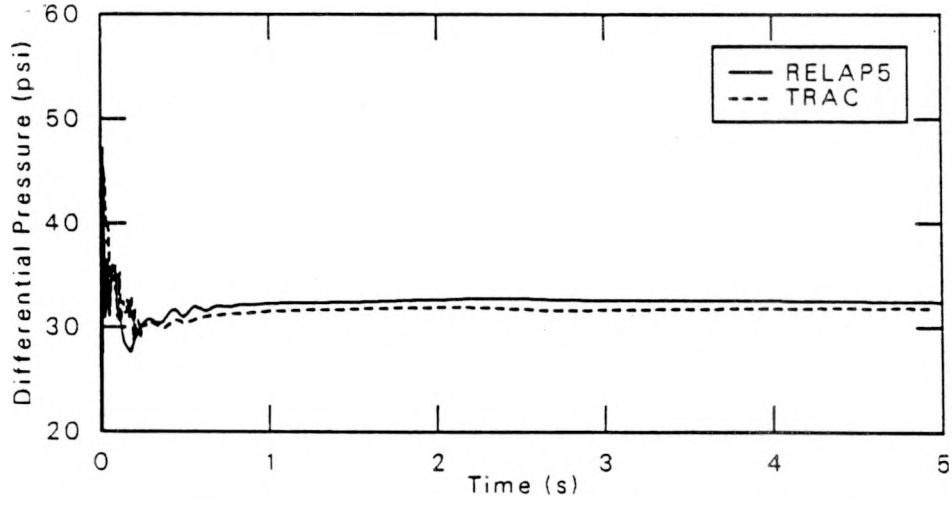

Figure A-12. A comparison of calculated differential pressures across the assemblies in ring 1 sector 4.

CBD0689 A10-12

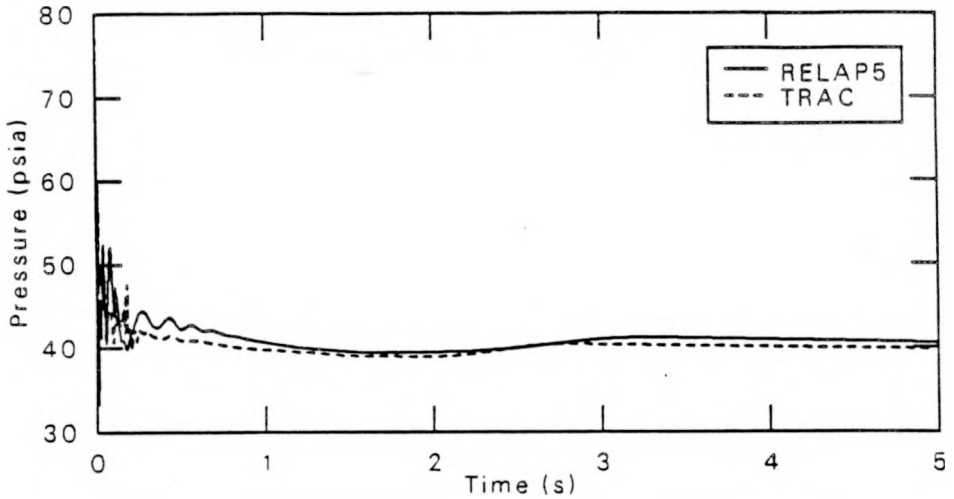

Figure A-13. A comparison of calculated pressures in ring 1 sector 5 of the water plenum.

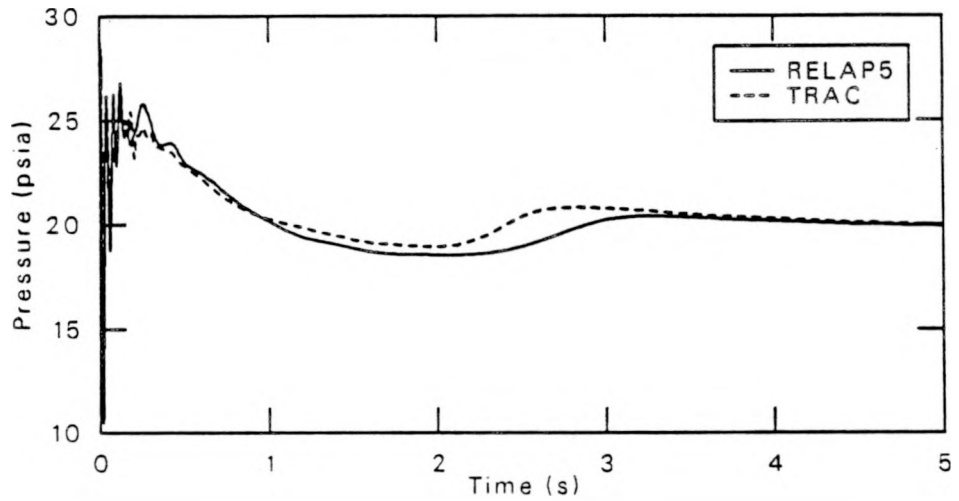

Figure A-14. A comparison of calculated pressures in ring 1 sector 5 at the tank bottom.

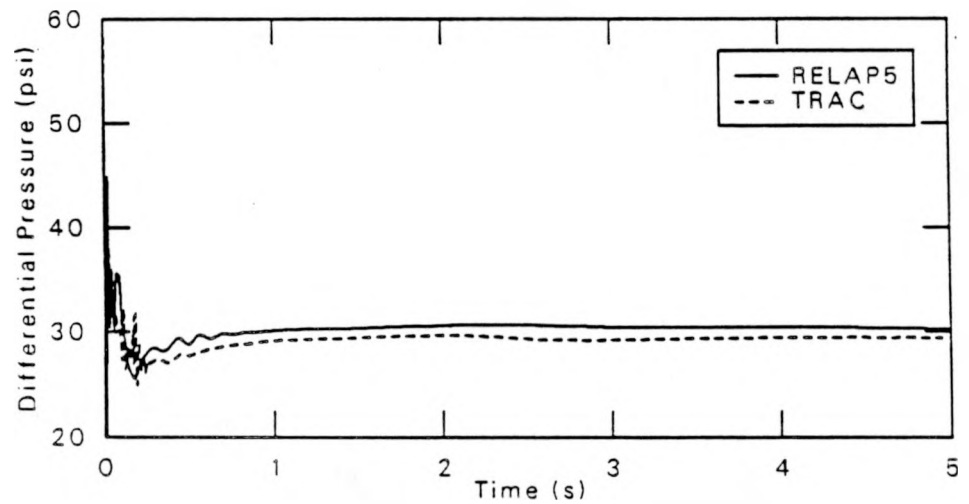

Figure A-15. A comparison of calculated differential pressures across the assemblies in ring 1 sector 5.

CBD0689 A13-15

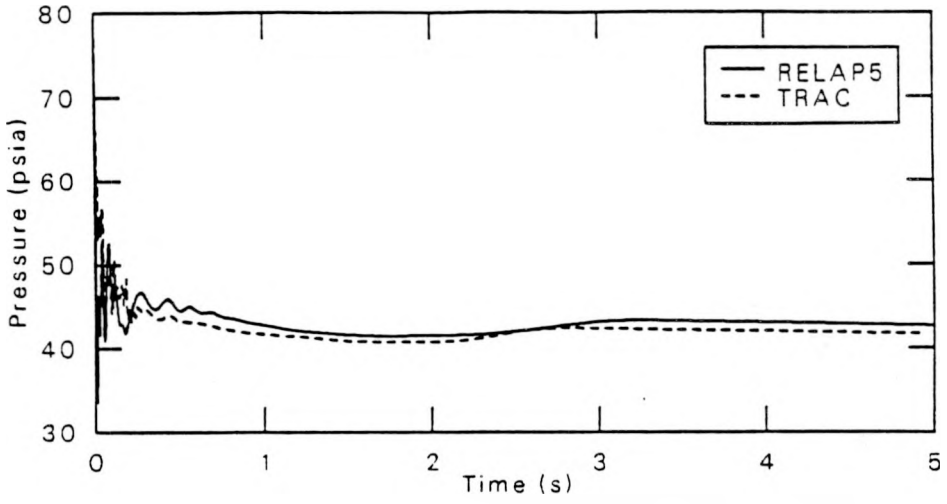

Figure A-16. A comparison of calculated pressures in ring 1 sector 6 of the water plenum.

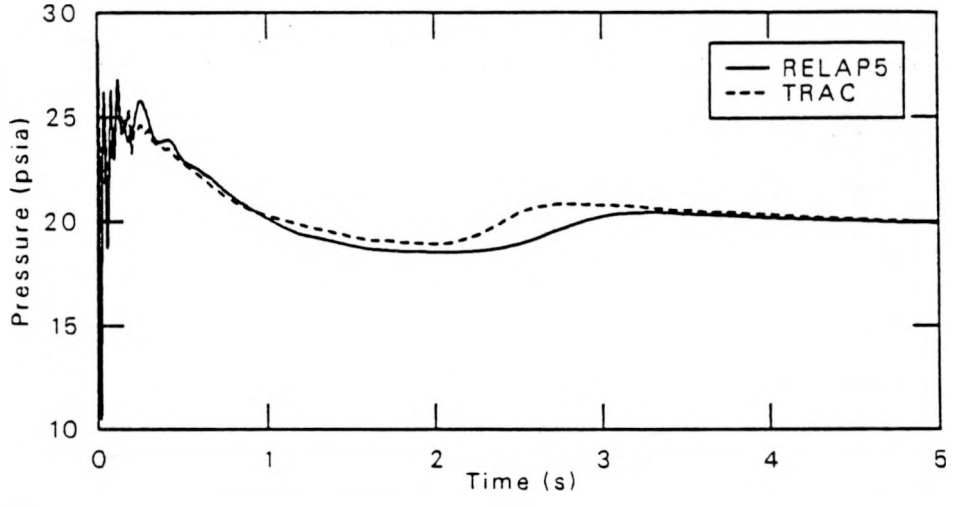

Figure A-17. A comparison of calculated pressures in ring 1 sector 6 at the tank bottom.

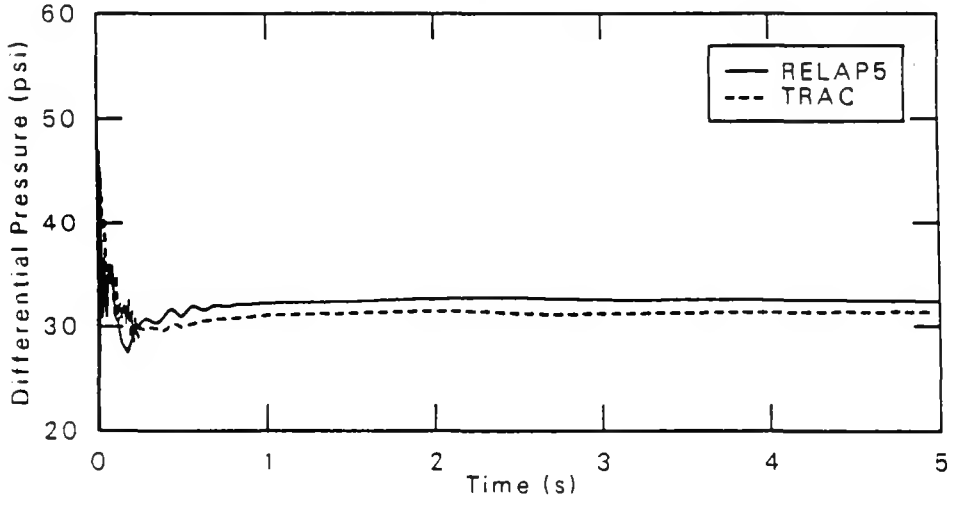

Figure A-18. A comparison of calculated differential pressures across the assemblies in ring 1 sector 6.

CBD0689 A16-18

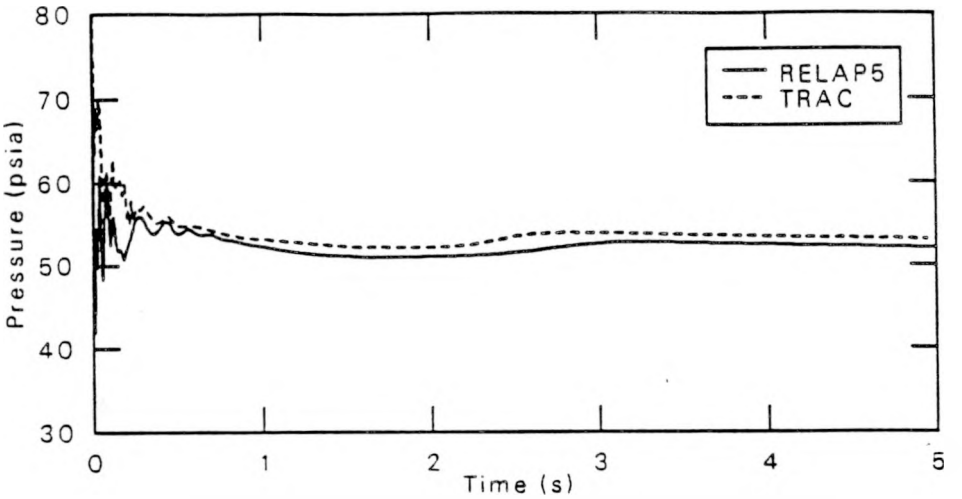

Figure A-19. A comparison of calculated pressures in ring 2 sector 1 of the water plenum.

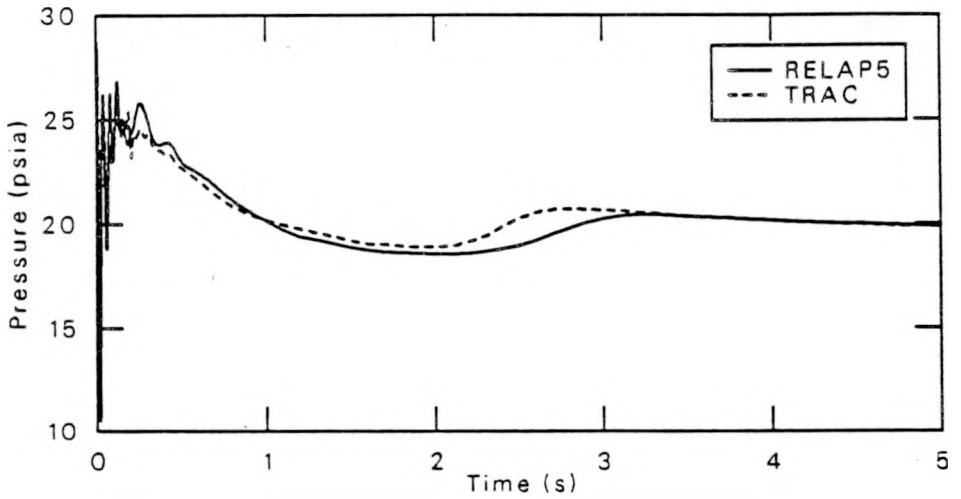

Figure A-20. A comparison of calculated pressures in ring 2 sector 1 at the tank bottom.

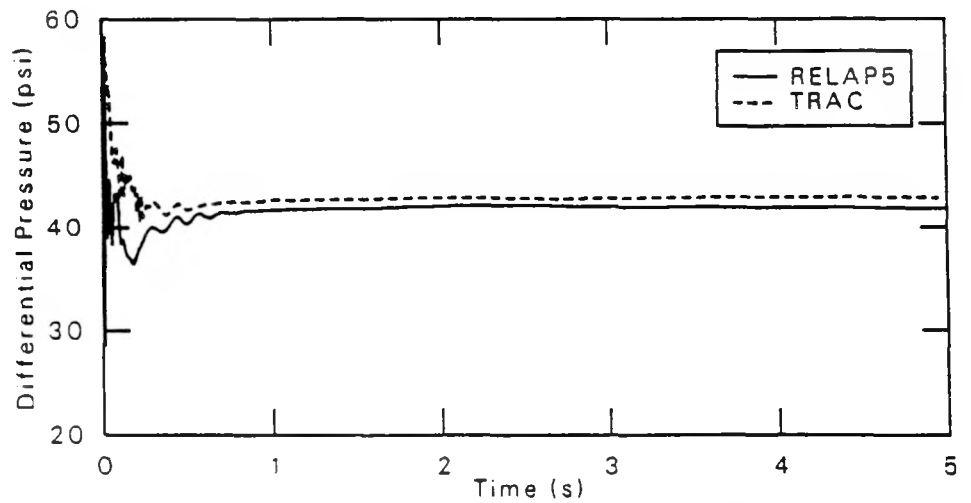

Figure A-21. A comparison of calculated differential pressures across the assemblies in ring 2 sector 1.

CBD0689 A19-21

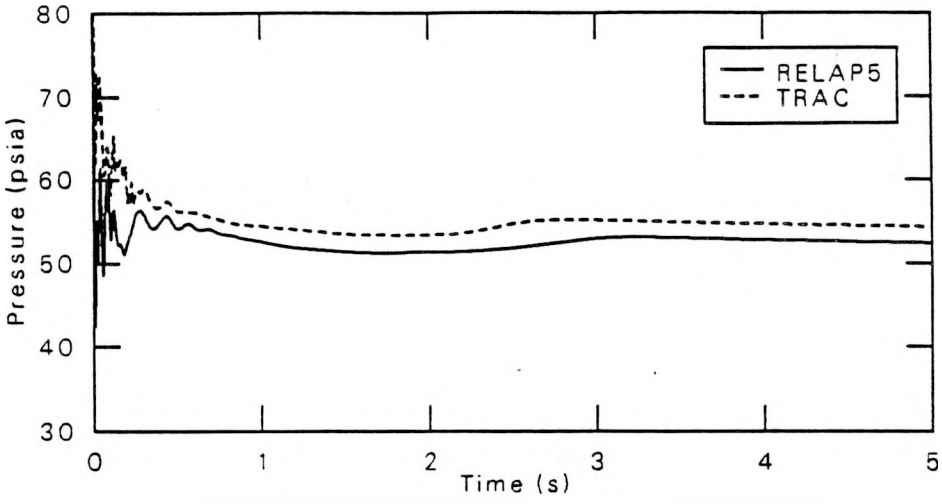

Figure A-22. A comparison of calculated pressures in ring 2 sector 2 of the water plenum.

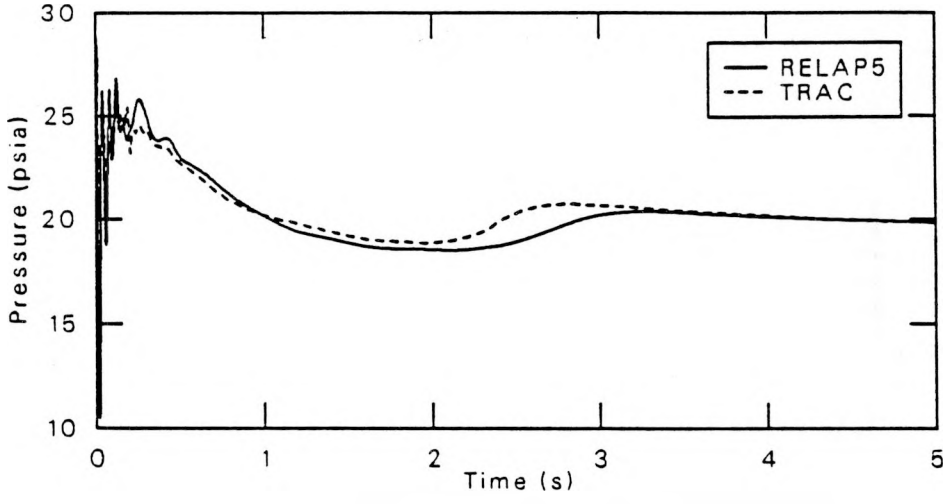

Figure A-23. A comparison of calculated pressures in ring 2 sector 2 at the tank bottom.

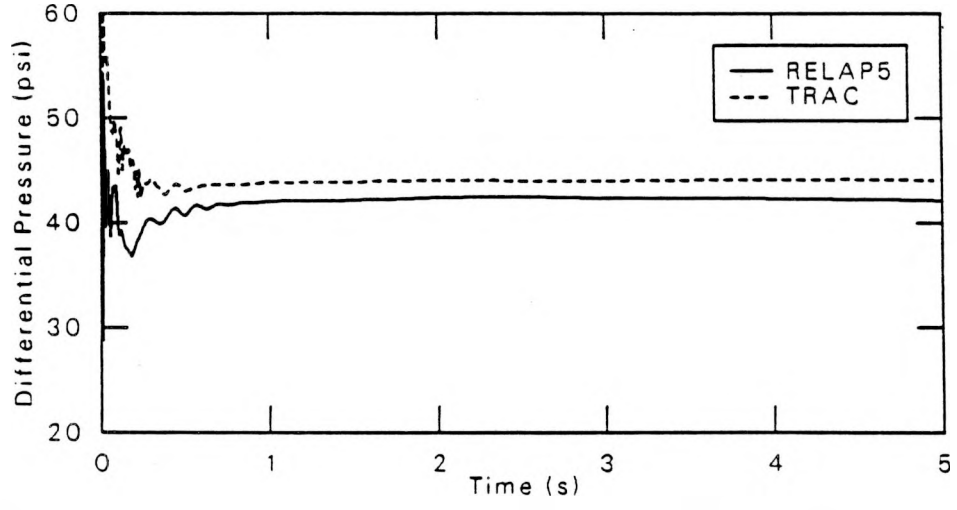

Figure A-24. A comparison of calculated differential pressures across the assemblies in ring 2 sector 2.

CBD0689 A22-24

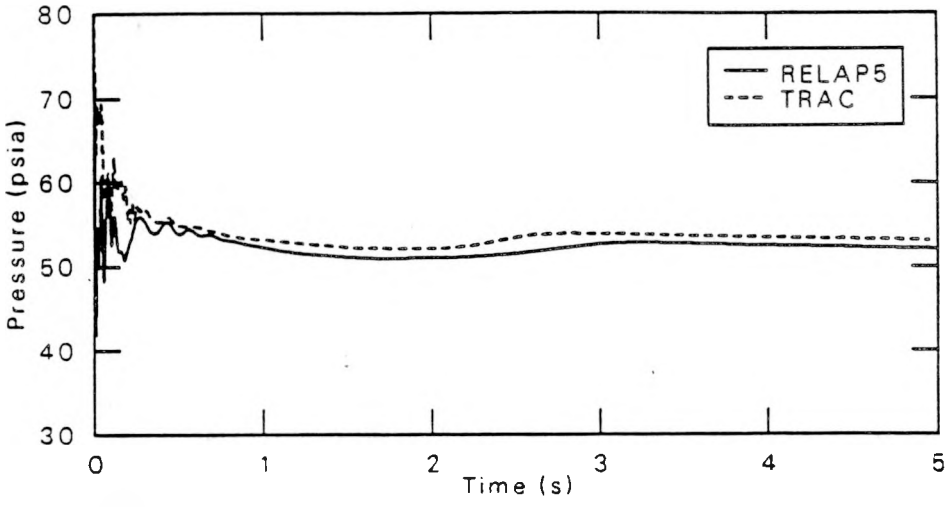

Figure A-25. A comparison of calculated pressures in ring 2 sector 3 of the water plenum.

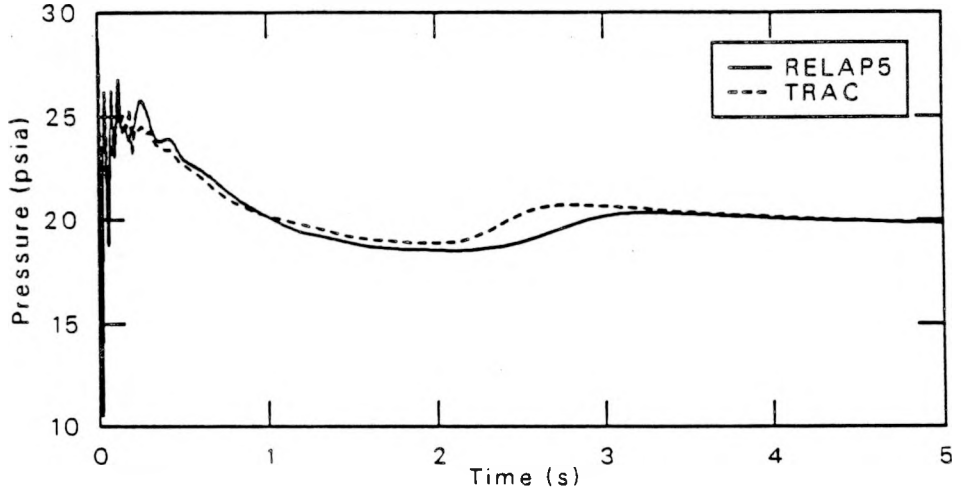

Figure A-26. A comparison of calculated pressures in ring 2 sector 3 at the tank bottom.

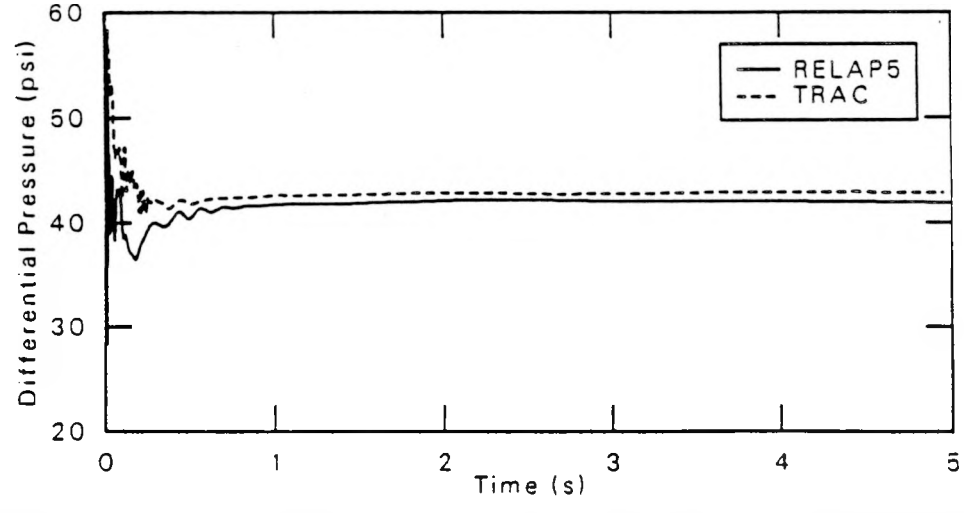

Figure A-27. A comparison of calculated differential pressures across the assemblies in ring 2 sector 3.

CBD0689 A25-27

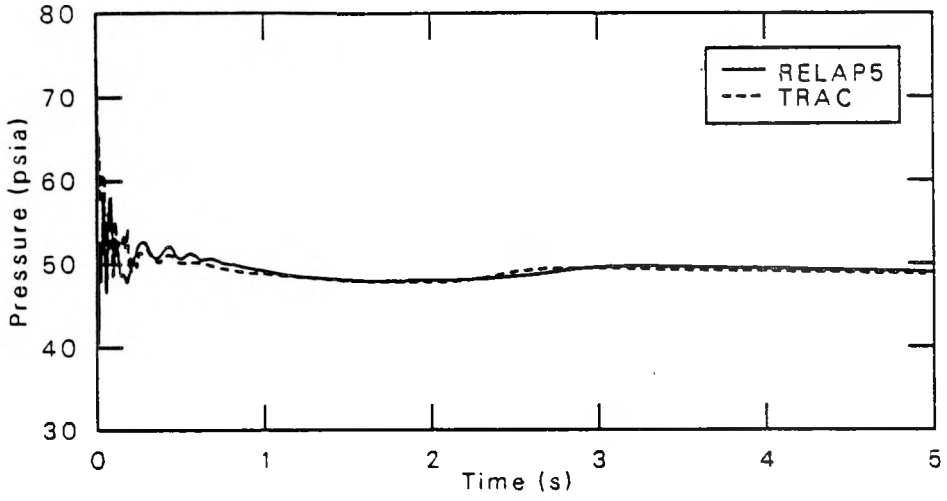

Figure A-28. A comparison of calculated pressures in ring 2 sector 4 of the water plenum.

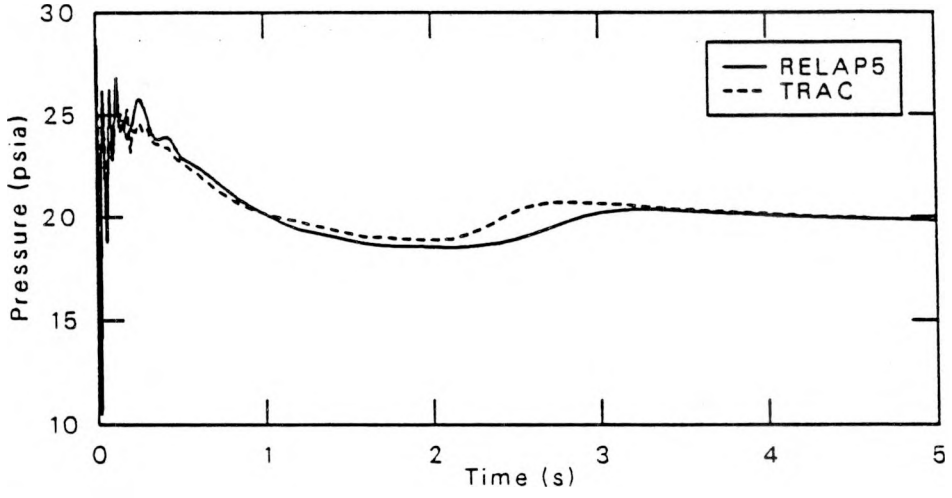

Figure A-29. A comparison of calculated pressures in ring 2 sector 4 at the tank bottom.

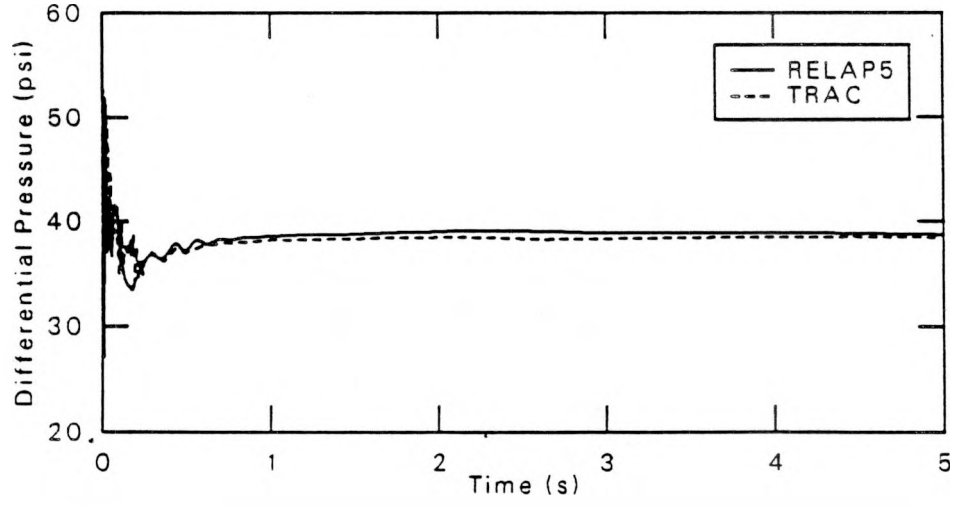

Figure A-30. A comparison of calculated differential pressures across the assemblies in ring 2 sector 4.

C8D0689 A26-30

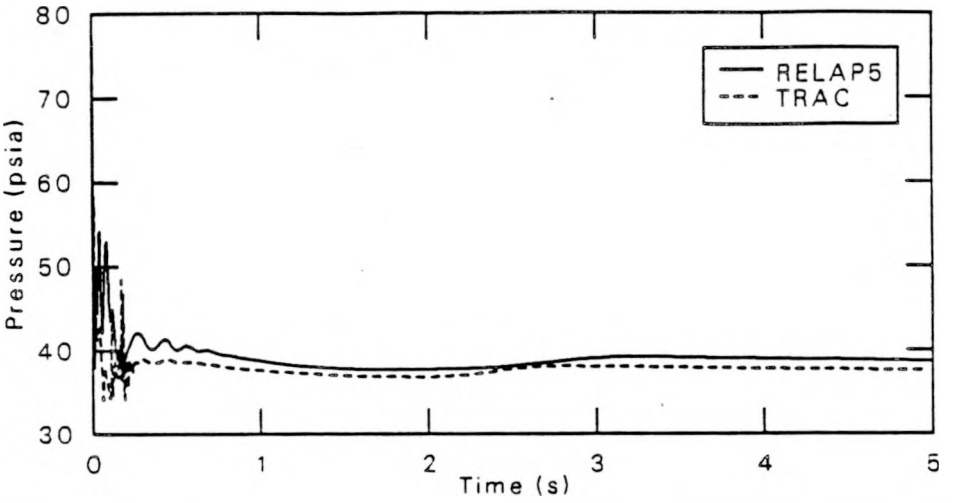

Figure A-31. A comparison of calculated pressures in ring 2 sector 5 of the water plenum.

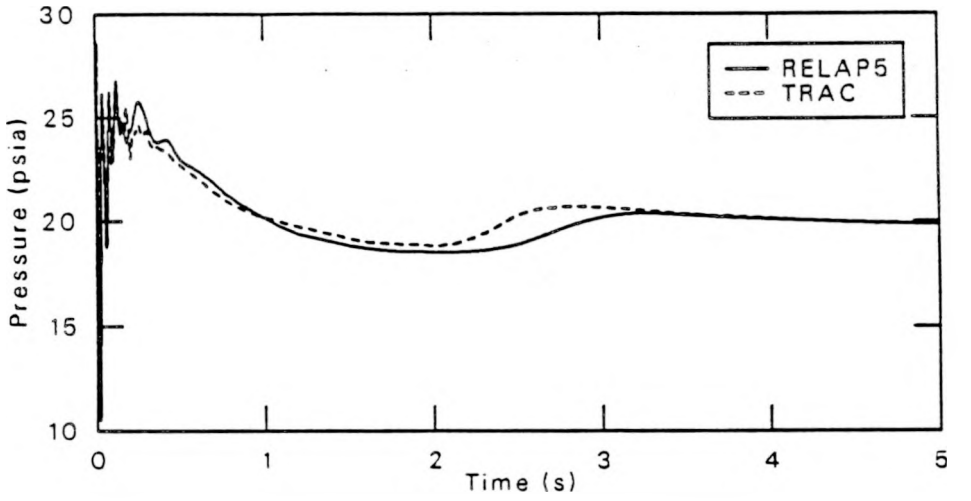

Figure A-32. A comparison of calculated pressures in ring 2 sector 5 at the tank bottom.

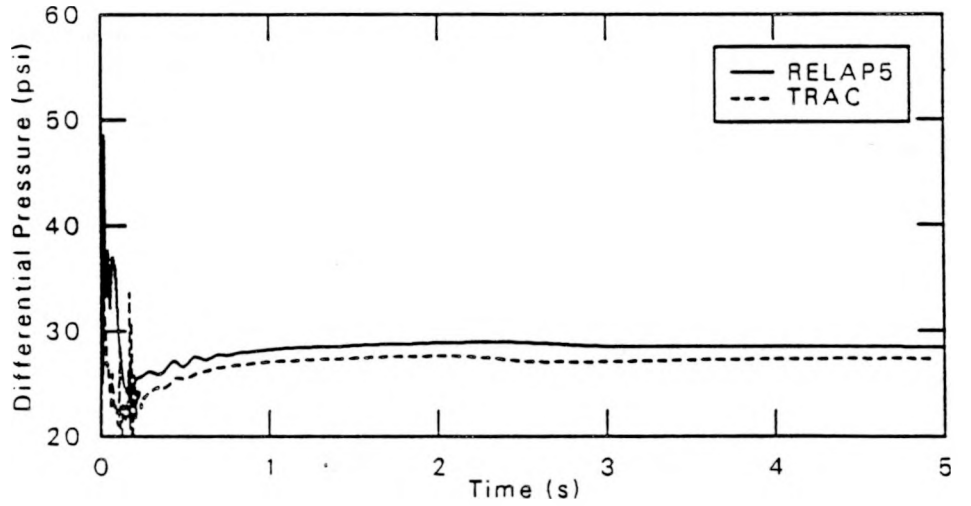

Figure A-33. A comparison of calculated differential pressures across the assemblies in ring 2 sector 5.

C8D0689 A31-33

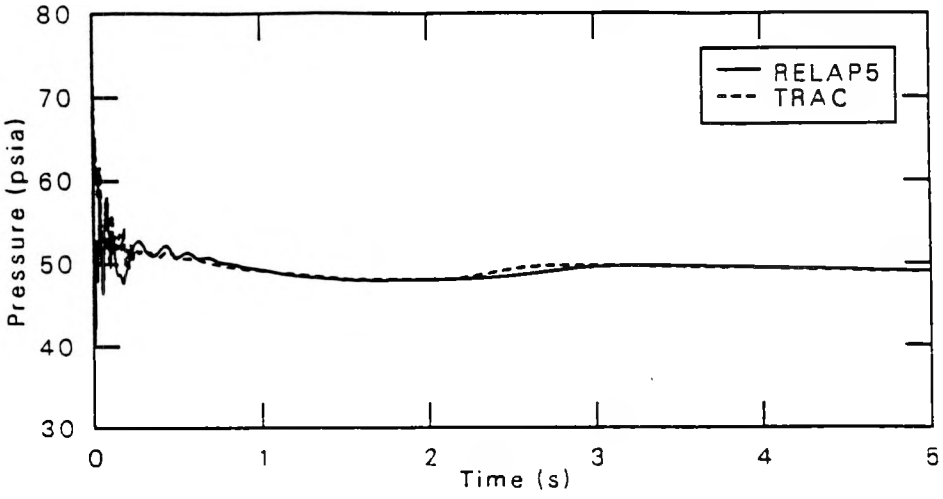

Figure A-34. A comparison of calculated pressures in ring 2 sector 6 of the water plenum.

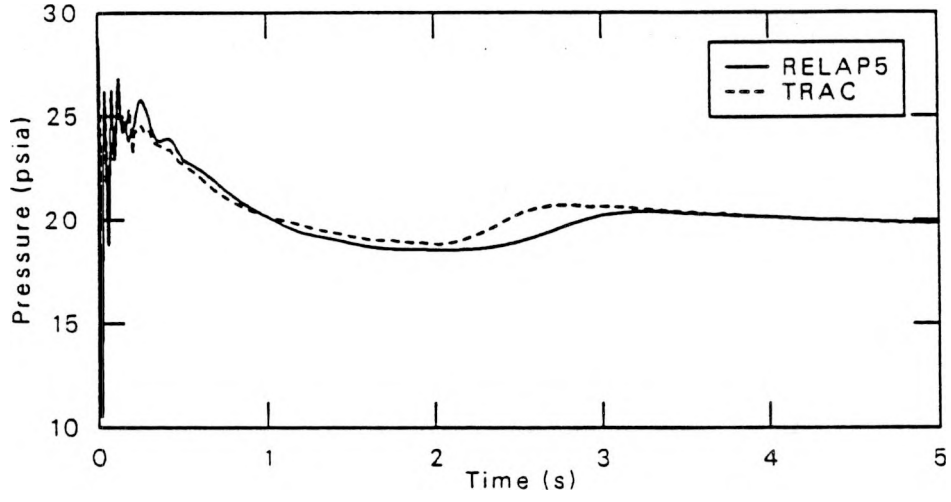

Figure A-35. A comparison of calculated pressures in ring 2 sector 6 at the tank bottom.

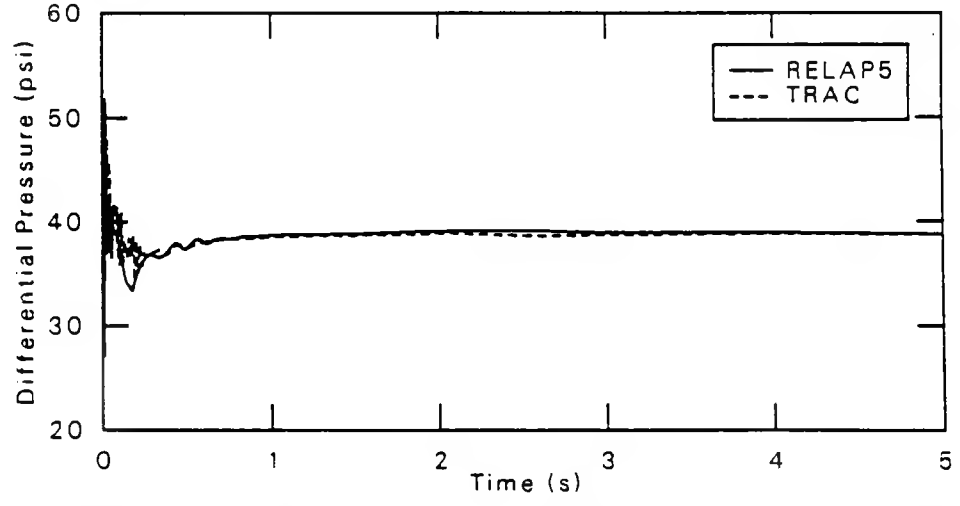

Figure A-36. A comparison of calculated differential pressures across the assemblies in ring 2 sector 6.

CBD0689 A34-36

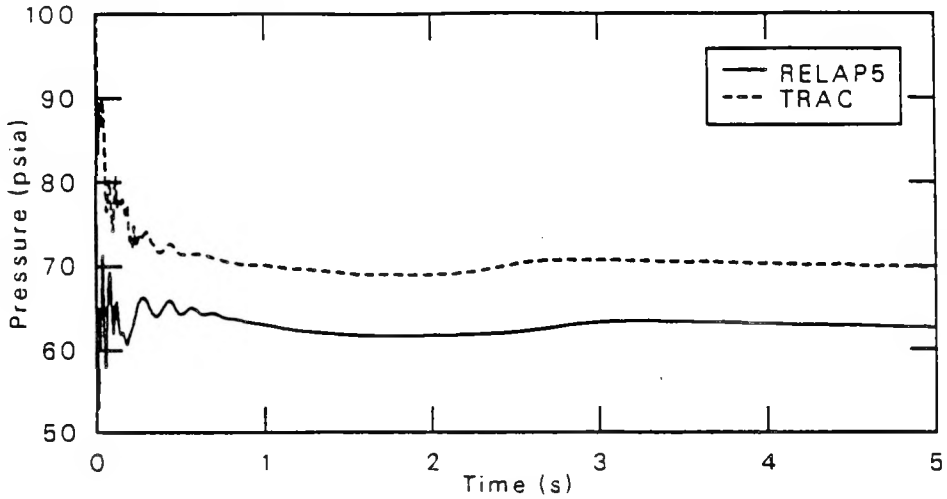

Figure A-37. A comparison of calculated pressures in ring 3 sector 1 of the water plenum.

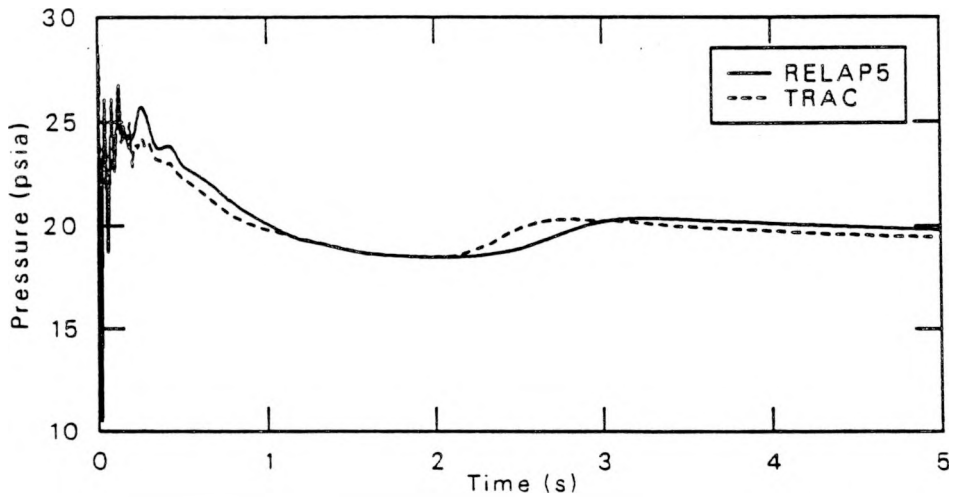

Figure A-38. A comparison of calculated pressures in ring 3 sector 1 at the tank bottom.

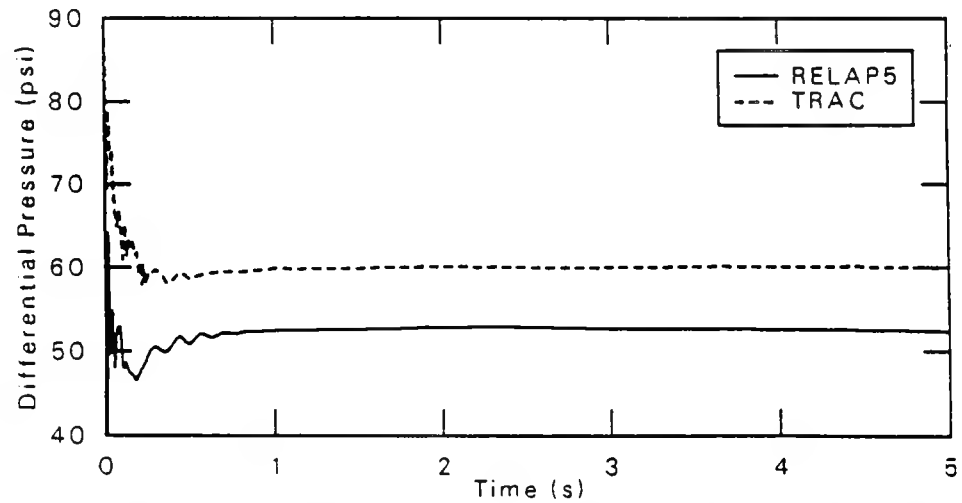

Figure A-39. A comparison of calculated differential pressures across the assemblies in ring 3 sector 1.

CBD0689 A37-39

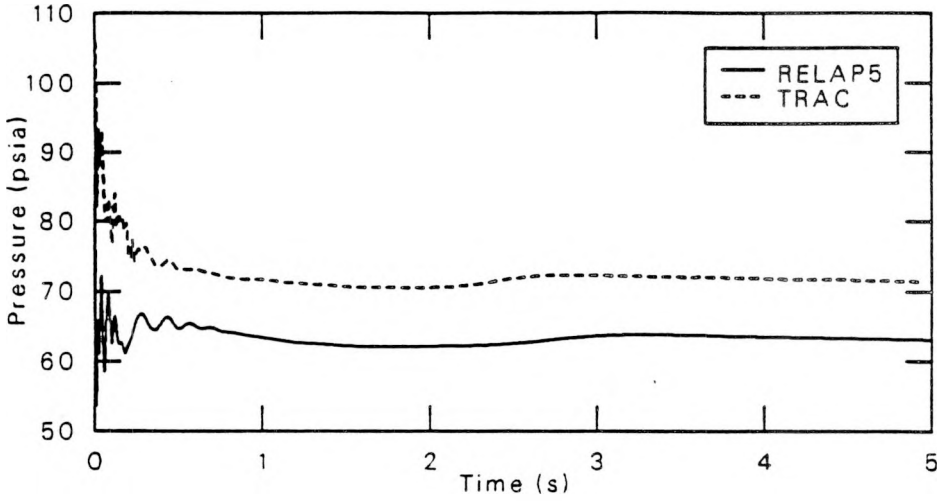

Figure A-40. A comparison of calculated pressures in ring 3 sector 2 of the water plenum.

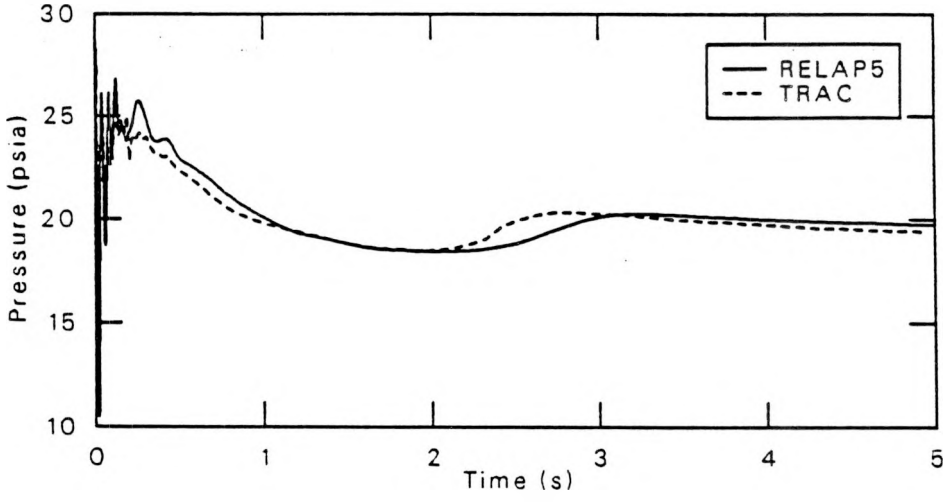

Figure A-41. A comparison of calculated pressures in ring 3 sector 2 at the tank bottom.

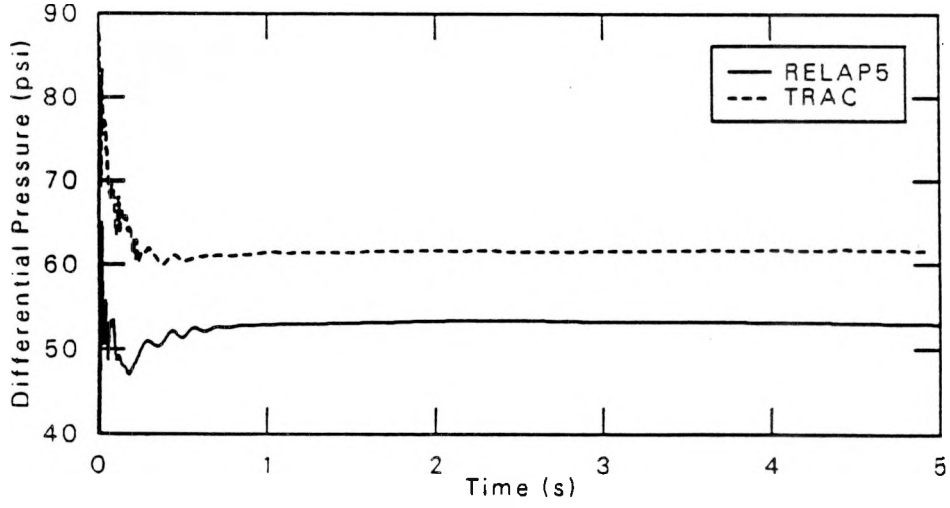

Figure A-42. A comparison of calculated differential pressures across the assemblies in ring 3 sector 2.

CBD0689 A40-42

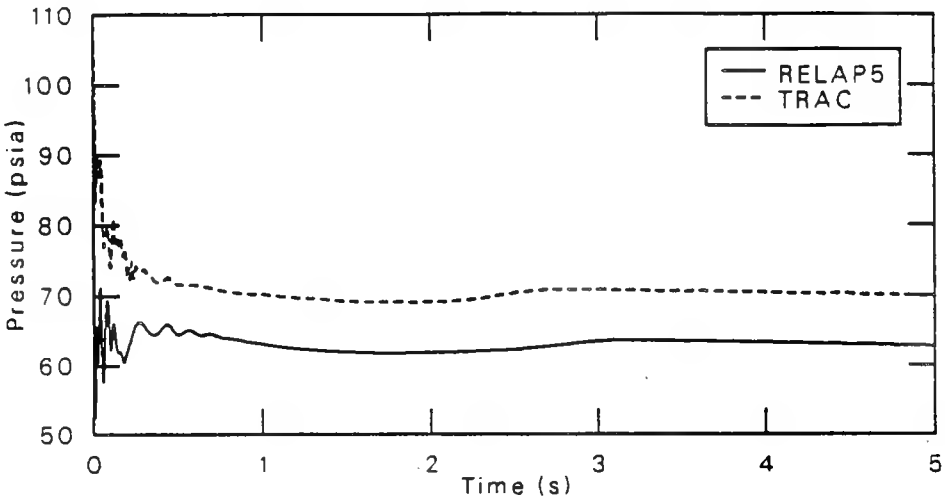

Figure A-43. A comparison of calculated pressures in ring 3 sector 3 of the water plenum.

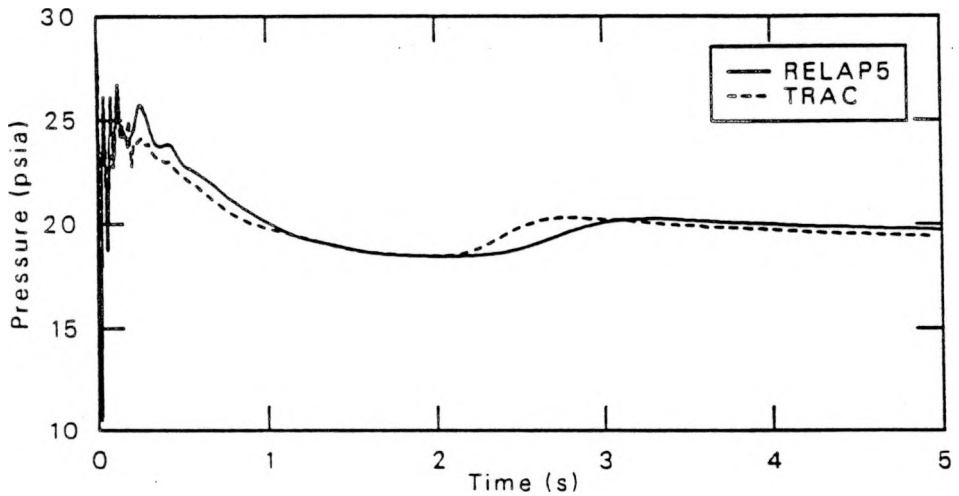

Figure A-44. A comparison of calculated pressures in ring 3 sector 3 at the tank bottom.

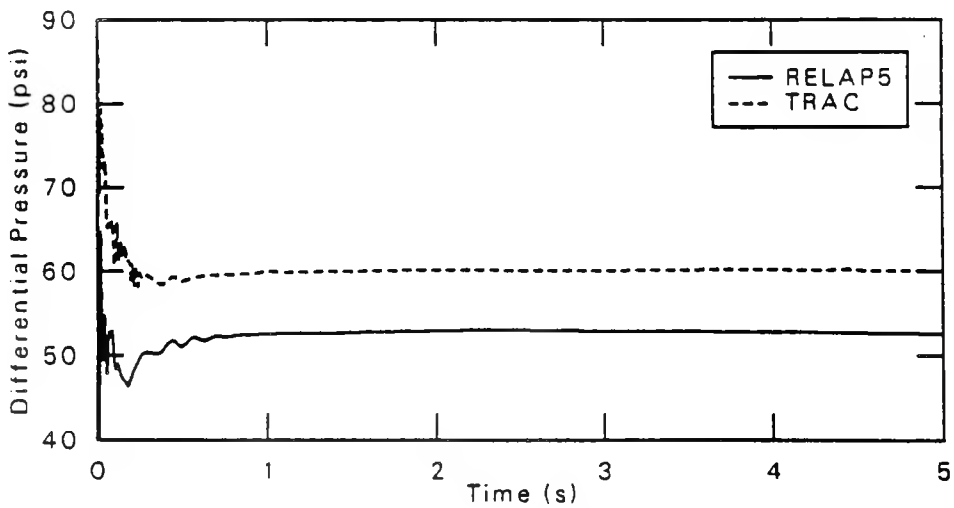

Figure A-45. A comparison of calculated differential pressures across the assemblies in ring 3 sector 3.

CBD0689 A43-45

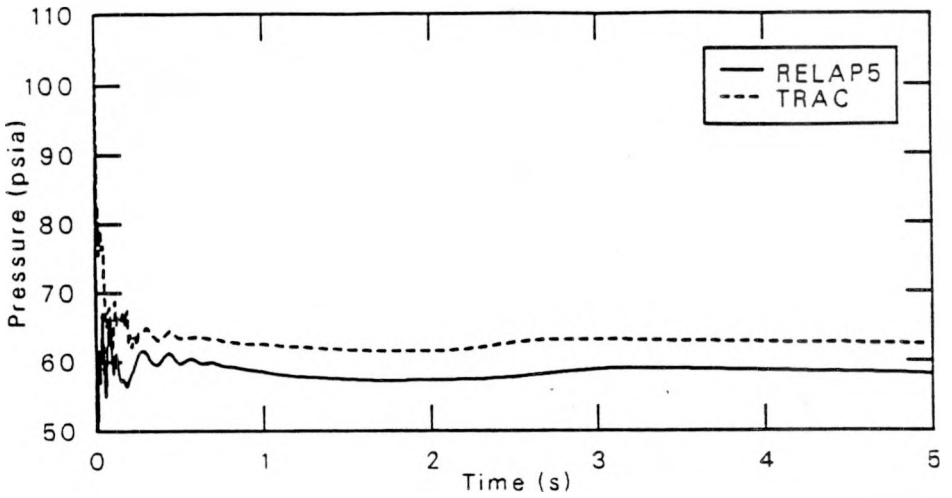

Figure A-46. A comparison of calculated pressures in ring 3 sector 4 of the water plenum.

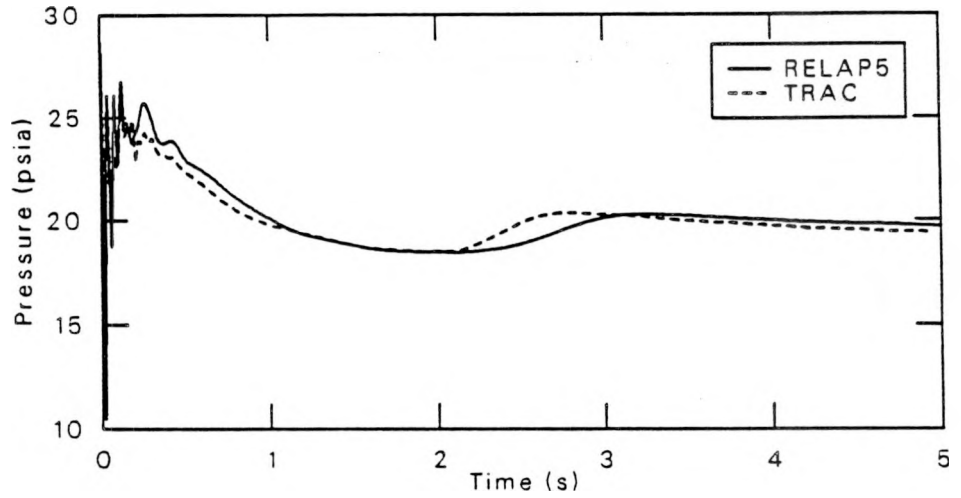

Figure A-47. A comparison of calculated pressures in ring 3 sector 4 at the tank bottom.

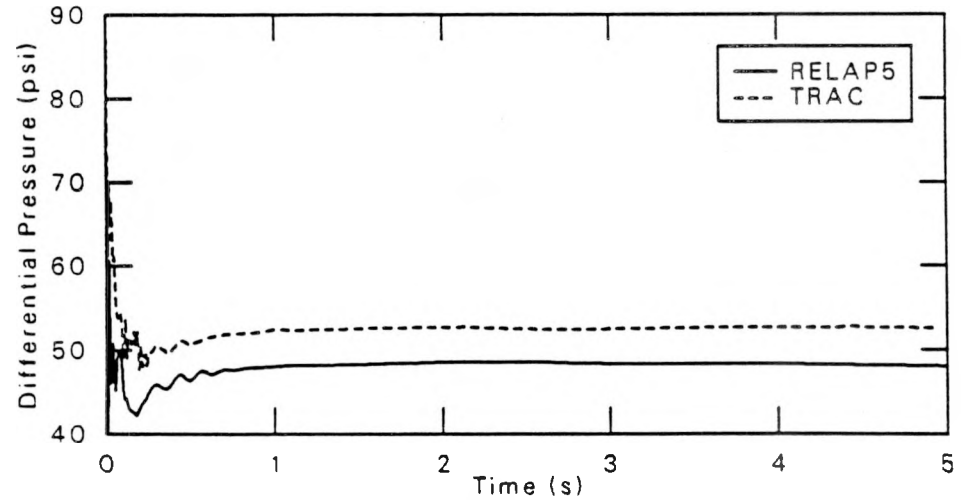

Figure A-48. A comparison of calculated differential pressures across the assemblies in ring 3 sector 4.

CBD0689 A46-48

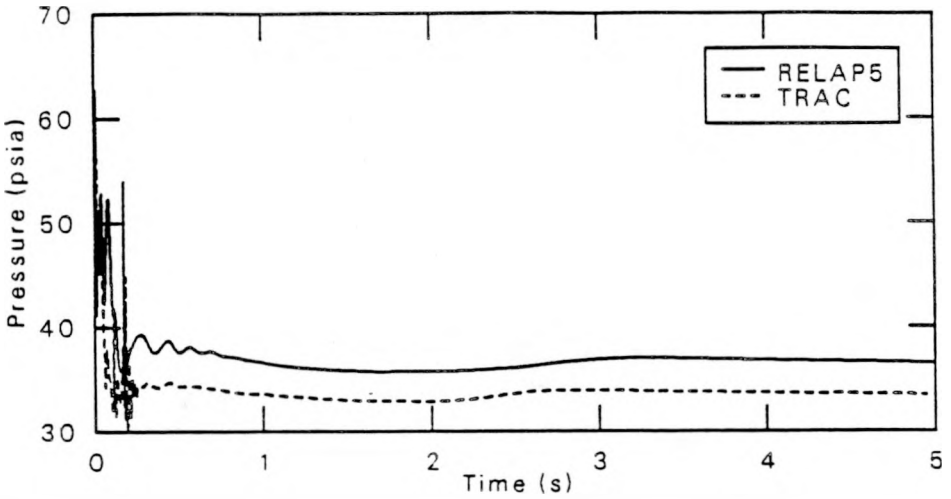

Figure A-49. A comparison of calculated pressures in ring 3 sector 5 of the water plenum.

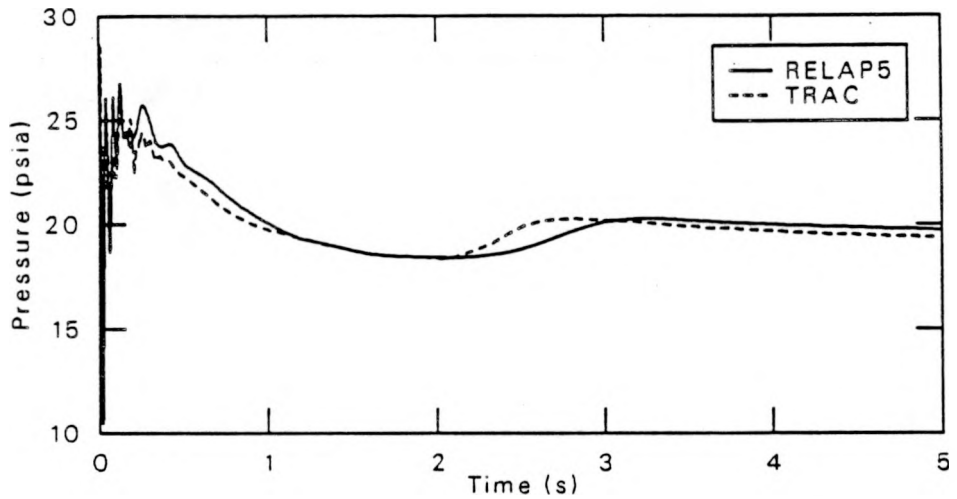

Figure A-50. A comparison of calculated pressures in ring 3 sector 5 at the tank bottom.

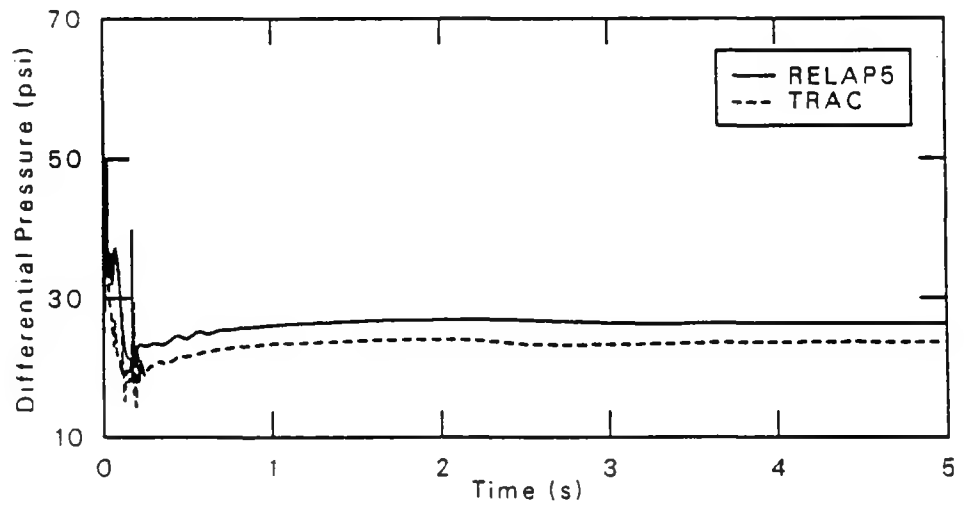

Figure A-51. A comparison of calculated differential pressures across the assemblies in ring 3 sector 5.

C8D0689 A49-51

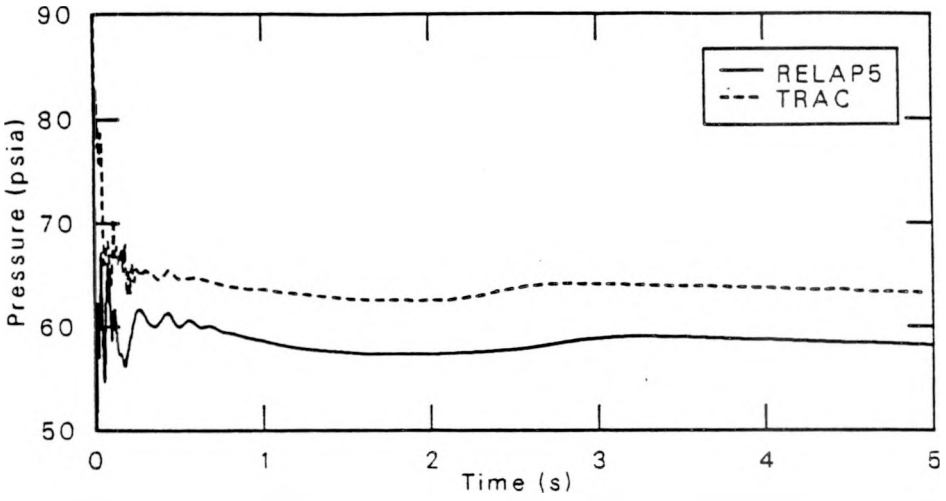

Figure A-52. A comparison of calculated pressures in ring 3 sector 6 of the water plenum.

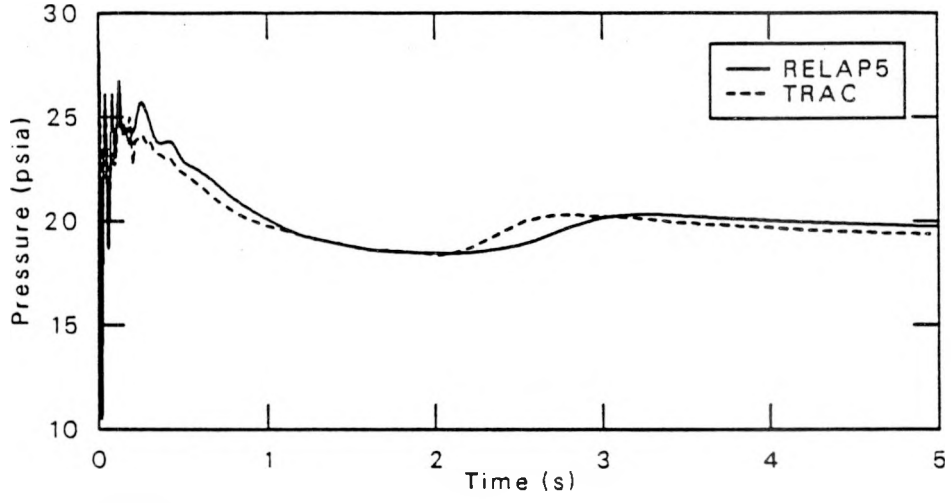

Figure A-53. A comparison of calculated pressures in ring 3 sector 6 at the tank bottom.

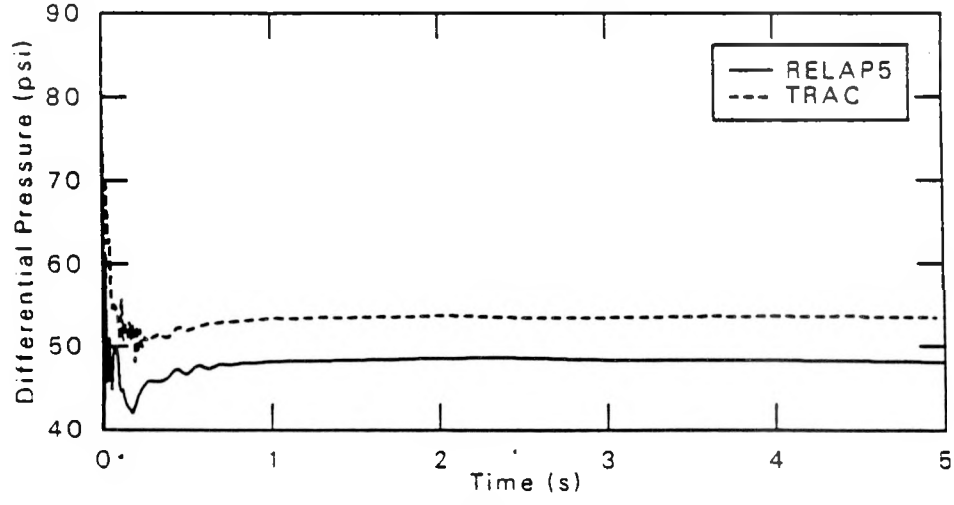

Figure A-54. A comparison of calculated differential pressures across the assemblies in ring 3 sector 6.

CBD0689 A52-54

APPENDIX B
GAS EXPANSION HAND CALCULATIONS

APPENDIX B
GAS EXPANSION HAND CALCULATIONS

Hand calculations were performed to estimate the effective polytropic coefficient based on the gas expansion calculated by RELAP5 and to determine the maximum possible bias in the RELAP5 calculations described in the main body of this report. The hand calculations, which were based on a volume balance, represented the expansion of the gas in the gas plenum and also accounted for the gas flowing into the plenum from other sources, such as the blanket gas system.

Consider the situation illustrated in Figure B-1. At time t_o, the blanket gas is at equilibrium and at pressure P_o. Suppose that at some final time, t_f, the gas volume has increased by an amount ΔV because of a break elsewhere in the system. The purpose of the hand calculations is to determine the final gas pressure, P_f, at time t_f. For ease of analysis, the blanket gas is divided into three components: the gas initially in the gas plenum, which occupies volume V_{ao}, the gas which will flow into the plenum between times t_o and t_f, which initially occupies volume V_{bo}, and the remainder of the blanket gas. It is assumed that the gas initially in the plenum and the gas that will enter the plenum expand identically and that this expansion may be represented with a polytropic coefficient, k, as

$$P_o \, V_{ao}{}^k = P_f \, V_{af}{}^k \qquad \text{(B-1)}$$

and

$$P_o \, V_{bo}{}^k = P_f \, V_{bf}{}^k \qquad \text{(B-2)}$$

The final gas volume within the plenum may be written as

$$V_{af} + V_{bf} = V_{ao} + \Delta V \qquad \text{(B-3)}$$

where V_{af} and V_{bf} are the final volumes of the two gas components

after expansion. Solving for P_f, one obtains

$$P_f = P_o \left[(V_{ao} + V_{bo}) / (V_{ao} + \Delta V) \right]^k \quad \text{(B-4)}$$

where the quantity inside the brackets is simply the initial gas volume divided by the final gas volume. Solving for the polytropic coefficient, one obtains

$$k = [\ln (P_f/P_o)] / \ln [(V_{ao} + V_{bo})/(V_{ao} + \Delta V)] \quad \text{(B-5)}$$

Equation B-5 was used to estimate the effective polytropic coefficient from the expansion calculated by RELAP5. t_o and t_f were chosen to be 0.0 and 1.5 s into the loss-of-coolant accident, respectively. The value for t_f was selected as the approximate time at which the flow instability power limits would be set. V_{bo} was calculated by integrating the gas mass flow rates into the plenum from the blanket gas system, the vacuum breakers, and the U-tube between 0.0 and 1.5 s, summing and then dividing by the gas density at 0.0 s. Note that between 0.0 and 1.5 s, the gas flow from the vacuum breaker and the U-tube represents flow of gas initially trapped between the gas plenum and the corresponding water seals and does not represent clearing of the vent path. ΔV was calculated as the integrated volumetric flow out the breaks less the volume of liquid entering the gas plenum from the vacuum breakers and the gas ports. The volume of liquid was calculated by integrating the liquid mass flow rates between 0.0 and 1.5 s, summing and then dividing by the liquid density. A small, additional term representing the volume of gas entering the moderator tank from the gas ports, which cleared at about 1 s in the calculations, was also subtracted from ΔV. The gas from the gas ports was treated differently than the gas from the other sources because it was initially at atmospheric pressure rather than at gas plenum pressure (19.7 psia) and thus did not experience the same expansion. Specifically, the small, additional term was calculated by integrating the gas mass flow rate from the gas ports between 0.0 and 1.5 s and then divided by the gas density at atmospheric pressure.

The calculations of V_{bo} and ΔV described above were combined with Equation B-5 to determine the effective polytropic coefficients from the RELAP5 calculated expansions. The results of the hand calculations for air

and helium were polytropic coefficients of 1.11 and 1.09, respectively. The hand calculations showed that the expansion calculated by RELAP5 was nearly isothermal.

Hand calculations were also performed to bound the maximum bias in the gas plenum pressures calculated by RELAP5. A bounding pressure was obtained by using Equation B-4 with the polytropic coefficients set to the isentropic values: 1.40 for air and 1.66 for helium. t_f was again chosen to be 1.5 s, and V_{bo} and ΔV were calculated as described previously. According to the hand calculations, isentropic expansions resulted in gas plenum pressures at 1.5 s that were 1.4 and 2.4 psi lower than calculated with RELAP5 for air and helium, respectively. Thus, 1.4 and 2.4 psi represent upper bounds on the possible bias in the RELAP5 calculated gas plenum pressures at 1.5 s based on the uncertainty in the type of gas expansion (isentropic versus nearly isothermal). The 1.4 and 2.4 psi biases are upper bounds for two reasons. First, an isentropic expansion bounds the possible expansions. Second, the increase in flow from the blanket gas system that would accompany the lower gas plenum pressures resulting from an isentropic expansion was not accounted for.

The uncertainty associated with the gas expansion calculated by RELAP5 is a function of pressure and thus time. The uncertainty in the calculated pressure generally increases with time because the difference between isentropic and isothermal expansions increases with final gas volume. Thus, the bias in pressure before 1.5 s would be less than the values obtained at 1.5 s. The uncertainty in the calculated gas pressure also decreases significantly after the the vacuum breakers clear near 2.0 s. After the vacuum breakers clear, the gas pressure is no longer controlled by the gas expansion but instead returns to near atmospheric pressure because the gas flow through the vacuum breakers is sufficient to compensate for the break flow.

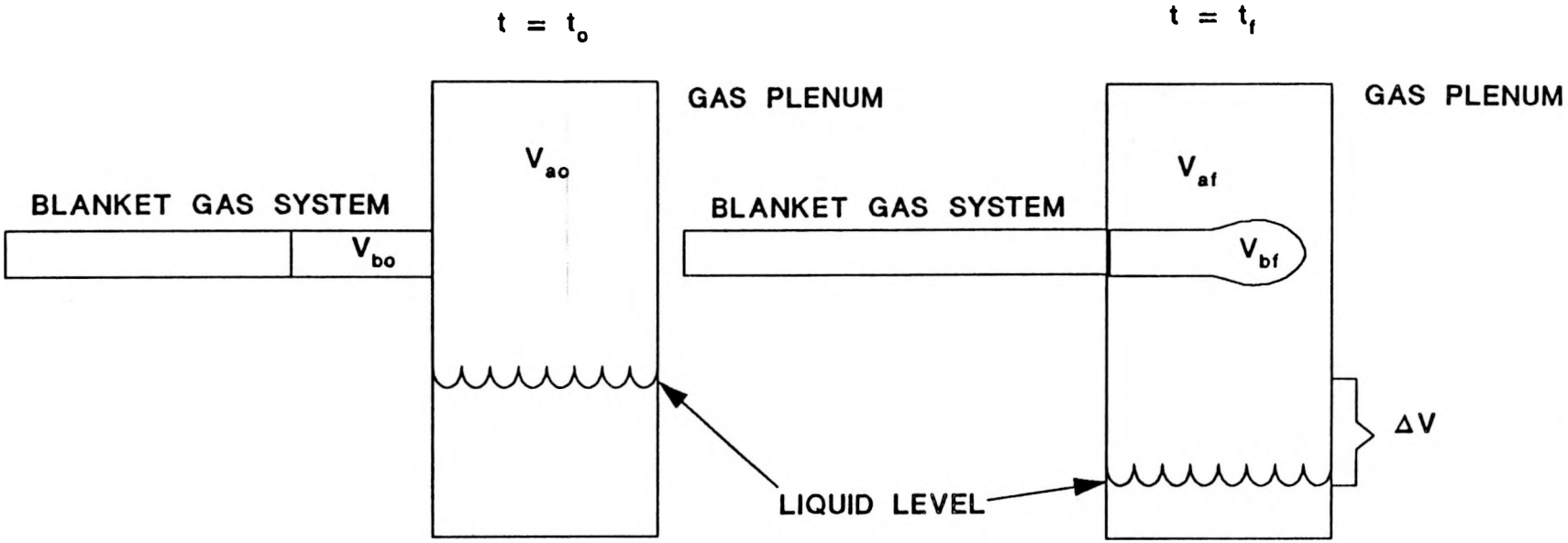

Figure B–1. Illustration of the gas expansion process.

JEN00731